INFORMATION TO USERS

This manuscript has been reproduced from the microfilm master. UMI films the text directly from the original or copy submitted. Thus, some thesis and dissertation copies are in typewriter face, while others may be from any type of computer printer.

The quality of this reproduction is dependent upon the quality of the copy submitted. Broken or indistinct print, colored or poor quality illustrations and photographs, print bleedthrough, substandard margins, and improper alignment can adversely affect reproduction.

In the unlikely event that the author did not send UMI a complete manuscript and there are missing pages, these will be noted. Also, if unauthorized copyright material had to be removed, a note will indicate the deletion.

Oversize materials (e.g., maps, drawings, charts) are reproduced by sectioning the original, beginning at the upper left-hand corner and continuing from left to right in equal sections with small overlaps.

Photographs included in the original manuscript have been reproduced xerographically in this copy. Higher quality 6" x 9" black and white photographic prints are available for any photographs or illustrations appearing in this copy for an additional charge. Contact UMI directly to order.

ProQuest Information and Learning
300 North Zeeb Road, Ann Arbor, MI 48106-1346 USA
800-521-0600

Université d'Ottawa • University of Ottawa

Abstract

This thesis deals with the preparation, characterization and reactivity of silica-supported titanium(IV) complexes. The room temperature reactions of excess $Ti(O^iPr)_4$ with the hydroxyl groups of a nonporous silica yield *dinuclear* surface complexes regardless of the degree of partial dehydroxylation of the silica. The surface reactions were studied by *in situ* IR transmission spectroscopy, DRUV-vis, ^{13}C CP/MAS NMR, GC/MS and elemental analysis. The spontaneous stoichiometric formation of both 2-propanol and propene during grafting indicates that interaction of $Ti(O^iPr)_4$ with the silica surface induces disproportionation of alkoxide ligands with concomitant formation of a Ti-O-Ti bridge. A synthetic route to *mononuclear* silica-supported Ti alkoxide complexes was developed by reaction of grafted amide complexes $(\equiv SiO)_nTi(NEt_2)_{4-n}$ (n = 1 or 2) with alcohols. Subsequent reactions of the mononuclear surface alkoxide complexes with $Ti(O^iPr)_4$ yield dinuclear species identical to those prepared by the direct reaction of $Ti(O^iPr)_4$ with silica.

Both mono- and dinuclear supported alkoxide complexes undergo ligand exchange reactions with *tert*-butylhydroperoxide, but only the dinuclear alkylperoxo titanium surface complexes react with olefins to generate epoxides, which are formed quantitatively as the exclusive product at short reaction times. At longer contact times, the yield of epoxide decreases, without the appearance of other volatile oxidation products. It was discovered that the epoxide reacts with the catalyst and the product blocks the active site, inhibiting further epoxidation reaction with *tert*-butylhydroperoxide.

Acknowledgements

I do not have enough room to thank all the people who have helped me over the past five years. Susannah L. Scott for giving me the opportunity to work in her lab for the purposes of this research. I would like to thank her not only for her guidance, patience and willingness to debate chemistry problems, but also for being a very understanding person.

I would like to thank Dr. Rice for performing the quantification of ligand-derived volatiles during grafting of $Ti(O^iPr)_4$.

I would also like to thank everyone I had the pleasure of working with over the years, undergraduates, graduate students and postdocs. I would particularly like to thank Marcel Beaudoin, Gordon Rice and Jamila Amor, who have been with me since I started in the lab.

I would like to thank the entire Chemistry Department support staff, particularly John Hopkins, Don Hopkins and Lee Sorensen. I would also like to thank Dr. Glenn Facey for running the solid NMR spectra.

I would like to thank my friends Dao Nguyen with whom I had a good time over the last year in the lab and Dino Amoroso for running the solution NMR spectra of my polymers.

Finally, I would like to thank my family whom I love very much: my mother Nima Abdillahi, my brothers Fayçal, Rachid, Asseyteh, Sahal and my sister Anissa.

This thesis is due to your effort and helps. Thank you.

Table of Contents

List of Figures

List of Schemes

List of Tables

Chapter 1

Introduction

1.1 Olefin oxidation

Olefin oxidation is practised industrially on a scale of millions of tons per year.[1] One class of oxidation products, the epoxides, are particularly versatile intermediates for the preparation of a variety of valuable organic products. Stoichiometric epoxidation is practised using organic compounds containing electrophilic oxygen, such as peracids and dioxiranes.[2] For non-activated olefins, this homogeneous epoxidation is slow and accompanied by the formation of by-products.[3]

Transition metal catalysts for the epoxidation reaction have received a great deal of attention because of their ability to direct the regio- and/or stereoselectivity of the epoxidation reaction through the choice of appropriate ligands. The catalysts contain a metal from one of group IV (Ti), group V (V), group VI (Mo, W) or group VIII (Re, Mn), generally in its highest oxidation state (*i.e.*, electronic configuration d^0).[3] The choice of ligand complement for the metal is crucial to the activity, and is limited by the requirement for stability under oxidizing conditions. Well-defined, soluble systems include Herrmann's catalyst CH_3ReO_3,[4] Jacobsen's catalyst Mn(salen),[5] Sharpless' catalyst $Ti(OR)_4$/diethyltartrate,[6] and $MoO(O_2)_2$(hmpa) (where hmpa is hexamethylphosphoramide),[7] discovered by Mimoun and subsequently commercialized as the Halcon process. A slightly modified version of Mimoun's catalyst, containing a phosphine oxide ligand,[8] was recently patented as a biphasic catalyst by BASF.[9]

Less well-defined but commercially very useful are the heterogeneous epoxidation catalysts. The oldest version is polycrystalline silver, which catalyzes the epoxidation of ethylene by molecular O_2.[10] Unfortunately, this catalyst is not effective for any substituted olefins. Researchers at Shell discovered that amorphous Ti/SiO_2 catalyses the epoxidation of higher olefins by anhydrous ^tBuOOH. More recently, a catalyst prepared by the isomorphous substitution of a small amount of titanium into the pentasil framework of Silicalite-1 was discovered by Italian researchers at Enichem.[11] This titanosilicate molecular sieve, called TS-1, is highly selective for the epoxidation of olefins and hydroxylation of phenol and linear alkanes by H_2O_2.[12] Initial reports of this remarkable reactivity launched an international research effort to prepare related supported epoxidation catalysts and to understand the nature of the active site.

1.2 Mechanism of epoxidation

Homogeneous transition metal catalysts for epoxidation are generally prepared by interaction of a metal complex with a peroxide source, either H_2O_2 or ROOH. Although dilute aqueous H_2O_2 is cheap and generates no organic byproducts, many epoxides are sensitive to hydrolysis, and in these cases non-aqueous reactions are preferable; *tert*-BuOOH is widely used[13] since the *tert*-BuOH product is readily recycled by reoxidation. In all cases except for Jacobsen's catalyst, the binding of the intact peroxide to the transition metal serves to render the peroxo oxygen more electrophilic. The rate of oxygen transfer to substrate is usually not very sensitive to steric effects, but is quite

sensitive to electronic effects, thus more nucleophilic (electron-rich) olefins tend to react faster with the electrophilic metal-peroxo complex.

The reaction mechanism for epoxidation has been the subject of a long controversy. The original proposal, inspired by the observation that the reactivity of Mimoun's catalyst is inhibited by the presence of donor solvents, had the olefin coordinate to the metal then undergo [2+2] insertion to yield a five-membered metallaoxetane intermediate, Scheme 1.1, path a.[7]

Scheme 1.1. Proposed epoxidation mechanisms for transition metal peroxo complexes

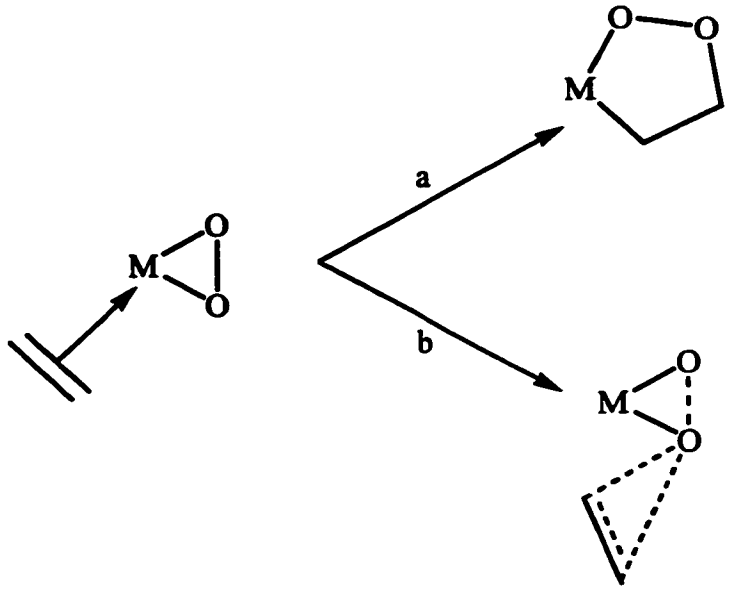

However, seven-coordinate (L-L)MoO(η^2-O_2)$_2$ complexes without an open coordination site were also shown to catalyse epoxidation.[14] Furthermore, calculations suggest that the barrier for olefin insertion is substantially higher (ca. 10 kcal)[15, 16] than for direct attack of the substrate on the peroxo oxygen, resulting in concerted oxygen transfer, Scheme 1.1, path b.[6] Density functional calculations do not confirm or preclude olefin

precoordination, where sterically possible, followed by "slippage" of the olefin towards the peroxo oxygen.[17]

Although the LUMO of the transition metal oxidant is one of its d orbitals, the predominant orbital overlap between the metal complex and the incoming olefin in the transition state is that between the olefin HOMO and the empty σ^* orbital of the peroxo ligand, Scheme 1.2.[18]

Scheme 1.2. Orbital interactions in the olefin-metal peroxide system

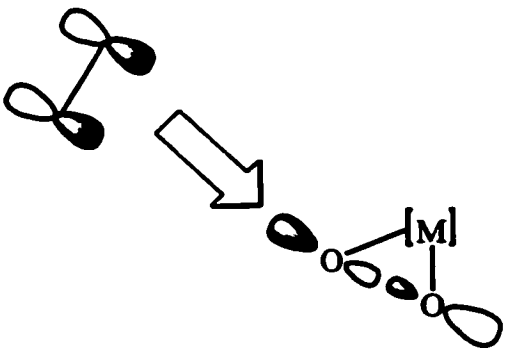

During the reaction, electron density is transferred from the olefin's filled π orbital to this σ^* orbital. The transition state prefers a spiro rather than a coplanar structure, in which the olefinic C-C bond is orthogonal to the plane of the metal-peroxo group.[15]

Two competing factors affect the reactivity of metal-peroxo complexes: the strength of the O-O bond, and the electrophilicity of the peroxide oxygens. Coordination of the peroxide to the metal reduces the antibonding character of the O-O interaction and hence strengthens the O-O bond, deactivating the peroxide ligand for oxygen abstraction. The higher the energy of the σ^* orbital, the higher is the barrier for reaction,[15] since the O-O bond is correspondingly sronger (and shorter).[19] However, the electrophilicity of the

peroxide oxygens increases as a result of their electron donation to the metal. Coordination of a base to the metal centre increases the electron density on the peroxide oxygens, thereby reducing their electrophilicity and shutting down the reaction (explaining Mimoun's observation).[16] Likewise, the replacement of the parent η^2-O_2^{2-} ligand by an alkylperoxo ligand η^2-O_2R makes the peroxo oxygen less electrophilic as a result of the electron-donating character of the alkyl substituent, although the geometry of the metal peroxo complex remains virtually unchanged.[16]

Nearly all structurally characterized catalysts are seven-coordinate diperoxo complexes with pentagonal bipyramidal geometries. However, six-coordinate diperoxo species with pentagonal pyramidal structures, which are unstable intermediates formed by dissociation of coordinated base, are calculated to be even more active, since their peroxide ligands are more electrophilic, for the reasons described above.[15] Although oxygen transfer from both diperoxo and monoperoxo complexes are exothermic, the reaction energies are much smaller for the monoperoxo complexes. Furthermore, the barriers for oxygen transfer from the diperoxo species are much lower than for the corresponding monoperoxo species.[15]

A final complication in the understanding of metal peroxo reactivity was revealed only by computational methods. The activity of the peroxo complexes of the group VI metals follows the order Cr<Mo<W, however, this order does not correlate with the thermodynamic driving forces for the reaction. While Cr has the largest driving force, it also has the largest activation barrier.[19] The major effect on the activation barriers is relativistic. Thus for W, the metal-O(peroxo) bonds are shorter and stronger due to relativistic effects, making the O-O bond weaker.

1.3 Characterization of the active sites in heterogeneous epoxidation catalysts

While group VI metal complexes, particularly of Mo and W, exhibit the highest activity and selectivity in homogeneous catalytic epoxidations, they do not make particularly good supported epoxidation catalysts. The peroxide (either H_2O_2 or ROOH) causes extensive and irreversible leaching of the metal from the oxide support, leading to loss of activity. In contrast, Ti(IV) is a relatively poor homogeneous epoxidation catalyst but once immobilized on or in a siliceous support, it shows superior activity. Apparently the greater strength of the Ti-O-Si interaction more effectively resists leaching.

The metal-support interaction is crucial in one more sense to the epoxidation activity. Unsupported TiO_2 catalyzes the unproductive decomposition of H_2O_2 by disproportionation to O_2 and H_2O.[20] Dispersion of Ti(IV) in a non-titania matrix is required to create the epoxidation active sites. The preferred support is silica, which lacks significant acidity. Acidic sites on other potential oxide supports, such as clays, catalyse epoxide ring-opening and other side reactions. Nonetheless, Ti-K10 montmorillonite has been reported to be an efficient catalyst for the asymmetric epoxidation of primary allylic alcohols in the presence of tartrate.[21]

The first Ti/silica catalyst, discovered by researchers at Shell, is prepared by impregnation of amorphous silica with $TiCl_4$, followed by high temperature calcination.[22] During thermal activation, the titanium is suggested to migrate into the silica lattice. The active centres were originally suggested to consist of titanyl groups on the surface, bound to siloxide ligands, Scheme 1.3.[23]

Scheme 1.3. Proposed titanium active sites in Ti/silica catalysts

titanyl dipodal tripodal tetrapodal

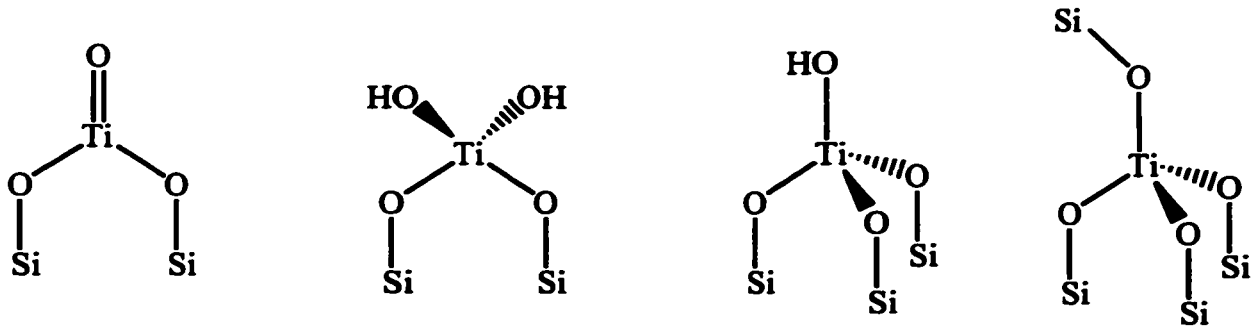

An intense band at 920-960 cm^{-1} in the vibrational spectra (IR, Raman) of these materials was suggested to correspond to ν(Ti=O), however, it was later demonstrated that this feature is characteristic of silicotitanates without titanyl groups, and has been definitively assigned to the $[O_3Si\text{-}O]^{\delta-}[Ti]^{\delta+}$ stretching mode.[24]

The amorphous nature of the Shell catalyst makes characterization understandably difficult. In contrast, the titanosilicate molecular sieve TS-1 is crystalline and has been exhaustively characterized.[25] The active sites appear to be Ti(IV) centres substituted isomorphously for Si into the silicalite framework, $Si_{96-x}Ti_xO_{192}$ (with x up to 2.5). The low amount of Ti relative to Si suggests that almost all the Ti sites are isolated. However, the standard synthetic technique[12,25] for TS-1 involves co-hydrolysis of $Si(OEt)_4$ with a titanium alkoxide, typically $Ti(OEt)_4$, so that the possibility of formation of titanium oxoalkoxides exists. In fact, if the Ti/Si ratio exceeds 2.5 wt.%, extraframework Ti appears in the form of TiO_2, which is said to be detected by the appearance of absorbance above 350 nm in the UV-visible spectrum.[25]

The Ti K-edge XANES spectrum of TS-1 shows a sharp pre-edge peak characteristic of the A_1-T_2 transition of tetrahedral Ti,[26] while the DRUV-vis spectrum shows a band at ca. 212 nm,[27] assigned to the Ti^{IV}-$O^{2-} \rightarrow Ti^{III}$-$O^{-}$ ligand-to-metal charge transfer transition of tetrahedrally-coordinated Ti.[28] These results are consistent with dipodal, tripodal and tetrapodal structures shown in Scheme 1.3. Multiple-scattering analysis of the EXAFS of TS-1 was recently claimed to reveal four O nearest neighbours and four Si next-nearest neighbours, in support of the tetrapodal site.[29] The Ti may occupy defect sites associated with hydroxyl "nests", leading to a structure with very little residual acidity which makes the epoxidation reaction highly selective. However, it should be recognized that all of the structures presented in Scheme 1.3 are really precursors to the true active sites, since the interaction with the peroxide is not considered.

1.4 Catalytic properties of framework-substituted materials

While the Shell catalyst is hydrophilic and deactivated by water, the TS-1 structure is hydrophobic and tends to exclude water from the active sites. This property allows catalysis to take place using aqueous H_2O_2, without deactivation of the catalyst or hydrolysis of the epoxide.[30] Neutron diffraction studies show a preference for Ti occupation in only some of the 12 crystallographically distinct sites of the silicalite framework, with the Ti sites fortuitiously located primarily at the channel intersections where they are accessible to substrate.[31] However, TS-1 and other microporous solid

catalysts have a significant disadvantage in that the channel size, ca. 5.5 Å, precludes epoxidation of all but the smallest, unhindered olefins.[32]

Titanium inserted into larger pore zeolites, as in Ti-β,[33,34] or amorphous mesoporous materials such as Ti-MCM-41,[35] is capable of epoxidizing larger olefins, but neither the conversion nor the selectivity are high. Furthermore, hydrolytic leaching is a severe problem for these materials. Post-synthesis silylation increases hydrophobicity and consequent resistance to leaching.[36] In general, selectivity improves with *tert*-BuOOH as the oxidant, rather than H_2O_2.[35] The major disadvantage of incorporating Ti into a silicate framework is that there is no possibility to modify the ligand environment of Ti in order to alter selectivity (*e.g.*, stereoselectivity).

1.5 Catalytic properties of grafted catalysts

An alternate preparative method to the framework substitution of Si by Ti involves the post-synthesis modification of a silicate by a Ti-containing molecular precursor. If the material is not subjected to a high temperature calcination treatment, some of the original ligands associated with the molecular complex remain associated with Ti, and are therefore able to influence subsequent reactions. The most common Ti reagents used for modification of silica surfaces are $TiCl_4$ and $Ti(OR)_4$, both of which react rapidly and irreversibly with the hydroxyl groups at room temperature. Cp_2TiCl_2 has also been used to graft Ti onto MCM materials.[28] Other Ti/silica catalysts have been prepared from TiF_4[37] and $TiNp_4$.[38]

Generally, hydrolysis or calcination is performed to remove remaining ligands prior to catalytic testing. Although the grafted Ti sites are presumed to remain isolated, evidence for this assumption is rarely sought. In fact, the simultaneous loss of hydrocarbon ligands and the appearance of ν(SiO-H) modes as seen by IR tends to suggest that hydrolysis/calcination is accompanied by detachment of grafted Ti from the silica surface. The unsupported Ti is then susceptible to oligomerization.

A rare report of grafted catalysts used without high temperature activation caught our attention. Supported silica catalysts were prepared using three reagents: $TiCl_4$, $Ti(O^iPr)_4$ and $TiCl_2(O^iPr)_2$.[39] The products in the first two cases were presumed to be primarily $(\equiv SiO)_2TiCl_2$ and $(SiO)_2Ti(O^iPr)_2$, respectively. Curiously, reaction of silica with $TiCl_2(O^iPr)_2$ gave a material which spectroscopically resembled neither of these. Nor did the elemental analysis agree with these assignments: $TiCl_4$/silica contained 1.2 Cl/Ti, while $Ti(O^iPr)_4$/silica contained 1.5 ^iPr/Ti. $TiCl_2(O^iPr)_2$/silica contained no Cl and only 0.5 ^iPr/Ti. Evidently the grafting reactions are more complex than the preliminary report suggested.

Nonetheless, these materials are active catalysts for olefin epoxidation by ^tBuOOH.[40] In fact, $Ti(O^iPr)_4$/silica is reported to be significantly more active than any of the zeolite-based catalysts, and more selective than Ti-exchanged K10 montmorillonite. Astonishingly, the catalyst is active even with 30% aqueous H_2O_2 as the oxidant, and is air-stable,[41] unlike the highly sensitive Shell catalyst. These properties are all the more remarkable for a catalysts based on hydrolytically-sensitive molecular precursors. $Ti(OR)_4$ complexes are notoriously prone to hydrolysis giving higher nuclearity oxoalkoxides.[42] Deactivation of the recycled catalyst in subsequent runs was not a

significant leaching (< 10%); in fact, the catalyst gained carbon during the epoxidation runs.[41] Adsorption of products and/or byproducts on the active sites was suggested, as well replacement of ^{i}PrO groups by sterically more bulky ^{t}BuO groups from the solvent (^{t}BuOH).

With this background in mind, we undertook to investigate the nature of the active sites of Ti($O^{i}Pr$)$_4$/silica upon grafting, during the epoxidation chemistry of simple olefins, as well upon deactivation.

1.6 References

1. Wittcoff, H. A.; Reuben, B. G. *Industrial Organic Chemicals*; Wiley: New York, 1996.
2. Hoveya, A. H.; Evans, D. A.; Fu, G. C. *Chem. Rev.* **1993**, *93*, 1307-1370.
3. Jørgensen, K. A. *Chem. Rev.* **1989**, *89*, 431-458.
4. Gisdakis, P.; Antonczak, S.; Köstlmeier, S.; Herrmann, W. A.; Rösch, N. *Angew. Chem., Int. Ed. Engl.* **1998**, *37*, 2211-2214.
5. Palucki, M.; Finney, N. S.; Posposil, P. J.; Guler, M. L.; Ishida, T.; Jacobsen, E. N. *J. Am. Chem. Soc.*, **1998**, *120*, 948-954.
6. Sharpless, K. B.; Townsend, J. M.; Williams, D. R. *J. Am. Chem. Soc.*, **1972**, *94*, 295.
7. Mimoun, H.; De Roch, I. S.; Sajus, L. *Tetrahedron*, **1970**, *26*, 37-50.
8. Wahl, G; Kleinhenz, D.; Schorm, A.; Sundermeyer, J.; Stowasser, R.; Rummey, C.; Bringmann, G.; Fickert, C.; Kiefer, W. *Chem. Eur. J.* **1999**, *5*, 3237.
9. Schulz, M.; Teles, J. H.; Sundermeyer, J.; Wahl, G. (BASF AG) WO 10054, 1995.
10. Sachtler, W. M. H.; Backx, C.; Van Santen, R. A. *Catal. Rev.-Sci. Eng.* **1981**, *23*, 127.
11. Taramasso, M.; Perego, G.; Notari, B. US Patent 4,410501, 1983.
12. Notari, B. *Adv. Catal.* **1996**, *41*, 253.
13. Thiel, W. R.; Eppinger, J. *Chem. Eur. J.* **1997**, *3*, 696-705.
14. Thiel, W. R.; Priermeier, T. *Angew. Chem. Int. Ed. Engl.* **1995**, *34*, 1737-1738.

15. Di Valentin, C.; Gisdakis, P.; Yudanov, I. V.; Rösch, N. *J. Org. Chem.* **2000**, *65*, 2996.

16. Yudanov, I. V.; Gisdakis, P.; Di Valentin, C.; Rösch, N. *Eur. J. Inorg. Chem.* **1999**, 2135-2145.

17. Jørgensen, K. A.; Hoffmann, R. *Acta Chem. Scand. B* **1986**, *40*, 411-419.

18. Deubel, D. V.; Frenking, G.; Senn, H. M.; Sundermeyer, J. *Chem. Commun.* **2000**, 2469.

19. Deubel, D. V. *J. Phys. Chem. A*, **2001**, 105, 4765-4772.

20. Huybrechts, D. R. C.; Bruskens, P. I.; Jacobs, P. A. *J. Mol. Catal.* **1992**, *71*, 129.

21. Choudary, B. M.; Valli, V. L. K.; Durga Prassad, A. *J. Chem. Soc., Chem. Commun.* **1990**, 1186.

22. Wulff, H. P. U.S. Patent. 3,932,843 (1975).

23. Sheldon, R. A. *Stud. Surf. Sci. Catal.* **1991**, *59*, 33.

24. Su, Y.; Balmer, M. L.; Bunker, B. C. *J. Phys. Chem. B* **2000**, *104*, 8160-8169.

25. Vayssilov, G. N. *Catal. Rev.-Sci. Eng.* **1997**, *39*, 209-251.

26. Trong On, D.; Kaliaguine, S.; Bonneviot, L. *J. Catal.* **1995**, *157*, 235.

27. Geobaldi, F.; Bordiga, S.; Zecchina, A.; Giamello, F.; Leofanti, G.; Petrini, G. *Catal. Lett.* **1992**, *16*, 109.

28. Maschmeyer, T.; Rey, F.; Sankar, G.; Thomas, J. M. *Nature* **1995**, *378*, 159.

29. Gleeson, D.; Sankar, G.; Catlow, C. R. A.; Thomas, J. M.; Spanó, G.; Bordiga, S.; Zecchina, A.; Lamberti, C. *Phys. Chem. Chem. Phys.* **2000**, *2*, 4812-4817.

30. Murugavel, R.; Roesky, H. W. *Angew. Chem., Int. Ed. Engl.* **1997**, *36*, 477.

31. Hijar, C. A.; Jacubinas, R. M.; Eckert, J.; Henson, N. J.; Hay, P. J.; Ott, K. C. *J. Phys. Chem. B* **2000**, *104*, 12157-12164.

32. Notari, B. *Catal. Today* **1993**, *18*, 163.

33. Corma, A.; Esteve, P.; Martínez, A.; Valencia, S. *J. Catal.* **1995**, *152*, 18.

34. Camblor, M. A.; Corma, A.; Martínez, J.; Pérez-Pariente, J.; Primo, J. *Stud. Surf. Sci. Catal.* **1993**, *78*, 393.

35. Blasco, T.; Corma, A.; Navarro, M. T.; Pérez-Pariente, J. *J. Catal.* **1995**, *156*, 65.

36. Tatsumi, T.; Koyano, K. A.; Igarashi, N. *Chem. Commun.* **1998**, 325.

37. Jorda, E.; Tuel, A.; Teissier, R.; Kervennal, J. *J. Catal.* **1998**, *175*, 93.

38. Holmes, S. A.; Quignard, F.; Choplin, A.; Teissier, R.; Kervennal, J. *J. Catal.* **1998**, *176*, 173.

39. Fraile, J. M.; García, J.; Mayoral, J. A.; Proietta, M. G.; Sánchez, M. C. *J. Phys. Chem.* **1996**, *100*, 19484-19488.

40. Cativiela, C.; Fraile, J. M.; García, J. I.; Mayoral, J. A. *J. Mol. Catal. A: Chem.* **1996**, *112*, 259-267.

41. Fraile, J. M.; García, J. I.; Mayoral, J. A.; Vispe, E. *J. Catal.* **2000**, *189*, 40-51.

42. Bradley, D. C.; Mehrotra, R. C.; Gaur, D. P. *Metal Alkoxides*, Academic: London, 1978.

Chapitre 2

Techniques Expérimentales

2.1 Les réactifs

2.1.1 La silice

La silice utilisée pour notre étude est une silice amorphe, Aerosil-200, provenant de Degussa Corporation. Elle a une surface de 200 m^2/g. Cette silice nonporeuse de haute pureté est pyrogène, ce qui signifie qu'elle est fabriquée par la pyrolyse de $SiCl_4$ dans une flamme, éq. 2.1 et 2.2.[1]

$$SiCl_4 + O_2 \rightarrow SiO_2 + 2\,Cl_2 \qquad (2.1)$$

$$2\,H_2O + 2\,Cl_2 \rightarrow 4\,HCl + O_2 \qquad (2.2)$$

2.1.2 Les complexes métalliques

Les complexes de surface traités dans cette thèse sont préparés à partir de trois précurseurs différents de titane. Le premier est le $Ti(O^iPr)_4$ (99.999%, Aldrich). Avant chaque expérience, son impureté de 2-propanol est séparée de ce dernier par une distillation piège-à-piège, utilisant un bain d'azote liquide et un bain composé de sel et de glace. Une procédure similaire a été employée pour enlever le $HNEt_2$ contenu dans le

$Ti(NEt_2)_4$ (99.99%, Alfa-Aesar) et le $HNMe_2$ dans le $Ti(NMe_2)_4$ (99.9%, Alfa-Aesar). Les trois réactifs de titane sont stockés sous atmosphère d'azote dans des tubes de Schlenk.

2.2.3 Les liquides et solvants

Le 2-propanol et le *tert*-butanol sont distillés sous atmosphère d'azote, transférés et stockés dans des tubes de Schlenk à haut vide en présence des tamis moléculaires activés (3 Å). Les alcools deuterés $(CD_3)_2CDOD$ (98%, Aldrich) et $(CD_3)_3COD$ (99%, Aldrich) sont séchés sous agitation dans des Schlenks sur des tamis moléculaires activés, suivi d'une distillation piège-à-piège, et stockés dans des réacteurs en présence des tamis moléculaires activés. Le *tert*-butylhydroperoxyde (99%, anhydre, 5 à 6 M dans le décane, Aldrich) est séché sous agitation dans un Schlenk contenant du $MgSO_4$ et stocké sur des tamis moléculaires activés. Le cyclohexène (99%, stabilisé par 0.001% de 2-*tert*-butyl-*p*-cresol, Aldrich) et l'oxyde de cyclohexène (98%, Aldrich) sont séchés sous agitation dans des Schlenks sur des tamis moléculaires activés suivi d'une distillation piège-à-piège, et stockés dans des tubes de Schlenk en présence des tamis moléculaires activés, munis de robinets à haut vide Téflon (Young). Avant son utilisation, chaque réactif liquide est l'objet de 3 cycles gel-vide-dégel. Ensuite, sa vapeur est transférée à travers la rampe à haut vide avec l'aide d'un piège d'azote liquide.

2.1.4 Les gaz

L'oxyde de propylène (99.5%) est acheté de Aldrich et le propène (99.6%) provient de Matheson Gas Products. Ils sont stockés dans des ballons en verre en présence des tamis moléculaires activés. L'oxygène provient de Air Products (Ultrapure Carrier Grade). Une pression précise de gaz est transférée dans le réacteur via la rampe à haut vide en utilisant une jonction en «T» à laquelle est connectée un manomètre à capacitance.

2.2 Préparation de la silice

2.2.1 Déshydroxylation partielle

Un protocole standard de prétraitement de la silice est suivi pour rendre les réactions de surface reproductibles. La température à laquelle la silice est chauffée détermine la densité des groupes hydroxyles sur sa surface. Une silice Aerosil partiellement déshydroxylée à 200 et 500°C contient 2.6 et 1.2 OH/nm^2, respectivement.[1] Ces matériaux sont indiqués par silice-200 et silice-500, respectivement, où le chiffre en appendice indique la température à laquelle la silice a été traitée avant sa réaction avec un complexe métallique quelconque. La silice-500 est préparée par calcination en présence de 200 Torr d'oxygène à 500°C pour au moins quatre heures afin d'éliminer les impuretés d'hydrocarbures, suivi d'une déshydration et déshydroxylation partielle pour un minimum de quatre heures à 500°C sous vide dynamique ($<10^{-4}$ Torr). Pour préparer

la silice-200, l'étape de calcination est omise. La silice est simplement chauffée à 200°C sous vide dynamique pour au moins 4 heures.

2.2.2 Marquage de la silice par isotopes d'oxygène

L'enrichissement de la silice en isotopes d'oxygène est effectué de la manière suivante: la pastille de silice est tout d'abord déshydroxylée à 500°C. Ensuite, on l'expose à quatre à six cycles de vapeur d'eau marquée ($H_2{}^{18}O$) à 400°C. Après le cycle final, la température est augmentée à 500°C suivi d'un vide dynamique à 500°C pendant une heure. Le degré d'enrichissement des groupes hydroxyles en ^{18}O est estimé à >80% à partir de la diminution en intensité de la bande $\nu(Si^{16}O\text{-}H)$ à 3747 cm^{-1} dans les spectres IR des pastilles. Cette méthode d'enrichissement isotopique est une version modifiée d'une méthode de la littérature.[2]

2.3 Modification de la surface de la silice

2.3.1 Techniques de haut vide

Toutes les expériences ont été réalisées avec un système à haut vide en verre. Le système est constitué d'une rampe principale à vide et d'une rampe à gaz, mutuellement connectées par des robinets à haut vide; chaque rampe est connectée à la pompe à diffusion à mercure en série avec une pompe à palettes (Edwards). Chaque rampe est équipée de deux manomètres à capacitance, lisant des pressions de 10^{-3} à 1000 Torr. Un

piège d'azote liquide est situé entre les rampes et la pompe à diffusion Les réacteurs sont attachés à la rampe à vide par voie des joints sphériques.

2.3.2 Techniques de "breakseal"

A l'origine, le terme technique qui décrit le réacteur de transfert comprend le mot anglais «breakseal». La traduction exacte du terme n'existe pas en français, et en France on utilise le terme "queue de cochon" car le bout du réacteur de transfert ressemble à une "queue de cochon" en miniature. Toutefois, nos réacteurs n'ayant pas l'allure d'une "queue de cochon", on a pris la liberté de les appelés "réacteurs de breakseal".

Le réacteur montré dans la Figure 2.1 est préparé par soufflage de verre, et son étanchéité est verifée sur la rampe à haut vide. Un réactif liquide est transféré dans le réacteur par seringue, sous courant d'azote. Le réacteur contenant le produit sous atmosphère azotée est connecté à la rampe à haut vide. Le produit est ensuite gelé dans de l'azote liquide et l'atmosphère dans le réacteur est éliminée. Le réactif est ensuite l'objet de trois cycles de gel-vide-dégel sur la rampe à haut vide afin d'éliminer les gaz dissous. Pour l'étape finale, on garde le breakseal dans de l'azote liquide (le produit est donc gelé) et on scelle le réacteur au niveau du rétrécissement avec la flamme d'un chalumeau. On obtient le complexe métallique scellé dans le breakseal sous vide statique. Un marteau, habituellement un morceau de fer scellé à l'intérieur d'un tube de verre, est inséré dans le bout ouvert du breakseal. On fixe un aimant à l'extérieur du breakseal au niveau du marteau afin d'éviter de casser l'ampoule contenant le produit. Ensuite, on prépare un deuxième rétrécissement du côté du marteau pour faciliter

l'élimination du breakseal après la réaction. Enfin, le bout ouvert du tuyau est soudé aux différents réacteurs comme le montrent les Figures 2.2 et 2.4.

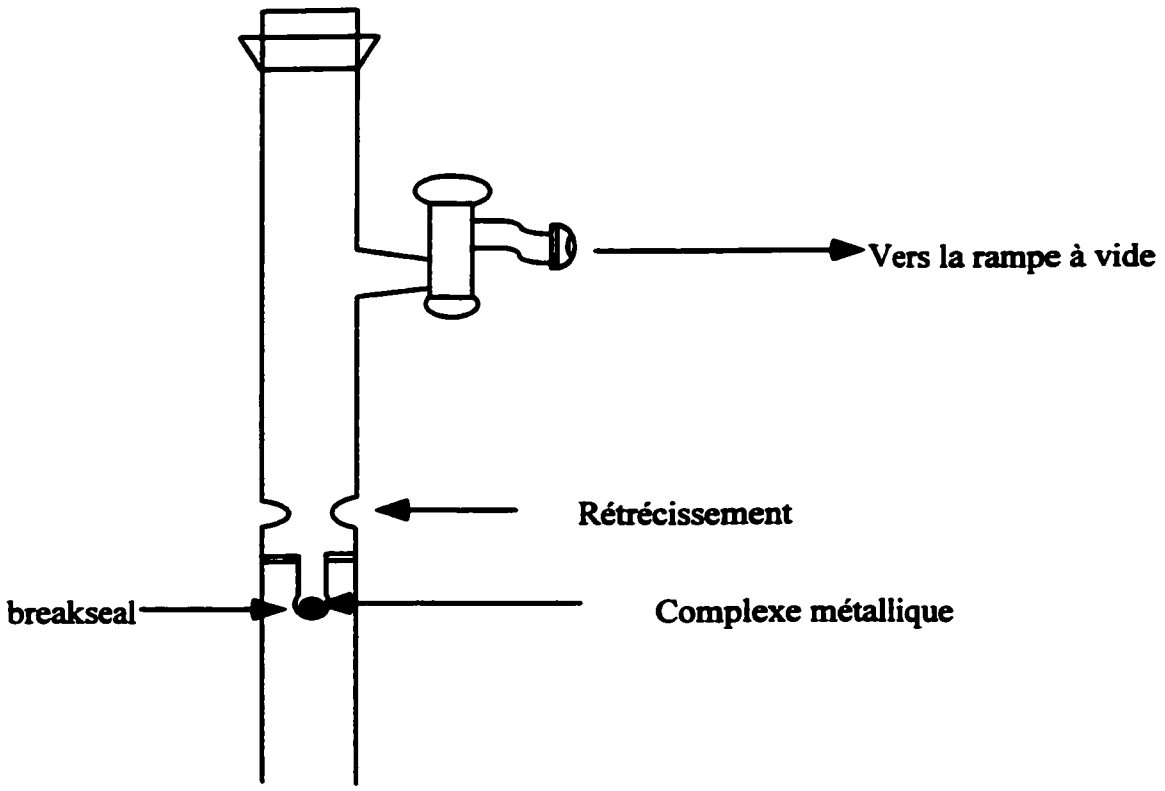

Figure 2.1. Schéma d'un réacteur de "breakseal"

2.3.2 Greffage du complexe métallique

Après le prétraitement thermique et le refroidissement à température ambiante de la silice en poudre ou en pastille, le breakseal contenant le produit métallique est cassé à l'aide du marteau. Pour introduire le $Ti(O^iPr)_4$ à la pastille, on déplace le porte-échantillon contenant la silice au-dessus du breakseal de manière à ce que la sublimation du produit se fasse perpendiculairement et ceci à température ambiante. Pour introduire le $Ti(NR_2)_4$, la zone du prétraitement thermique est plongée dans un bain d'azote liquide et le produit est sublimé du breakseal aux parois froides selon sa volatilité (R=Me, une heure de sublimation; R=Et, 16 heures de sublimation). Ensuite, on enlève le bain d'azote liquide et on laisse réagir le $Ti(NR_2)_4$ avec la silice à température ambiante jusqu'à ce que la réaction soit complète, c'est-à-dire, de une à douze heures selon la volatilité du complexe métallique et la quantité de silice.

L'excès des réactifs et les produits volatils des réactions sont ensuite désorbés vers le breakseal en utilisant un piège d'azote liquide. En général, la désorption s'éffectue sur plusieurs heures (en général la même période que la réaction de greffage). Ensuite, le breakseal est scellé au niveau du rétrécissement et l'on isole ainsi la silice modifiée par le complexe métallique pour des manipulations ultérieures.

2.4 Caractérisation des complexes métalliques supportés sur la silice

2.4.1 Spectroscopie infrarouge

Les expériences de spectroscopie infrarouge sont réalisées *in situ* dans des cellules IR ayant un volume approximatif de 300 mL, Figure 2.2. Elles sont équipées de fenêtres transparentes au faisceau infrarouge, soit de KCl soit de ZnSe, soudées sur la cellule avec le TorrSeal (Varian). Les cellules sont capables de maintenir un vide statique (< 10^{-4} Torr) pendant plusieurs jours.

Les spectres IR sont enregistrés en mode transmission par un spectrophotomètre FTIR Mattson Research Series équipé d'un détecteur DTGS. Le compartiment où le faisceau rencontre l'échantillon est purgé par de l'air dépourvu d'eau et de gaz carbonique. Pour la ligne de base, ainsi que pour les spectres des échantillons, 32 balayages sont enregistrés avec une résolution de 2 cm^{-1}.

2.4.1.1 Spectroscopie infrarouge des pastilles de silice

Entre 5-15 mg de silice sont pressées (125 kg/m^2) sous forme de pastille de 1.6 cm de diamètre. Les pastilles sont tenues dans un porte-échantillon dans la cellule infrarouge, Figure 2.2. Le porte-échantillon est d'abord situé dans la zone du traitement thermique de la cellule infrarouge, lieu où la calcination et la déshydroxylation vont se faire. Après refroidissement du porte-échantillon à la température ambiante, on enregistre un spectre de la pastille, Figure 2.3, et des fenêtres de la cellule infrarouge. Ensuite, on introduit le complexe métallique comme décrit précédemment. La réaction en surface est suivie en enregistrant des spectres de l'échantillon à différentes étapes de l'expérience. Ces spectres sont obtenus en glissant le porte-échantillon vers la tête de la cellule infrarouge où l'on place de manière à ce que la pastille soit perpendiculaire au faisceau infrarouge.

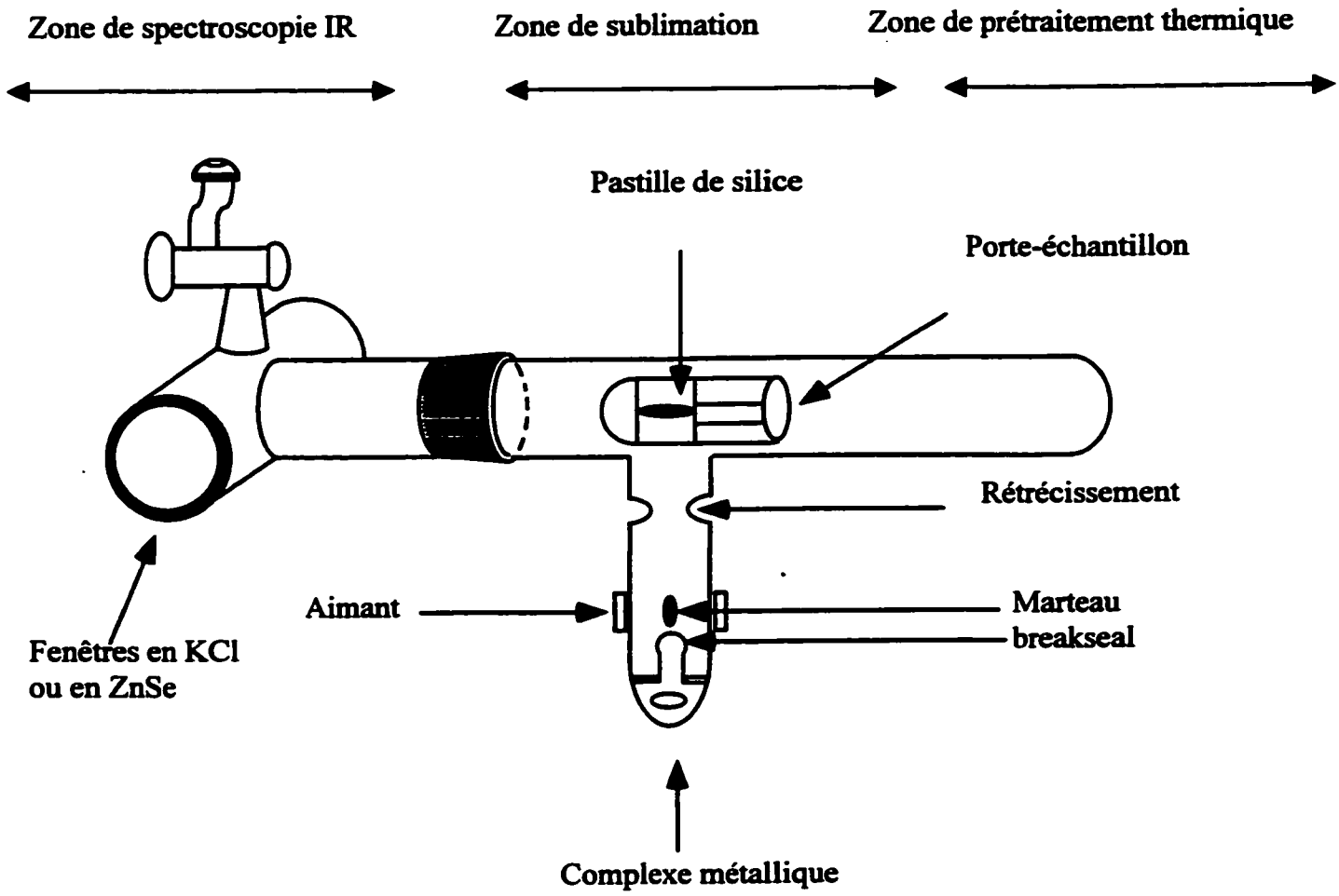

Figure 2.2. Schéma de la cellule infrarouge (vue de côté)

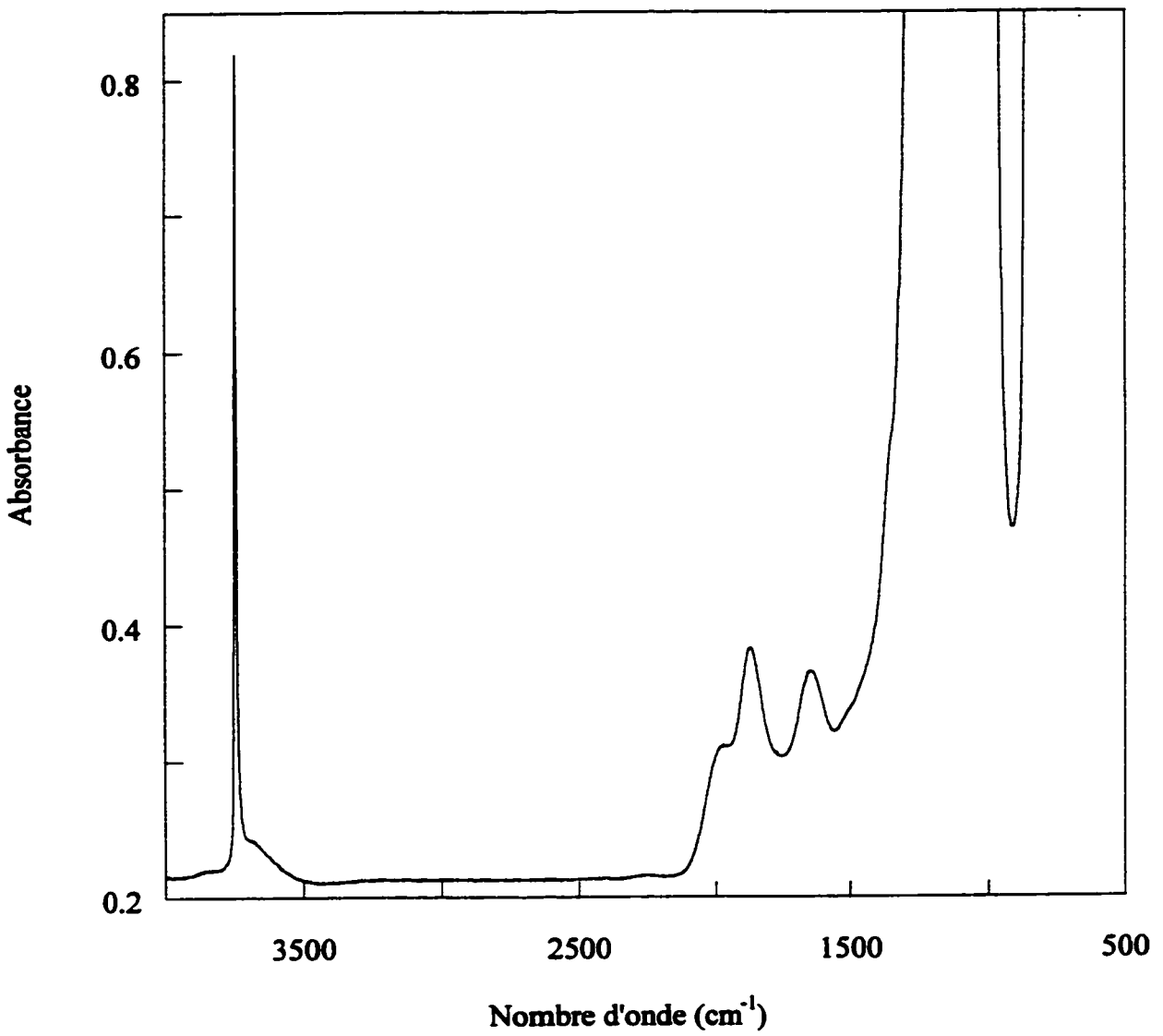

Figure 2.3. Spectre infrarouge d'une pastille de silice calcinée et partiellement déshydroxylée sous vide à 500°C .

Les spectres des produits dans la phase gaz sont obtenus en déplaçant légèrement le porte-échantillon de la tête vers le milieu de la cellule infrarouge laissant ainsi le faisceau traverser que les fenêtres.

2.4.1.2 Spectroscopie infrarouge des couches minces de silice

Les expériences avec des couches minces de silice ont été réalisées avec des cellules infrarouge spécialement conçues, Figure 2.4. La cellule infrarouge a été modifiée pour porter un disque de ZnSe de diamètre 25 mm. Le porte-échantillon peut glisser de la tête vers le bout de la cellule sans rotation, de manière à ce que le disque de ZnSe reste toujours parallèle aux fenêtres de la cellule infrarouge.

La silice (0.1-0.5 mg de silice/cm^2) est répandue sur la fenêtre de ZnSe avec une spatule, de façon à obtenir une couche mince relativement uniforme. L'ensemble est suspendu avec l'aide du porte-échantillon à l'intérieur de la cellule infrarouge modifiée. Une couche mince idéale (dont le spectre ne contient pas trop de bruit de fond) a une absorbance qui ne dépasse pas 1.2. Le traitement thermique de la couche mince est effectué de la même façon que pour les pastilles de silice, mais la température maximum est de 450°C au lieu de 500°C afin d'éviter de faire fondre le disque de ZnSe. Après son refroidissement, la cellule est portée au spectrophotomètre et la couche mince de silice est alignée perpendiculairement au faisceau infrarouge. Une fois alignée, ni la couche mince ni la cellule infrarouge ne doivent bouger pendant toute la durée de l'expérience afin d'obtenir des soustractions spectrales précises.

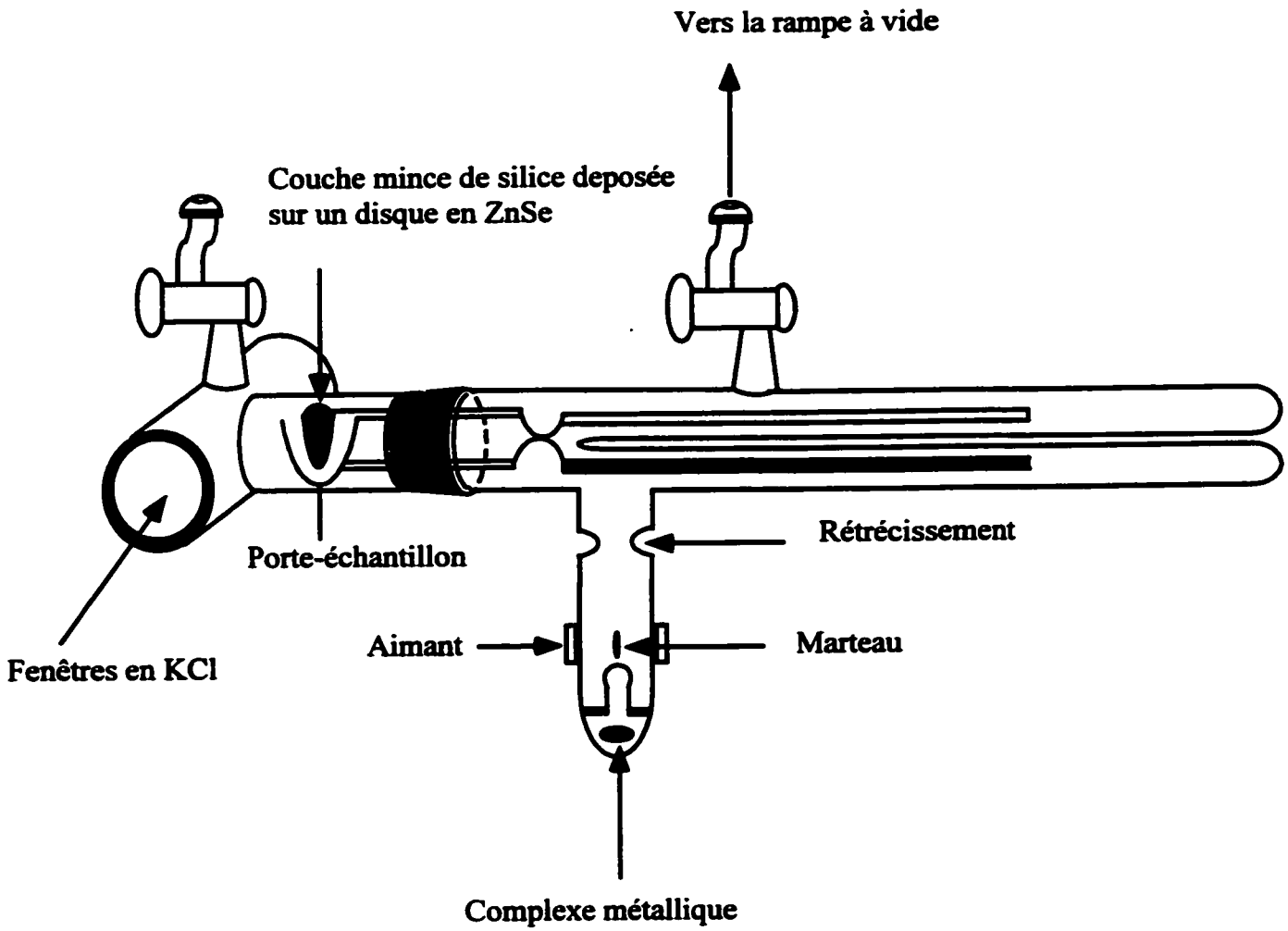

Figure 2.4. Schéma de la cellule infrarouge pour couche mince (vue de côté)

Les conditions expérimentales utilisées sont les mêmes que celles utilisées pour les pastilles, c'est-à-dire, la résolution et le nombre de balayages sont identiques.

Un tuyau en polyéthylène de longueur 1.5 m et de diamètre 5 mm portant à ses deux extrémités des joints sphériques mâles en verre de diamètre 19 mm sert de connecter la rampe à vide à un deuxième robinet situé dans la zone de sublimation de la cellule infrarouge. Les complexes métalliques sont introduits dans la cellule par le biais d'un breakseal. Par contre, les réactifs organiques sont introduits dans la cellule par la voie du tuyau en polyéthylène. Avant d'introduire ces derniers, on effectue d'abord un vide dynamique d'une heure dans le tuyau pour assurer l'absence totale d'humidité.

2.4.2 Spectroscopie RMN de l'état solide

Pour les expériences de RMN, la silice est compactée sous forme de pastilles épaisses (20-30 mg) qui sont ensuite finement broyées dans un mortier. On obtient ainsi de la silice compactée, qui sera transférée dans un réacteur de type Schlenk équipé d'un robinet à haut vide et portant à la perpendiculaire un ou plusieurs tubes de RMN en pyrex de diamètre 5 mm et de longueur 30 mm, Figure 2.5.

Après avoir déshydroxylé la silice compactée à la température recherchée (500 ou 200°C), et suite à son refroidissement à la température ambiante, on greffe les complexes métalliques sur la silice compactée de la façon décrite précédemment pour les pastilles de silice. Entre 30 et 50 mg de la silice compactée est transférée *in vacuo* dans un des tubes de RMN qui sera scellé par chalumeau à une longueur de 25-30 mm. On obtient ainsi des tubes de RMN sous vide contenant de la silice modifiée qui s'insèrent dans des rotors en

zircone. Les spectres RMN du ^{13}C ont été enregistrés en mode CP/MAS (Cross-Polarization/Magic–Angle-Spinning) avec un spectromètre Bruker ASX-200. Les spectres ont été accumulés sur plusieurs heures en utilisant des pulsions à proton à 90° de 4.4 msec avec un temps de contact de 2 msec et un délai de relaxation de 2 s.

La technique du déphasage dipolaire est utilisée pour discerner le signal du méthyle de celui du méthylène. On applique deux pulsions séparées entre elles par un délai de 40 μsec situé entre le temps de contact et le temps d'acquisition. Au cours de ce délai, le signal correspondant au méthylène disparaît. Seul le signal du méthyle est observé puisque l'interaction dipolaire entre le C et le H est réduite due à une rotation rapide du groupe méthyle.

2.4.3 Spectroscopie UV-visible à réflectance diffuse (DRUV-Vis)

Les échantillons pour la spectroscopie UV-visible à réflectance diffuse sont préparés de la même manière que les échantillons RMN. Cependant, au lieu de transférer la poudre de silice sous vide dans des tubes RMN, on les transfert dans des tubes rectangulaires de 2 x 5 mm en quartz. Les tubes sont soudés préalablement sur le réacteur en pyrex par l'intermédiaire des raccords quartz-pyrex. Ils sont par la suite scellés avec un chalumeau au-dessus de ce raccord. Les spectres UV-visible sont enregistrés avec un spectrophotomètre Varian Cary 1E équipé d'un accessoire à réflectance diffuse.

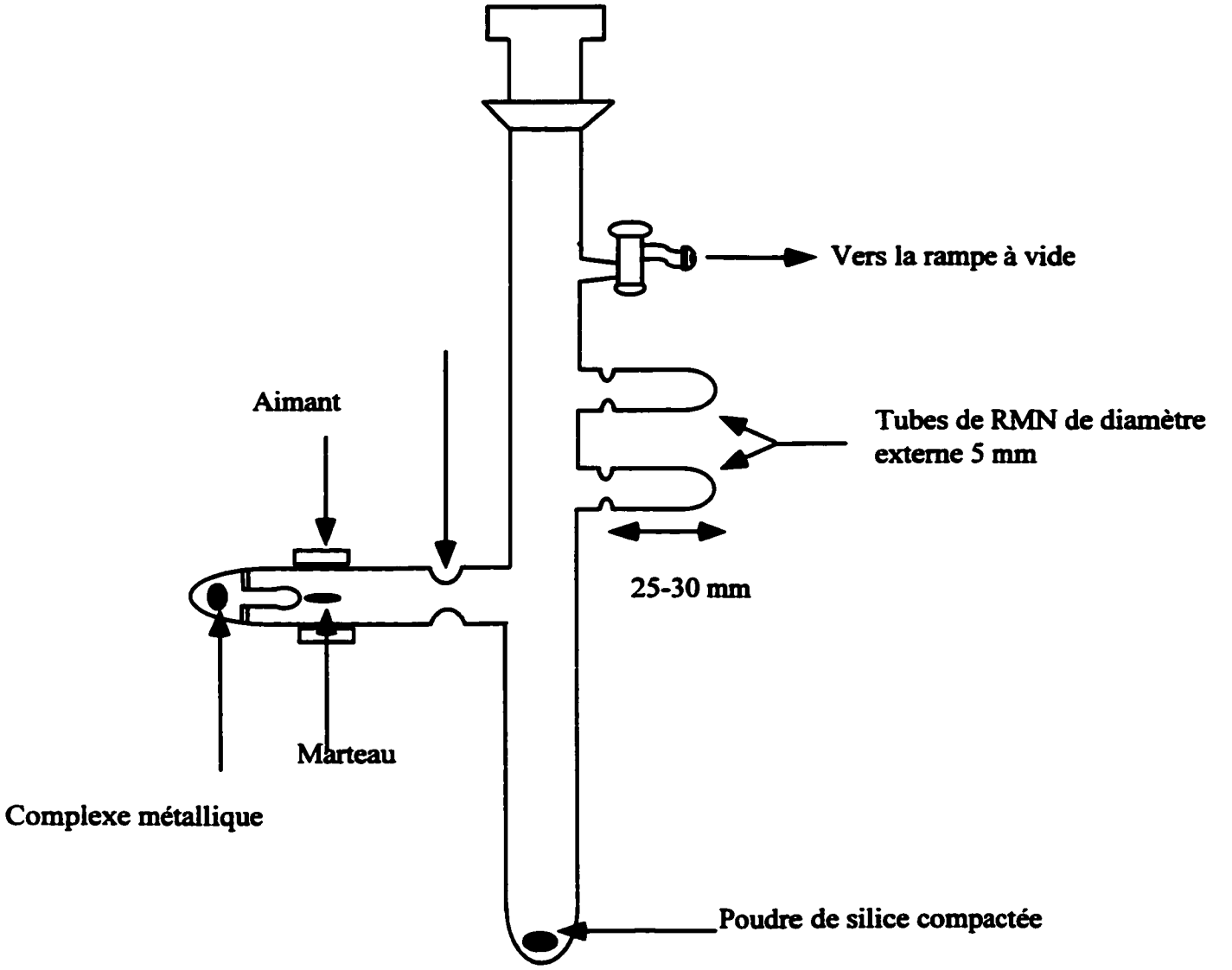

Figure 2.5. Schéma du réacteur RMN

2.4.4 Analyses élémentaires

À la fin de chaque expérience, la quantité de titane chimisorbée sur la silice est déterminée. Le titane est extrait quantitativement en agitant chaque échantillon de silice modifiée dans le H_2SO_4 3.6 M, afin d'obtenir des solutions contenant environ 0.5 mg Ti/mL. A ces solutions, on ajoute H_2O_2 (solution aqueuse à 30%, 0.03 mL/mL de solution de l'échantillon) pour former le complexe peroxo de titane de couleur jaune.[3,4] Les spectres UV-visible sont enregistrés dans des cuvettes en quartz, avec pour la référence une solution composée d'un mélange de H_2SO_4/H_2O_2. Les spectres sont enregistrés avec un spectrophotomètre Varian Cary 1E. L'absorbance à λ_{max} 408 nm est convertie en concentration de titane en utilisant une courbe d'étalonnage, Figure 2.6, obtenue à partir d'une solution standard de 1 g Ti/L (Aldrich) soumise aux mêmes conditions.

2.5 Identification et quantitation des produits volatils

2.5.1 Par spectroscopie infrarouge

Pour identifier les produits volatils de réaction, quand il s'agit d'un gaz unique libéré lors du greffage d'un complexe métallique sur la silice, on compare l'intensité du spectre infrarouge de la phase gaz avec celle d'une courbe d'étalonnage. Chaque courbe d'étalonnage est préparée en mesurant l'absorbance (soit l'intensité d'un pic choisi soit la surface intégrée d'une région spectrale) en fonction de la pression du produit pur.

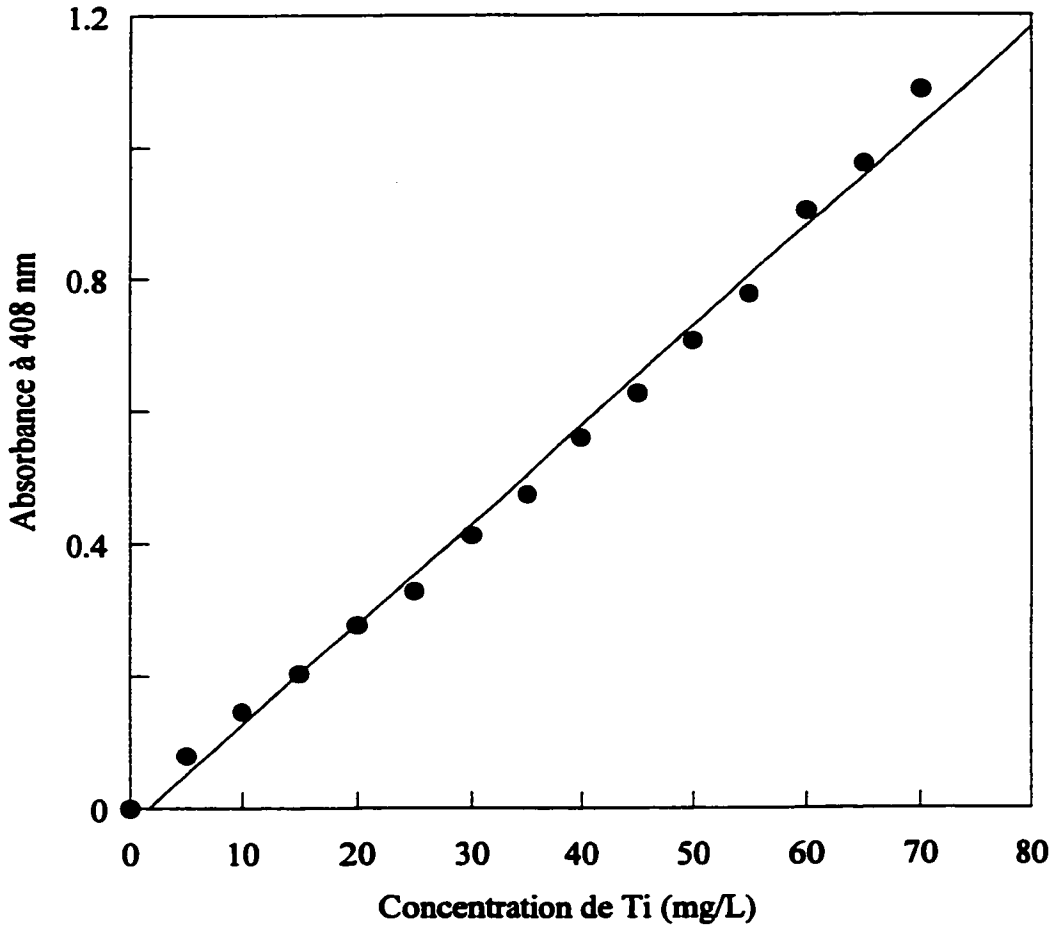

	Abs= a+ b [Ti]
a	-0.02 ± 0.01
b	0.0151± 0.0003
Chisq	0.0097447
R	0.997

Figure 2.6. Courbe d'étalonnage pour le titane

Bien sûr, cette méthode n'est utilisée que quand la phase gaz ne contient qu'un seul produit. Pour préparer la courbe d'étalonnage, le produit pur est transféré dans un réacteur en verre muni d'un robinet à haut vide. Ce réacteur est connecté à une cellule infrarouge vide à l'aide d'une jonction en «T» à laquelle est connectée directement un manomètre à capacitance avec une échelle soit de 10 soit de 1000 Torr selon l'intervalle de pression recherchée. Une pression de gaz connue est introduite dans la cellule infrarouge dont la distance entre les fenêtres IR est de 7 cm. Le spectre infrarouge est enregistré à une résolution de 2 cm^{-1}. Cette opération est répétée à plusieurs pressions dans la gamme des pressions obtenues pour les réactions. Des courbes d'étalonnage ont été préparées pour le ^{i}PrOH, ^{t}BuOH, $HNMe_2$, $HNEt_2$, et pour le CO_2, Figure 2.7-2.8.

2.5.2 Par GC/MS

Quand la phase gaz contient un mélange de produits, les gaz libérés sont analysés de préférence par GC/MS. L'instrument HP 5710A utilisant un gaz vecteur de He est équipé d'une colonne Porasil. Sur cette colonne et à température ambiante le 2-propanol et le propène ont des temps de rétention presque identiques, 2.0 et 1.9 minutes, respectivement. Il est donc impossible de les quantifier par intégration des pics. Par contre, le spectre de masse du 2-propanol contient un ion à m/z=45, alors qu'il est absent du spectre de propène. Il en est de même pour l'ion à m/z=41 dans le spectre de masse du propène. Il est donc possible de quantifier chacun de ces produits en déterminant l'abondance de ces deux ions. Des courbes d'étalonnage ont été préparées par injection des produits purs aux pressions partielles entre 1 et 10 Torr. Les équations 2.3 et 2.4

représentent l'abondance A des ions m/z= 41 et 45, respectivement, en fonction de la pression P du propène et du 2-propanol.

$$A= 1.214X10^{7} + (2.26X10^{6})P \quad (2.3)$$

$$A= -2.5751X10^{7} + (8.16X10^{6})P \quad (2.4)$$

Pour l'oxyde de cyclohexène et le cyclohexène, des courbes d'étalonnages ont été également préparées par injection du produit pur aux pressions partielles entre 1 et 10 Torr, Figure 2.9. Pour quantifier l'oxyde de cyclohexène et le cyclohexène, on a choisi l'ion à m/z=83 et 67.10, respectivement, dans leurs spectres de masse.

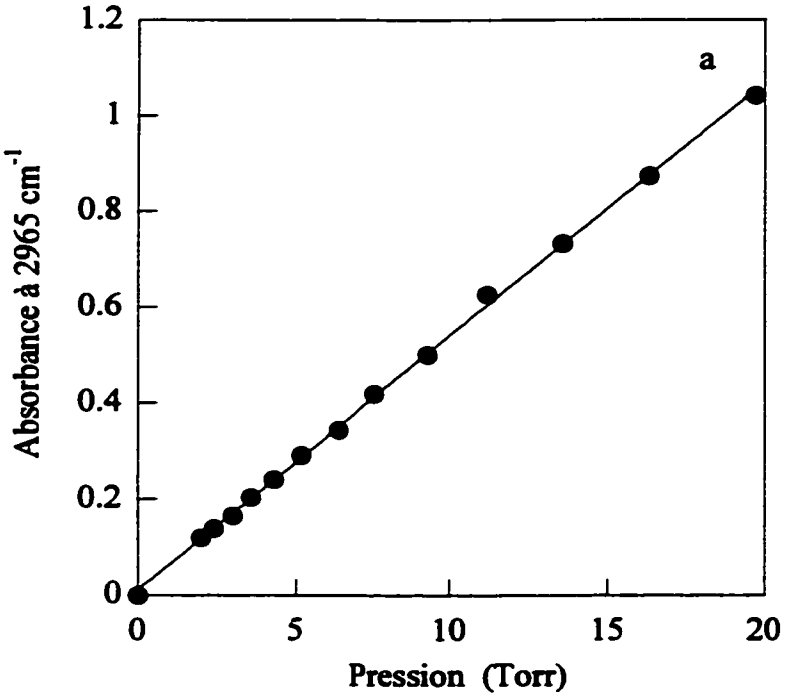

	Abs= a + bP
a	0.014 ± 0.004
b	0.0530± 0.0004
Chisq	0.00089978
R	0.997

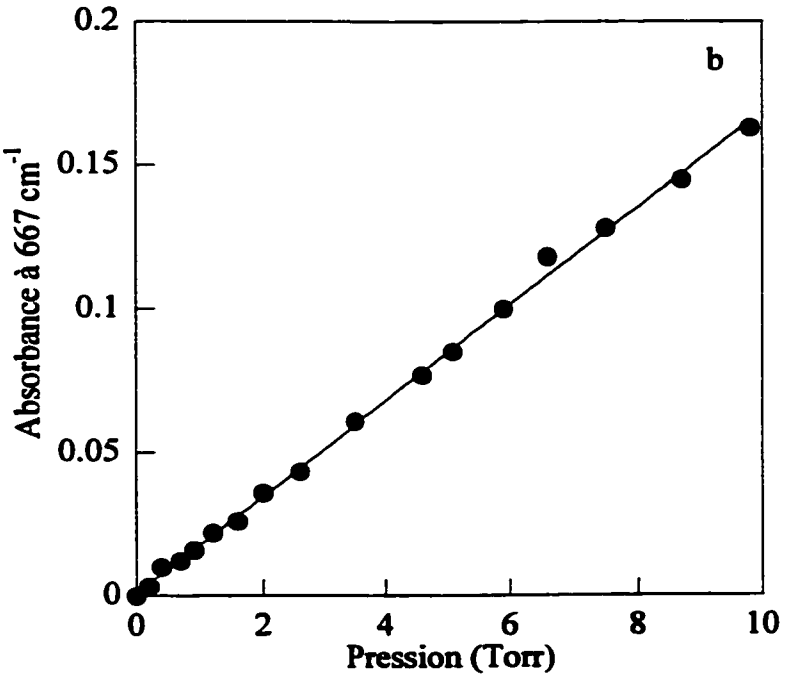

	Abs= a + bP
a	0.0010 ± 0.0008
b	0.0168± 0.0002
Chisq	0.000073333
R	0.992

Figures 2.7. Courbes d'étalonnage IR: a) du 2-propanol; b) du CO_2

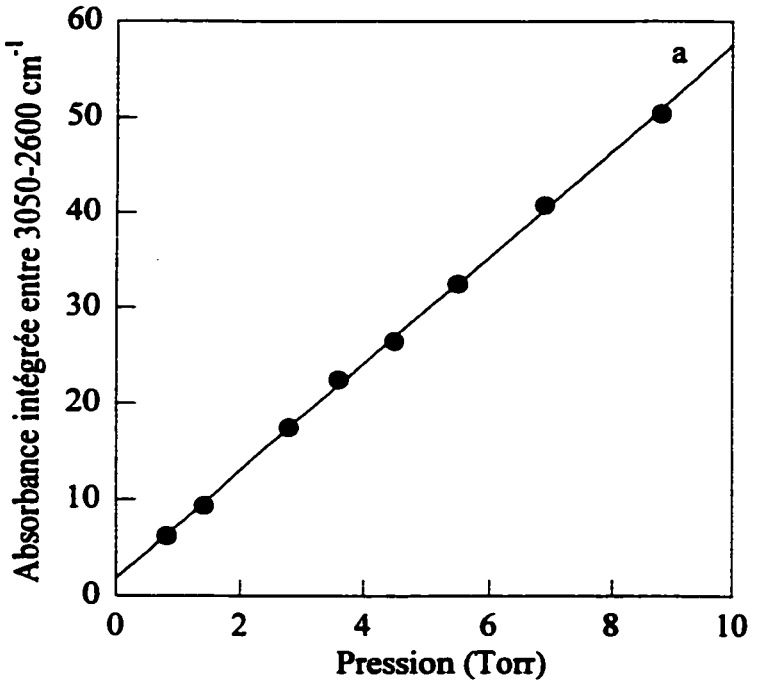

	Abs= a + bP
a	1.9± 0.3
b	5.57± 0.06
Chisq	1.0702
R	0.9967

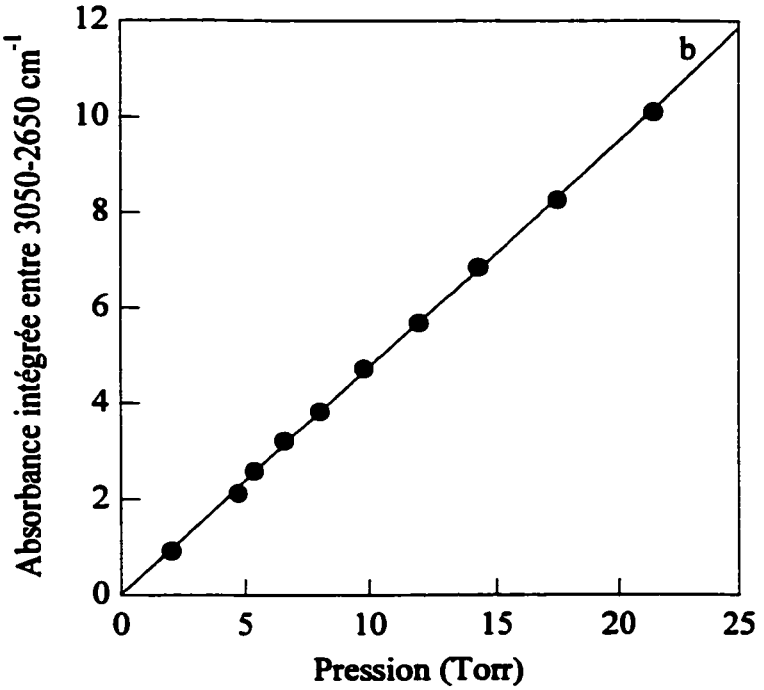

	Abs= a + bP
a	0.02 ± 0.04
b	0.474± 0.003
Chisq	0.032517
R	0.9998

Figures 2.8. Courbes d'étalonnage IR: a) du $HNEt_2$; b) du $HNMe_2$

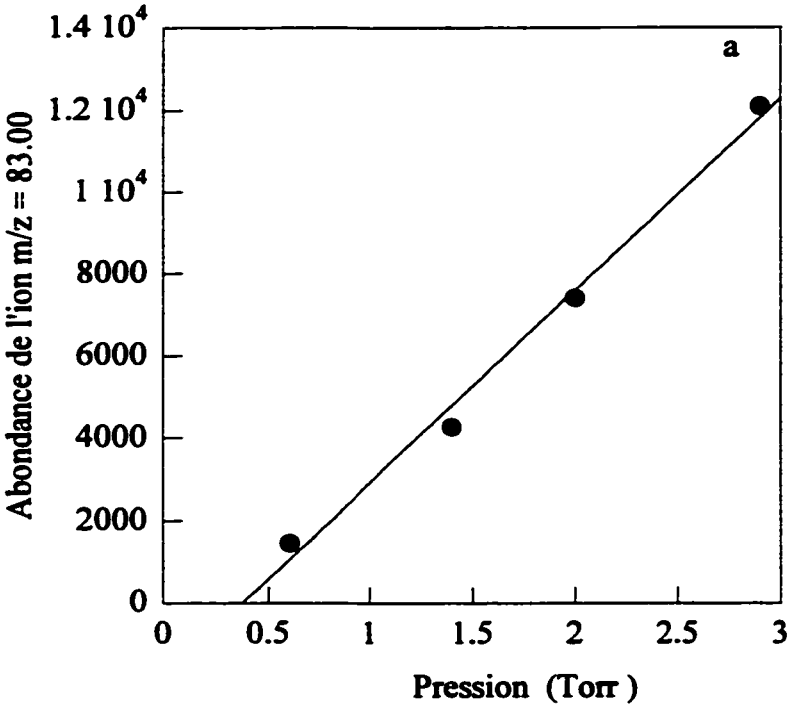

	Abs= a + bP
a	-1751± 600
b	4680± 313
Chisq	0.000055278
R	0.996

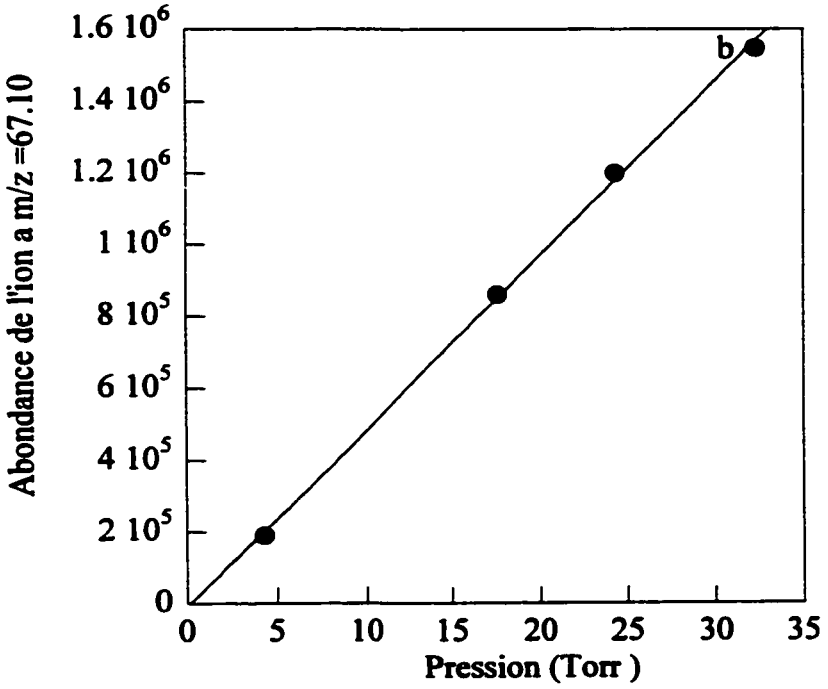

	Abs= a + bP
a	0.0010 ± 0.008
b	0.0168± 0.0002
Chisq	0.00007333
R	0.992

Figures 2.9. Courbes d'étalonnage GC/MS : a) du $C_6H_{10}O$; b) du C_6H_{12}

2.6 Références

(1) Heaney, P. J.; Prewitt, C. T.; Gibbs, G. V. *Silica: Physical Behavior, Geochemistry and Materials Applications*; Mineralogical Society of America: Washington, D. C 1994.

(2) Morrow, B. A.; Devi, A. *Can. J. Chem* **1970**, *48*, 2454-2456.

(3) Vogel, A. J. *A Textbook of Quantitative Inorganic Analysis*; Longman: London 1961.

(4) Haukka, S.; Saastamoinen, A. *Analyst* **1992**, *117*, 1381-1384

(5) G.L. Rice, Ph.D. Thesis, University of Ottawa, 1999.

Chapter 3

The Reaction of $Ti(O^iPr)_4$ with Silica

3.1 Introduction

Titanium catalysts supported on solid oxide substrates, especially siliceous ones, often show even higher activity than their homogeneous analogues in olefin epoxidation,[1,2] esterification[3] and transesterification,[4] hydroxylation of phenols,[5] oxyfunctionalization of alkanes,[6-8] Baeyer-Villiger oxidations,[9] and ammoximation of ketones.[10] The catalyst may contain Ti in the form of a Ti(IV) overlayer on the oxide support[11] or as Ti incorporated directly into the oxidic (*e.g.*, zeolitic) framework.[12] While the silica-supported catalyst is the most active for epoxidation and is used in a commercial process for propylene oxide,[13] it is highly water-sensitive. Zeolite-based catalysts such as TS-1[14] are hydrolytically stable but are less active, presumably due to restricted access of the substrate to the active site. Catalytic activity associated with low water sensitivity was recently reported for Ti grafted onto MCM-41[15] and other Ti-substituted mesoporous materials.[16,17]

Sol-gel processes for the preparation of Ti-Si mixed oxide catalysts are plagued by TiO_2 domain formation, which leads to undesirable side reactions such as peroxide disproportionation. An alternate method for preparing highly dispersed silica-supported Ti is the reaction of readily available volatile chloride and alkoxide compounds TiX_4 with surface hydroxyl groups to form chemisorbed species.

Ambient temperature grafting reactions in which an organometallic or coordination complex becomes anchored on an oxide surface are generally assumed to yield supported species of the same nuclearity as the molecular precursor complex. In some cases, the surface species have been extensively characterized and their nuclearity demonstrated. For example, the reaction of VOX_3 (where X is Cl or O^iPr) gives exclusively mononuclear $\equiv SiOVOX_2$ upon reaction with the surface hydroxyl groups of silica, regardless of the pretreatment temperature of the silica surface (and hence the density of the surface hydroxyl groups).[18] Previous studies[3,4,18-20] of the reactions of $Ti(OR)_4$ with silica have assumed the occurrence of simple grafting reactions which lead to mononuclear surface Ti complexes. Hydrolysis-condensation reactions in aqueous sol-gel processes, however, are notorious for generating polynuclear TiOTi species. Unlike for VOX_3 grafting reactions, multiple ligand substitutions of TiX_4 are usually considered likely. The grafting reactions are suggested to proceed by simple ligand displacement, yielding mononuclear surface species with liberation of HCl and/or ROH.[21-23] The following reactions have been proposed:

$$\equiv SiOH + TiX_4 \rightarrow (\equiv SiO)TiX_3 + HX \qquad (3.1)$$

$$2 \equiv SiOH + TiX_4 \rightarrow (\equiv SiO)_2TiX_2 + 2\,HX \qquad (3.2)$$

At a loading of $Ti(O^iPr)_4$ on silica roughly corresponding to the number of surface hydroxyl groups, monolayer coverage and molecular dispersion is assumed.[24] However, UV-vis[24] and EXAFS[19] analyses of the surface complexes are not fully consistent with the reactions shown in eqs 3.1-3.2. Mixed ligand precursors such as $(CH_3)Ti(O^iPr)_3$ and

$(N_3)_2Ti(O^iPr)_2$ have also been used,[3] as well as TiF_4[25] and $Ti(CH_2{}^tBu)_4$.[26] The kind of surface Ti complex obtained depends critically on the precursor used, and this has important implications for reactivity,[19] although the origins of such effects are not clear since the products of such grafting reactions, after calcination, are always presumed to be isolated pseudotetrahedral sites.

Proposals for the mechanisms of catalysis by supported Ti abound,[5,27-29] but in the absence of accurate knowledge about the structure of the active site(s), hypotheses are difficult to test. The activity of Ti-substituted zeolites for epoxidation is correlated with Ti dispersion.[30] This finding has been widely interpreted as evidence for tetrahedral site-isolated active site precursors, such as $(\equiv SiO)_4Ti$.[5] Similarly, the greater esterification activity of the surface complex assumed to be "$\equiv SiOTi(O^iPr)_3$" compared to homogeneous $Ti(O^iPr)_4$ was attributed to the inability of the former to dimerize due to its immobility.[3] TiOTi connectivity is believed to be detrimental to catalytic activity and selectivity. In this context, it is interesting to note that the active species in the extensively studied Sharpless homogeneous catalytic epoxidation process is a dinuclear oxygen-bridged Ti tartrate complex, which is much more active than the mononuclear complex.[31] Therefore, we decided to investigate the nuclearity of the active species in supported Ti catalysts, particularly in view of the much sought-after goal of extending the reactivity of supported metal complexes to heterogeneous enantioselective catalysis.

In this Chapter, we report the preparation and characterization of silica-supported titanium(IV) coordination complexes derived from $Ti(O^iPr)_4$.

3.2 Stoichiometry of the reaction of $Ti(O^iPr)_4$ with silica

When $Ti(O^iPr)_4$ vapor reacts with silica at room temperature in a closed reactor with an initial pressure of 10^{-4} Torr, an irreversible chemisorption takes place over a period of 1 h. In an *in situ* IR experiment, the initially transparent silica disk became opaque, and volatile organic products were liberated into the gas phase. This experiment was performed using silicas which had been partially dehydroxylated at two different temperatures. Silica-200, treated at 200 °C, contains (0.86± 0.02) mmol of OH/g, while silica-500 contains (0.40± 0.02) mmol of OH/g.[18] After approximately 1 hr of desorption of unreacted $Ti(O^iPr)_4$ to a liquid N_2 trap, the chemisorbed Ti was extracted and measured to be (3.91 ± 0.04) and (3.87 ± 0.03) wt % on silica-200 and -500, respectively. These values are reproducible, Table 3.1. However, the similarity of these results was unexpected, given that the number of surface groups on silica-200 is slightly more than double that on the same quantity of silica-500. The amount of chemisorbed Ti corresponds to 1.0 Ti/≡SiOH on silica-200 and 2.0 Ti/≡SiOH on silica-500, where ≡SiOH represents a surface hydroxyl group. In both cases, the surface coverage is 2.5 Ti/nm^2.

Volatile products were identified by GC and GC/MS as a mixture of 2-propanol and propene on each type of silica. A blank experiment showed that 2-propanol is not chemisorbed on the surface hydroxyl groups of silica at room temperature, nor is it dehydrated to propene in the presence of silica under these conditions. Absolute quantities measured by Dr. G. L. Rice, are shown in Table 3.2.

Table 3.1. Titanium content of materials prepared by chemisorption of $Ti(O^iPr)_4$ on silica at saturation coverage

silica support[a]	wt. % Ti	mmol Ti[b]	Ti/≡SiOH[c]
silica-200	3.92	0.84	0.98
	3.94	0.85	0.99
	3.86	0.82	0.95
average	3.91 ± 0.04	0.84 ± 0.02	0.97 ± 0.02
silica-500	3.90	0.81	2.02
	3.84	0.80	2.00
	3.86	0.79	1.98
average	3.87 ± 0.03	0.80 ± 0.01	2.00 ± 0.02

[a] The appended numbers refer to the temperature, in °C, at which the silica was partially dehydroxylated prior to the chemisorption reaction.

[b] Normalized per gram of solid.

[c] Calculated based on the number of surface hydroxyl groups on silica pretreated *in vacuo* at each temperature: 0.40 mmol/g (500°C) and 0.86 mmol/g (200°C).[18]

Table 3.2. Quantification of ligand-derived volatiles during grafting of $Ti(O^iPr)_4$ on modified and unmodified silicas

grafting reaction	wt. % Ti	mmol Ti[a]	mmol ^iPrOH[a]	mmol C_3H_6[a]	^iPrOH/Ti	C_3H_6/Ti
silica-500 + $Ti(O^iPr)_4$	3.87	0.81	0.86	0.38	1.06	0.47
	3.14	0.65	0.68	0.31	1.04	0.48
	2.28	0.48	0.51	0.23	1.07	0.47
silica-200 + $Ti(O^iPr)_4$	2.62	0.55	0.83	0.27	1.51	0.49

[a] Normalized per gram of solid.

The 2-propanol and propene are liberated in reproducible and stoichiometric amounts, Table 3.2, regardless of Ti loading in the range 2.28-3.87 wt % (where the highest value corresponds to maximum Ti loading). Less than maximum loading of Ti is achieved by terminating the grafting reaction before all of the surface hydroxyls have reacted.

Thus, regardless of the extent of reaction of the surface hydroxyls, grafting of $Ti(O^iPr)_4$ occurs with the stoichiometry shown in eqs 3.3-3.4 for silica-200 and silica-500, respectively. Calcination of **1** and **2** in 300 Torr O_2 at 750 °C completely removes the surface hydrocarbon fragments. The amount of CO_2 liberated corresponds to 6.1 and 7.6 CO_2/Ti, respectively (Table 3.3), confirming the empirical formulae of **1** and **2**.

$$2\,{\equiv}SiOH + 2\,Ti(O^iPr)_4 \rightarrow [({\equiv}SiO)Ti(O^iPr)_2]_2O + 3\,{}^iPrOH + C_3H_6 \qquad (3.3)$$

(silica-200) **1**

$${\equiv}SiOH + 2\,Ti(O^iPr)_4 \rightarrow ({\equiv}SiO)Ti_2(O^iPr)_5(O) + 2\,{}^iPrOH + C_3H_6 \qquad (3.4)$$

(silica-500) **2**

3.3 Spectroscopic characterization

3.3.1 Solid state NMR

The solid-state ^{13}C CP/MAS spectra of both chemisorbed surface complexes derived from $Ti(O^iPr)_4$ consist of two resonances at 25 and 78 ppm, Figure 3.1, similar to a reported spectrum.[3] These signals are assigned to the methyl and methine carbons of chemisorbed isopropyl groups, and agrees with the $^{13}C\{^1H\}$ spectrum of $Ti(O^iPr)_4$ in $CDCl_3$ with two peaks at 26.10 and 75.16 ppm.

Table 3.3. Quantification of carbon content of supported Ti complexes by calcination

surface complex	wt. % Ti	mmol Ti[a]	mmol CO_2[a]	CO_2/Ti observed	CO_2/Ti expected
$[(\equiv SiO)Ti(O^iPr)_2]_2O$, **1**	3.92	0.82	5.00	6.1	6.0
$(\equiv SiO)Ti_2(O^iPr)_5(O)$, **2**	3.86	0.80	6.10	7.6	7.5

[a] Normalized per gram of solid.

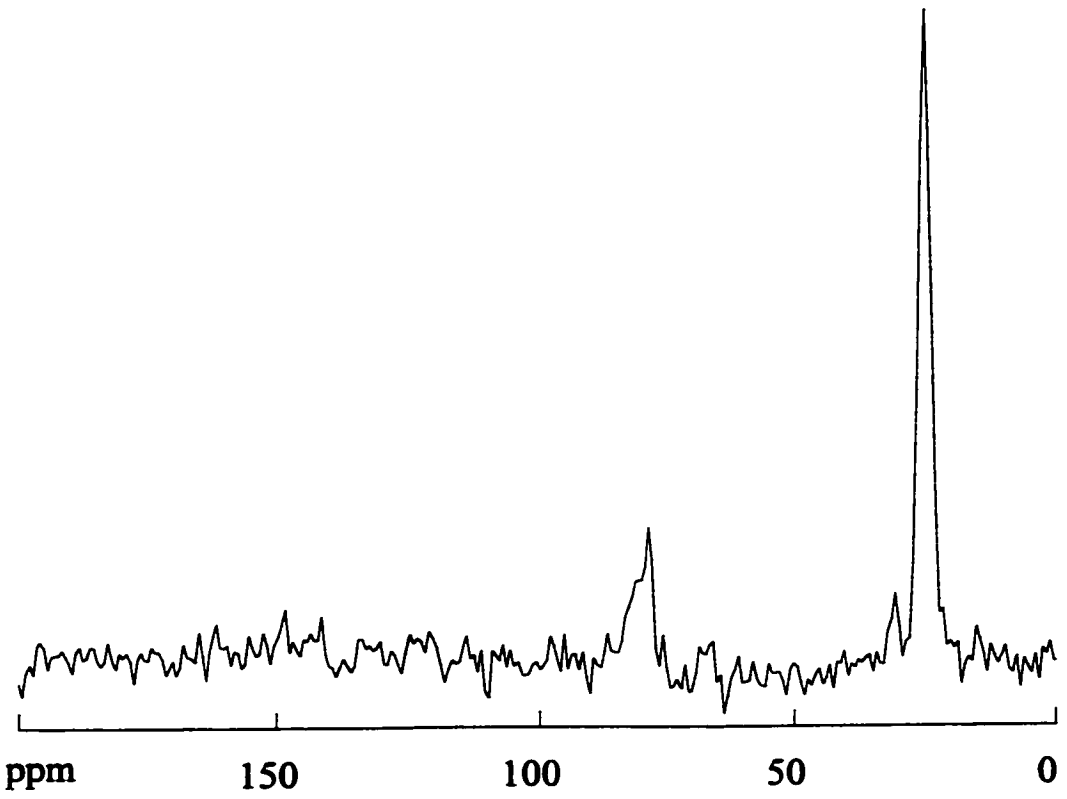

Figure 3.1. ^{13}C CP/MAS spectrum of silica-500 treated with $Ti(O^iPr)_4$ to give **2**, followed by desorption of unreacted starting material and evacuation of volatile products. Spin rate, 4 kHz.

3.3.2 Vibrational spectroscopy

In situ infrared spectroscopy confirms that the intense ν(SiO-H) mode of silica at 3747 cm^{-1} disappears from each type of silica during the grafting reaction, from which we infer the complete reaction of the surface hydroxyl groups. At the same time, new bands appear in the C-H stretching (2959, 2945, 2872, 2628 cm^{-1}) and deformation (1465, 1452, 1380, 1367, 1332 cm^{-1}) regions, assigned to 2-propoxide ligand vibrations, Figure 3.2a.[32,33] The low-frequency vibrations on each type of silica include bands at 1005 (ν(C-O)), 630 (ν(Ti-OC)),[32-34] 951, 857, 747 and 690 cm^{-1}, Figure 3.2b. The spectra of the supported Ti complexes on silica-200 and silica-500 are qualitatively very similar, although the ligand vibrations on silica-500 are slightly more intense.

The assignment of the IR band at 951 cm^{-1} is of particular interest, since the intensity of a band in this region often correlates with catalytic activity. Oxide-supported Ti complexes, including TS-1, have an intense band at ca. 960 cm^{-1} which has been attributed by various authors to ν(Ti=O),[6] ν_{as}(SiOTi),[35,36] the localized ν(SiO) of an SiOTi unit,[37] ν(SiO) of defect sites,[38] and ν(Si-OH) associated with Ti sites.[39] In **1** and **2**, the band at 957 cm^{-1} is unlikely to be due to the latter, since it is present even in the complete absence of unreacted silanol groups. Reaction of $Ti(O^iPr)_4$ with a silica in which the surface hydroxyl groups were labeled with ^{18}O (ca. 80% enrichment) was undertaken. The resulting spectrum contained the same band, essentially unshifted from the spectrum of Ti-modified unlabeled silica. However, an intense band at 964 cm^{-1} is also present in the IR spectrum of $Ti(O^iPr)_4$.[32,34] We therefore assign the vibration in the spectra of **1** and **2** to a skeletal vibration of the 2-propyl groups.[40]

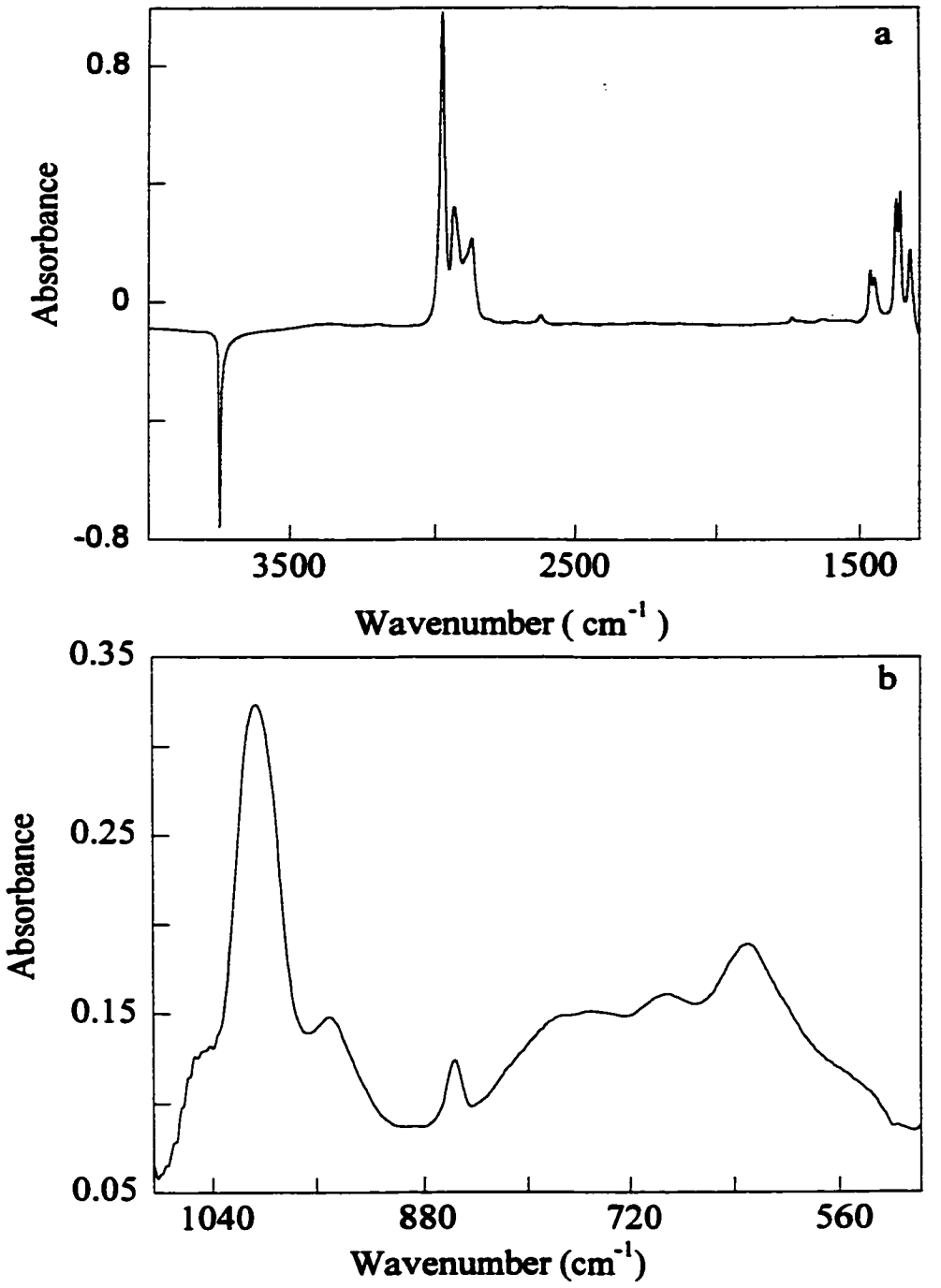

Figure 3.2. *In situ* IR difference spectrum of a self-supporting disk of silica-500 treated with $Ti(O^iPr)_4$ to give **2**, followed by desorption of unreacted starting material and evacuation of volatile products, in two frequency regions of partial transparency of the silica disk. The reference spectrum of silica-500 has been subtracted such that negative peaks correspond to vibrations which are no longer present on the silica surface after reaction.

3.3.3 UV-visible spectroscopy

The diffuse reflectance UV-visible spectrum of silica-200 modified with $Ti(O^iPr)_4$ consists of a peak at 254 nm, Figure 3.3a., compared to the solution spectrum of mononuclear $Ti(O^iPr)_4$, in cyclohexane with a maximum at 238 nm, Figure 3.3b. A red shift therefore occurs upon grafting $Ti(O^iPr)_4$ on silica. However, the absence of absorption above 350 nm indicates there is no anatase present in our samples.

3.4 Discussion

Our findings demonstrate that gas-solid reactions of $Ti(O^iPr)_4$ with silica, even with strict exclusion of water to preclude hydrolysis, are not as simple as previously supposed. The number of grafted Ti centers after complete reaction of the hydroxyl groups exceeds, on silica-500, the original number of surface hydroxyl groups by a factor of 2 (0.80 mmol of Ti/g present on silica which originally contained 0.40 mmol of OH/g), Table 3.1. To our knowledge, this is the first evidence for a single-step grafting procedure in which the number of chemisorbed molecular complexes exceeds the number of grafting sites. In the more usual case, after complete reaction of the surface silanols, excess metal complex is weakly physisorbed and is readily removed by evacuation or washing with solvent.

The possibility of grafting $Ti(O^iPr)_4$ on siloxane sites, ≡SiOSi≡, rather than silanols, is excluded by the low ratio of chemisorbed isopropyl groups per grafted Ti (observed: 2.5 ^iPr/Ti on silica-500). In the hypothetical siloxane reaction, all four

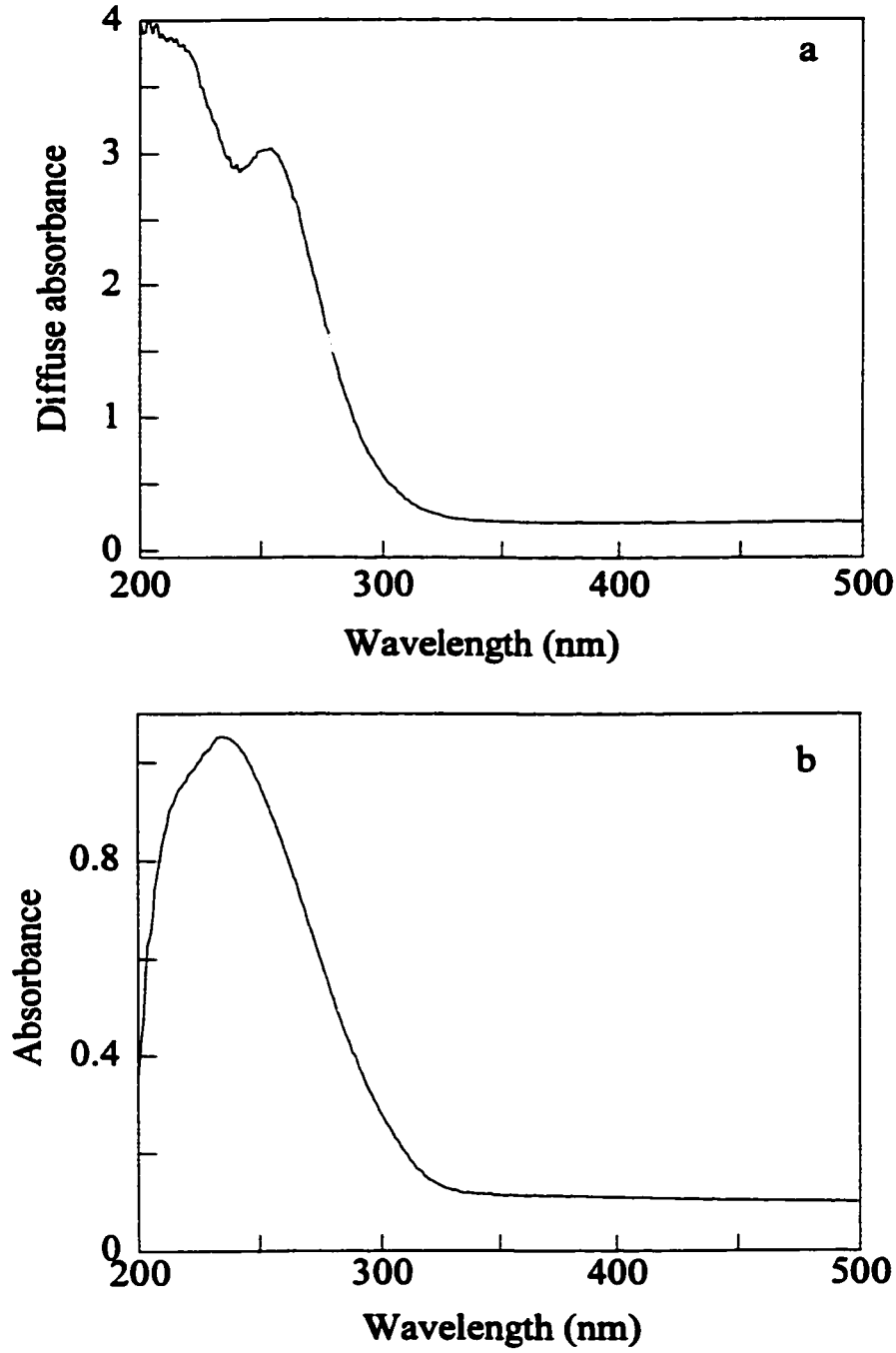

Figure 3.3. UV-visible spectra of (a) silica-200 modified with $Ti(O^iPr)_4$, recorded in diffuse reflectance mode, and (b) $Ti(O^iPr)_4$ in cyclohexane, recorded in transmission mode.

isopropyl groups would be retained on the surface, as in ≡SiOSi≡ + $Ti(O^iPr)_4$ → ≡$SiOTi(O^iPr)_3$ + ≡SiO^iPr.

On silica-200, 0.84 mmol of Ti/g is grafted on the silica surface which originally contained 0.86 mmol of OH/g. This stoichiometry has been interpreted[24] as evidence for a 1:1 reaction with surface hydroxyls, eq 3.5:

$$\equiv SiOH + Ti(O^iPr)_4 \rightarrow (\equiv SiO)Ti(O^iPr)_3 + {}^iPrOH \qquad (3.5)$$

Such a reaction would generate isolated Ti surface complexes and ^iPrOH, formed exclusively by protonolysis of the 2-propoxide ligands by surface silanols. However, the average number of 2-propoxide ligands present on the surface, as measured by their total combustion to CO_2, is 2.0/Ti, which is not consistent with eq 3.5. In addition, the gaseous products contain unanticipated propene as well as the expected 2-propanol. Therefore, we conclude that, on both silica-200 and -500 surfaces, the grafting reaction is more complex than a simple ligand-exchange reaction on Ti.

Exchange between coordinated ligands and free alcohol is known to be facile in Ti alkoxide and mixed halide-alkoxide systems.[41] In the first step of grafting, we propose that an exchange occurs between the alkoxide ligands and the "silanols", eq 3.6, analogous to reactions suggested for $VO(O^iPr)_3$[18] and $Zr(O^tBu)_4$[42] with silica surfaces.

$$n \equiv SiOH + Ti(O^iPr)_4 \rightarrow (\equiv SiO)_nTi(O^iPr)_{4-n} + n\ {}^iPrOH \qquad (3.6)$$

The propensity of Ti to coordinate additional ligands increases as bulky electron-donating alkoxide ligands are progressively substituted by electron-withdrawing ligands.[43] Substitution of an alkoxide ligand by a siloxide ligand derived from the silica surface will cause the Lewis acidity of Ti to increase due to the strongly electron-withdrawing character of the "siloxide" ligand.[18] The initially formed mononuclear chemisorbed complexes are therefore stronger Lewis acids than $Ti(O^iPr)_4$. The next step in the mechanism of direct grafting of $Ti(O^iPr)_4$ is therefore suggested to be coordination of additional $Ti(O^iPr)_4$, eq 3.7:[44]

$$(\equiv SiO)_nTi(O^iPr)_{4-n} + Ti(O^iPr)_4 \rightarrow \{(\equiv SiO)_nTi_2(O^iPr)_{8-n}\} \qquad (3.7)$$

Ia (n=2)

Ib (n=1)

The structures of the intermediate dinuclear alkoxo-siloxo complexes **I** may resemble structurally characterized bimetallic molecular complexes, such as dimeric $[TiCl_2(OEt)_2]_2$, in which Ti achieves five-coordination through formation of two alkoxide bridges.[45] If sterically allowed, participation of surface oxygens in **I** may augment the Ti coordination number and even generate six-coordinate, edge-sharing octahedra linked via pairs of bridging alkoxides.[46,47] In solution chemistry, oxygen-containing donors/solvents such as THF and Et_2O are known to coordinate to mixed chloride-alkoxide complexes of Ti when there are not enough free ligands available to complete the coordination sphere of Ti.[48]

The proposed intermediates **Ia** and **Ib** must undergo loss of coordinated 2-propoxide ligands in order to generate the stable surface complexes **1** and **2**. Metal alkoxides, including those of Ti,[49] undergo non-hydrolytic condensations to give polynuclear species containing μ-oxo bridges via elimination of dialkylethers[50,51] or equal amounts of alcohol/alkene,[52] eq 3.8:

$$2\ M(OR)_n \rightarrow (RO)_{n-1}M\text{-}O\text{-}M(OR)_{n-1} + R_2O \text{ or } (ROH + R(-H)) \qquad (3.8)$$

The silica surface may promote the formation of μ-oxo bridges in supported metal alkoxide complexes. A similar non-hydrolytic condensation was recently inferred in the reaction of silica-supported ≡SiOVO(O^iPr)$_2$ with Ti(O^iPr)$_4$.[53] In addition, we note that the condensation step (eq 3.8) must be fast relative to the initial grafting step (eq 3.6) in order to generate the same ratio of 2-propanol to propene even when the grafting reaction is not allowed to proceed to completion (*i.e.*, even when the surface loading of Ti is less than the maximum loading, as in the second and third entries in Table 3.2).

Although many molecular metal oxoalkoxide complexes are known,[54] there appears to be a strong tendency to isolate more stable, higher nuclearity clusters. Only one structurally characterized oxoalkoxide complex containing just two metal nuclei is known: $Ta_2O(O^iPr)_8(^iPrOH)$.[55] This complex consists of pairs of edge-sharing octahedra joined by one oxo and one 2-propoxo bridge. The surface complexes **1** and **2** may possess a similar oxo/alkoxo-bridged structural unit. We do not know whether the coordination number of Ti is as high as 6 (which would require additional coordination of surface siloxane oxygens). Nor does the solid-state ^{13}C CP/MAS NMR spectrum (Figure

3.1) reveal whether bridging as well as terminal 2-propoxide ligands are present, since only one OCH signal was detected at 78 ppm. This chemical shift is consistent with terminal 2-propoxide ligands as in monomeric[39] $Ti(O^iPr)_4$. Although a bridging 2-propoxide methine signal is expected to have a different chemical shift,[46] fluxionality and/or the breadth of the solid-state signal may have precluded its detection in our study.

3.5 Conclusion

Two silica-supported Ti alkoxides have been synthesized and characterized via the direct reaction of $Ti(O^iPr)_4$ with silica. In both cases, only dinuclear surface complexes were obtained, in which pairs of Ti(IV) atoms are linked via an oxo bridge.

3.6 References

(1) Cativiela, C.; Fraile, J. M.; García, J. I.; Mayoral, J. A. *J. Mol. Catal. A: Chem.* **1996**, *112*, 259-267.

(2) Hutchings, G. J.; Lee, D. F.; Minihan, A. R. *Catal. Lett.* **1996**, *39*, 83-90.

(3) Blandy, C.; Pellegatta, J.-L.; Choukroun, R.; Gilot, B.; Guiraud, R. *Can. J. Chem.* **1993**, *71*, 34-37.

(4) Blandy, C.; Pellegata, J.-L.; Cassoux, P. *Catal. Lett.* **1997**, *43*, 139-142.

(5) Notari, B. *Stud. Surf. Sci. Catal.* **1988**, *37*, 413-425.

(6) Huybrechts, D. R. C.; Valsen, I.; Li, H. X.; Jacobs, P. A. *Catal. Lett.* **1991**, *8*, 237.

(7) Tatsumi, T.; Nakamura, M.; Negeshi, S.; Tominaga, H. *J. Chem. Soc., Chem. Commun.* **1990**, 476.

(8) Clerici, M. G. *Appl. Catal.* **1991**, *68*, 249.

(9) Bhaumik, A.; Kumar, P.; Kumar, R. *Catal. Lett.* **1996**, *40*, 47-50.

(10) Roffia, P.; Padovan, M.; Alberti, G. U.S. Patent 4,745,221 (1988).

(11) Sheldon, R. A.; Dakka, J. *Catal. Today* **1994**, *19*, 215-246.

(12) Murugavel, R.; Roesky, H. W. *Angew. Chem., Int. Ed. Engl.* **1997**, *36*, 477-479.

(13) Wulff, H. GB. Patent 1,249,79,(1971).

(14) Taramasso, M.; Perego, G.; Notari, B. .U.S. Patent 4,410,501, (1983).

(15) Maschmayer, T.; Rey, F.; Sankar, G.; Thomas, J. M. *Nature* **1995**, *378*, 159-162.

(16) Corma, A.; Camblor, M. A.; Esteve, P.; Martinez, A.; Pérez-Pariente, J. *J. Catal.* **1994**, *145*, 151-158.

(17) Hutter, R.; Dutoit, D. C. M.; Mallat, T.; Schneider, M.; Baiker, A. *J. Chem. Soc., Chem. Commun.* **1995**, 163-164.

(18) Rice, G. L.; Scott, S. L. *Langmuir* **1997**, *13*, 1545-1551.

(19) Fraile, J. M.; García, J.; Mayoral, J. A.; Proietti, M. G.; Sánchez, M. C. *J. Phys. Chem.* **1996**, *100*, 19484-19488.

(20) Fraile, J. M.; García, J. I.; Mayoral, J. A.; de Ménorval, L. C.; Rachdi, F. *J. Chem. Soc., Chem. Commun.* **1995**, 539-540.

(21) Morrow, B. A.; Tripp, C. P.; McFarlane, R. A. *J. Chem. Soc., Chem. Commun.* **1984**, 1282-1283.

(22) Damyanov, D.; Velikova, M.; Ivanov, I.; Vlaev, L. *J. Non-Cryst. Solids* **1988**, *105*, 107-113.

(23) Haukka, S.; Lakomaa, E.-L.; Root, A. *J. Phys. Chem.* **1993**, *97*, 5085-5094.

(24) Gao, X.; Bare, S. R.; Fierro, J. L. G.; Banares, M. A.; Wachs, I. E. *J. Phys. Chem. B* **1998**, *102*, 5653-5666.

(25) Jorda, E.; Tuel, A.; Teissier, R.; Kervennal, J. *J. Chem. Soc., Chem. Commun.* **1995**, 1775.

(26) Holmes, S. A.; Quignard, F.; Choplin, A.; Teissier, R.; Kervennal, J. *J. Catal.* **1998**, *176*, 173-181.

(27) Huybrechts, D. R. C.; De Bruycker, L ; Jacobs, P. A. *Nature* **1990**, *345*, 240-242.

(28) Tatsumi, T.; Nakamura, M.; Tominaga, H. *Catal. Soc. Japan* **1991**, *33*, 444.

(29) Bellusi, G.; Carati, A.; Clerici, M. G.; Maddinelli, G.; Millini, R. *J. Catal.* **1992**, *133*, 220-230.

(30) Klein, S.; Thorimbert, S.; Maier, W. F. *J. Catal.* **1996**, *163*, 476-488.

(31) Woodard, S. S.; Finn, M. G.; Sharpless, K. B. *J. Am. Chem. Soc.* **1991**, *113*, 106-113.

(32) Barraclough, C. G.; Bradley, D. C.; Lewis, J.; Thomas, I. M. *J. Chem. Soc.* **1961**, 2601-2605.

(33) Hampden-Smith, M. J.; Williams, D. S.; Rheingold, A. L. *Inorg. Chem.* **1990**, *29*, 4076-4081.

(34) Kriegsmann, H.; Licht, K. *Zeit. Elektrochem.* **1958**, *62*, 1163-1174.

(35) Boccuti, M. R.; Rao, K. M.; Zecchina, A.; Leofanti, G.; Petrini, G. *Stud. Surf. Sci. Catal.* **1989**, *48*, 133.

(36) Bellusi, G.; Fattore, F. In *Zeolite Chemistry and Catalysis*; Jacobs, P. A., Jaeger, N. I., Kubelkova, L., Wichterlova, B., Eds., 1991; Vol. 69, p 79.

(37) Smirnov, K. S.; van de Graaf, B. *Micropor. Mater.* **1996**, 7, 133-138.

(38) Camblor, M. A.; Corma, A.; Pérez-Pariente, J. *J. Chem. Soc., Chem. Commun.* **1993**, 557-559.

(39) Holloway, C. E. *J. Chem. Soc., Dalton Trans.* **1976**, 1050-1054.

(40) Sheppard, N.; Simpson, D. M. *Quart. Rev. Chem. Soc.* **1953**, *7*, 19-55.

(41) Weingarten, H.; Wazer, J. R. V. *J. Am. Chem. Soc.* **1965**, *87*, 724-730.

(42) Miller, J. B.; Schwartz, J.; Bernasek, S. L. *J. Am. Chem. Soc.* **1993**, *115*, 8239-8347.

(43) Clark, R. J. In *Comprehensive Inorganic Chemistry*; Trotman-Dickson, A. F., Ed.; Compendium: Elmsford, New York, 1973; Vol. 3, p 386.

(44) Bradley, D. C.; Mehrotra, R. C.; Gaur, D. P. *Metal Alkoxides*; Academic Press: New York, 1978.

(45) Haase, W.; Hoppe, H. *Acta Cryst.* **1968**, *B24*, 281-282.

(46) Winter, C. H.; Sheridan, P. H.; Heeg, M. J. *Inorg. Chem.* **1991**, *30*, 1962-1964.

(47) Wu, Y.-T.; Y.-C., H.; Lin, C.-C.; Gau, H.-M. *Inorg. Chem.* **1996**, *35*, 5948-5952.

(48) Gau, H.-M.; Lee, C.-S.; Lin, C.-C.; Jiang, M.-K.; Ho, Y.-C.; Kuo, C.-N. *J. Am. Chem. Soc.* **1996**, *118*, 2936-2941.

(49) Schmid, R.; Mosset, A.; Galy, J. *J. Chem. Soc., Dalton Trans.* **1991**, 1999.

(50) Bradley, D. C.; Chakravarti, B. N.; Chatterjee, A. K. *J. Chem. Soc.* **1958**, 99.

(51) Turova, N. Y.; Kessler, V. G.; Kucheiko, S. I. *Polyhedron* **1991**, *10*, 2617-2628.

(52) Andrianainarivelo, M.; Corriu, R. J. P.; Leclercq, D.; Mutin, P. H.; Vioux, A. *Chem. Mater.* **1997**, *9*, 1098-1102.

(53) Rice, G. L.; Scott, S. L. *Chem. Mater.* **1998**, *10*, 620-625.

(54) Turova, N. Y.; Turevskaya, E. P.; Yanovskaya, M. I.; Yanovsky, A. I.; Kessler, V. G.; Tcheboukov, D. E. *Polyhedron* **1998**, *17*, 899-915.

(55) Turova, N. Y.; Korolev, A. V.; Tchebukov, D. E.; Belokon, A. I.; Yanovsky, A. I.; Struchkov, Y. T. *Polyhedron* **1996**, *15*, 3869-3880.

Chapter 4

The Reaction of $Ti(NEt_2)_4$ with Silica

4.1 Introduction

As a result of our observation that mononuclear silica-supported Ti complexes are not generated via the reaction of $Ti(O^iPr)_4$ with surface silanols, and because of the very widely-held belief in their importance in olefin oxidation, an alternate synthetic strategy was devised. The ligands of $Ti(NR_2)_4$ are susceptible to protonolysis, but the bulkiness of the dialkylamido ligands effectively impedes oligomerization. Furthermore, the non-hydrolytic alkoxide condensation reaction which leads to Ti-O-Ti is avoided by the use of amido complexes. Therefore an investigation of the reaction of $Ti(NEt_2)_4$ with silica was undertaken.

4.2 Stoichiometry of the reaction of $Ti(NEt_2)_4$ with silica

The gas-solid reactions of yellow $Ti(NEt_2)_4$ with silica-200 or -500 at room-temperature proceed with a color change of the solids from colorless to yellow. After 1 hr of reaction, $HNEt_2$ is the exclusive gas-phase product detected by IR spectroscopy and GC. On silica-200, the amount of chemisorbed titanium after complete reaction of the surface hydroxyl groups with $Ti(NEt_2)_4$ is (2.0 ± 0.1) wt %, which corresponds to 1.3 Ti/nm^2, or 0.47 Ti/≡SiOH, Table 4.1. Furthemore, (1.9 ± 0.1) equiv of $HNEt_2$ is liberated per chemisorbed Ti, consistent with the stoichiometry shown in eq 4.1:

Table 4.1 Mass balance for materials prepared by the room temperature chemisorption of $Ti(NEt_2)_4$ on silica

silica support[a]	wt. % Ti	mmol Ti[b]	Ti/≡SiOH[c]	mmol $HNEt_2$[b]	$HNEt_2$/Ti
silica-200	1.94	0.40	0.47	0.73	1.83
	1.86	0.39	0.45	0.80	2.05
	1.97	0.41	0.48	0.75	1.84
	2.00	0.42	0.49	0.85	2.03
average	1.94 ± 0.06	0.41 ± 0.01	0.47 ± 0.02	0.78 ± 0.05	1.94 ± 0.12
silica-500	2.14	0.45	1.12	0.44	0.98
	1.98	0.41	1.03	0.42	1.02
	1.96	0.41	1.02	0.40	0.98
	2.00	0.41	1.04	0.41	1.00
average	2.02 ± 0.08	0.42 ± 0.02	1.05 ± 0.05	0.42 ± 0.02	0.99 ± 0.02

[a] The appended numbers refer to the temperature, in °C, at which the silica was partially dehydroxylated prior to the chemisorption reaction.

[b] Normalized per gram of solid.

[c] Calculated based on the number of surface hydroxyl groups on silica pretreated *in vacuo* at each temperature: 0.40 mmol/g (500°C) and 0.86 mmol/g (200°C).

$$2\,{\equiv}SiOH + Ti(NEt_2)_4 \rightarrow (\equiv SiO)_2Ti(NEt_2)_2 + 2\,HNEt_2 \qquad (4.1)$$

(silica-200) **3**

On silica-500, the amount of chemisorbed titanium which corresponds to complete reaction of surface hydroxyl groups is (2.0 ± 0.1) wt %, and corresponds to 1.05 Ti/≡SiOH, Table 4.1. At the same time, 1.0 equiv of $HNEt_2$ is evolved per chemisorbed Ti during the grafting reaction. The stoichiometry of this surface reaction is shown in eq 4.2:

$$\equiv SiOH + Ti(NEt_2)_4 \rightarrow \equiv SiOTi(NEt_2)_3 + HNEt_2 \qquad (4.2)$$

(silica-500) **4**

Note that, on both types of silica, the amount of chemisorbed Ti after grafting $Ti(NEt_2)_4$ is exactly one-half the amount obtained by the reaction of $Ti(O^iPr)_4$ with each silica (Chapter 3). In view of this finding, and in contrast to the dinuclear formulations of **1** and **2**, we conclude that the supported amido complexes **3** and **4** are mononuclear.

4.3 Spectroscopic characterization of grafted amido complexes

4.3.1 Solid state NMR

The ^{13}C CP/MAS spectra of the solid products are qualitatively similar on silica-200 and -500 and consist of two resonances at 13.7 and 47.0 ppm, Figure 4.1, assigned

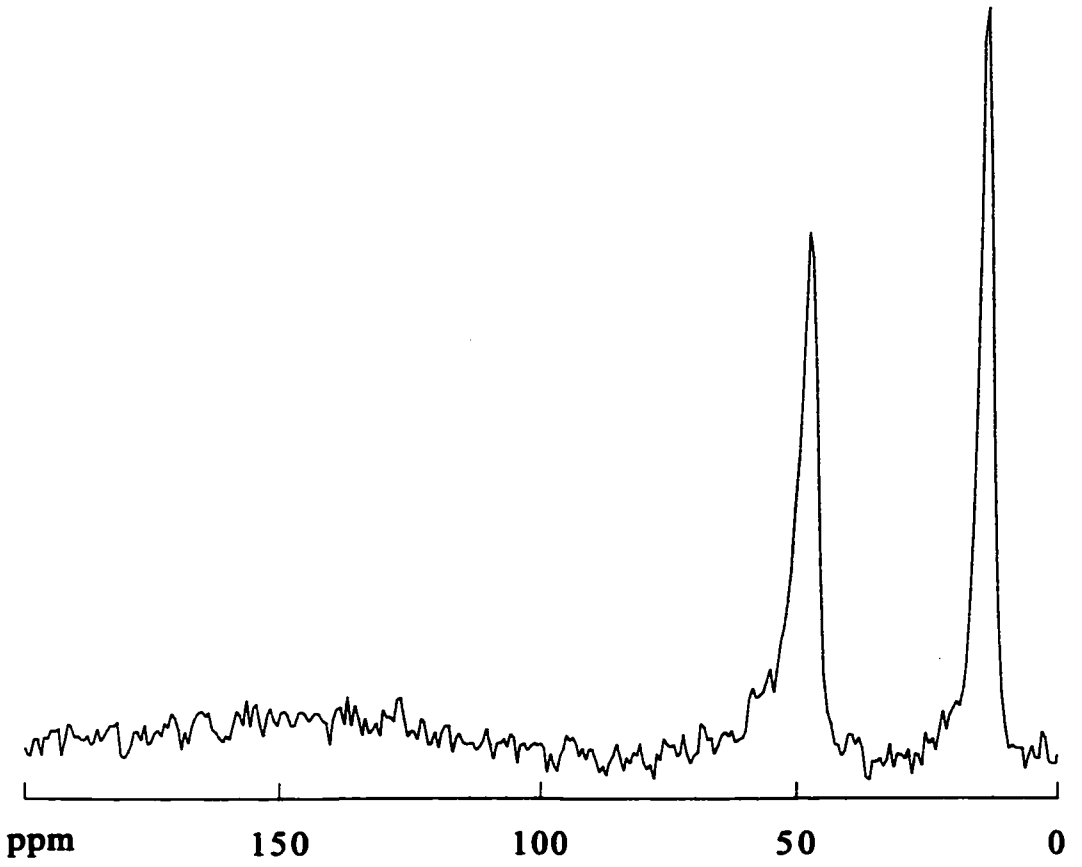

Figure 4.1. ^{13}C CP/MAS spectrum of silica-500 treated with $Ti(NEt_2)_4$ to give **4**, followed by desorption of unreacted starting material and evacuation of volatile products. Spin rate, 4 kHz.

to the methyl and methylene carbons of diethylamido ligands, respectively, by comparison to the $^{13}C\{^1H\}$ NMR spectrum of $Ti(NEt_2)_4$ in $CDCl_3$ (13.3 and 45.0 ppm).

4.3.2 Vibrational spectroscopy

In the IR spectrum, complete disappearance of the IR vibration at 3747 cm^{-1} due to surface hydroxyl groups was observed on both types of silica. Bands characteristic of the diethylamide ligands (2973, 2937, 2880, 2848, 1464, 1448, 1373, 1353, 992, 910, 882, 616 cm^{-1}) are clearly visible, as well as a new band at 957 cm^{-1}, Figure 4.2. The spectra of the supported Ti complexes on silica-200 and silica-500 are qualitatively very similar, although the ligand vibrations on silica-500 are slightly more intense. The vibrations at 992 and 616 cm^{-1} are assigned to $\nu_s(NC_2)$ and ν(Ti-N) on the basis of literature assignments for $Ti(NEt_2)_4$.[1] Reaction of $Ti(NEt_2)_4$ with ^{18}O-labeled surface hydroxyl groups[2], eq 4.3, resulted in a shift of the 957 cm^{-1} band to 936 cm^{-1}, Figure 4.3.

$$\equiv Si^{18}OH + Ti(NEt_2)_4 \rightarrow \equiv Si^{18}OTi(NEt_2)_3 + HNEt_2 \qquad (4.3)$$

On this basis, and by comparison to shifts of similar magnitude in the IR spectra of silica-supported, ^{18}O-labeled vanadium[3] and molybdenum[4] complexes, the vibration is assigned as ν(Si-OTi).

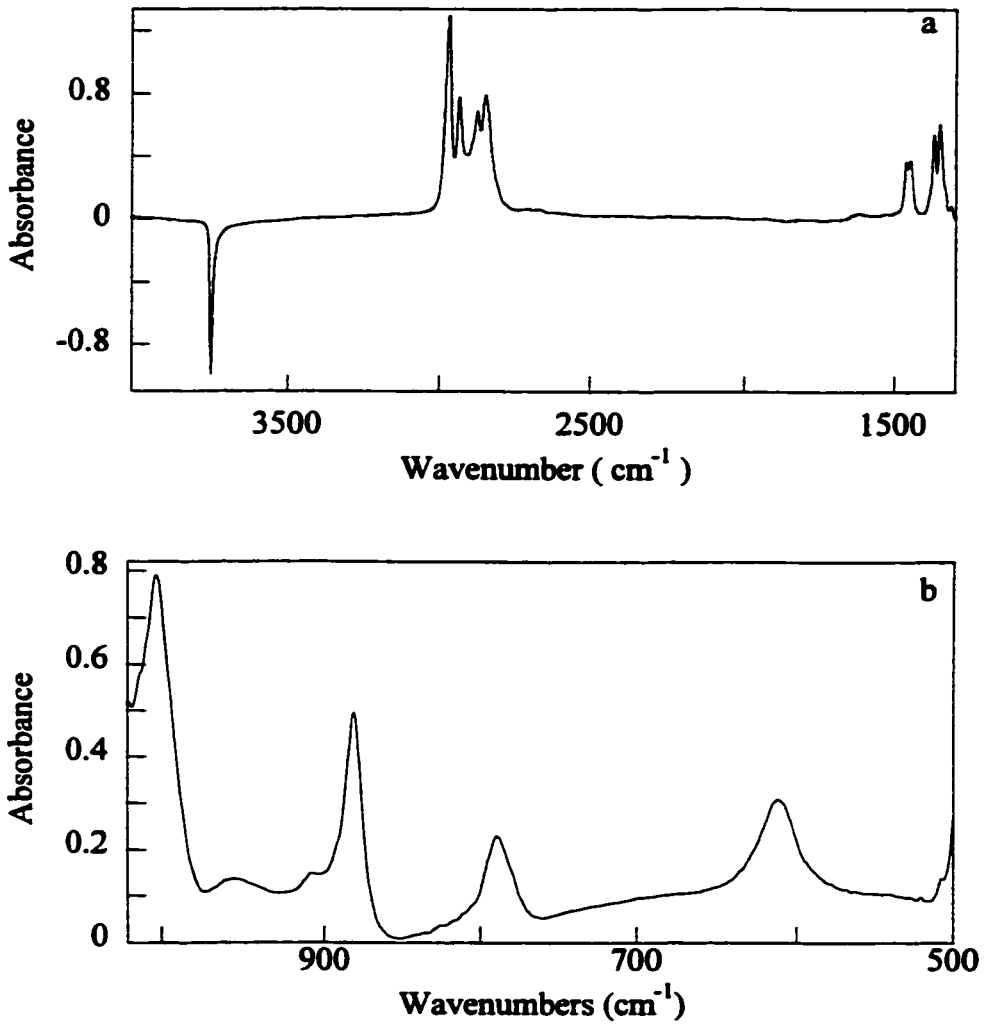

Figure 4.2. *In situ* IR difference spectrum of a self-supporting disk of silica-500 treated with $Ti(NEt_2)_4$ to give **4**, followed by desorption of unreacted starting material and evacuation of volatile products, in two frequency regions of partial transparency of the silica disk. The reference spectrum of silica-500 has been subtracted such that negative peaks correspond to vibrations which are no longer present on the silica surface after reaction.

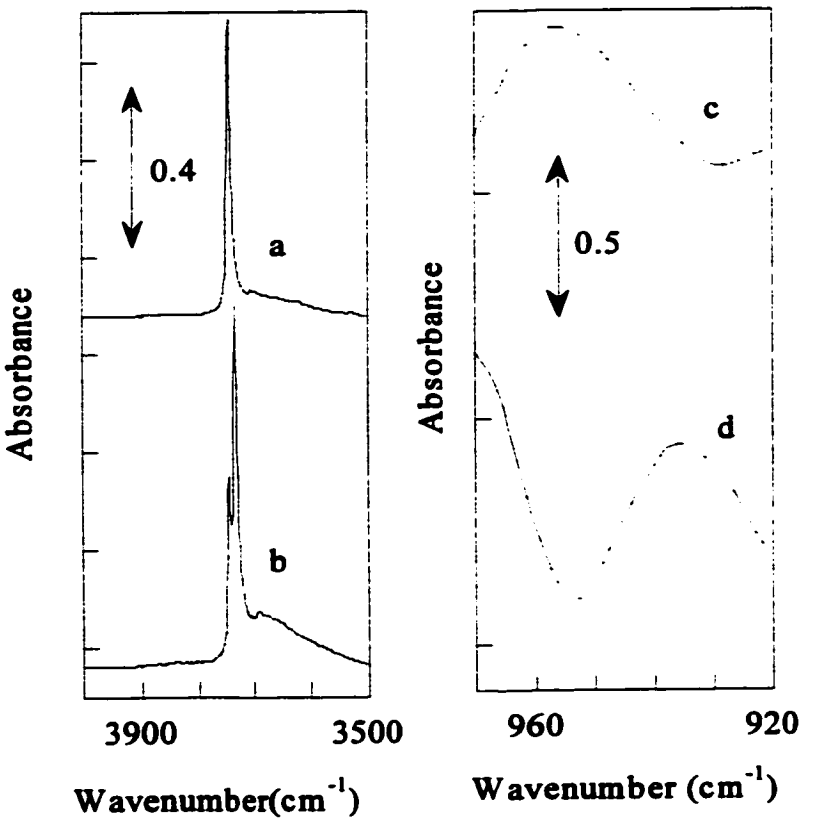

Figure 4.3. *In situ* IR difference spectra of self-supporting disks of silica-500 (a) unmodified, showing $\nu(Si^{16}O\text{-}H)$; (b) after exchange with $H_2{}^{18}O$, showing an additional band for $\nu(Si^{18}O\text{-}H)$; (c and d) after reaction of unmodified and ^{18}O-exchanged silicas, respectively, with $Ti(NEt_2)_4$ to give **4**.

4.3.3 UV-visible spectroscopy

The diffuse reflectance UV-visible spectrum of silica-200 modified with $Ti(NEt_2)_4$ consists of two peaks at 257 and 336 nm, Figure 4.4a. The presence of a feature at $\lambda >$ 300 nm in this spectrum is clearly the result of a LMCT band, which is also present in the yellow $Ti(NEt_2)_4$ precursor. It cannot be taken to indicate the presence of anatase in samples of $(\equiv SiO)_nTi(NEt_2)_{4-n}$, since displacement of the amido ligands by alcohol leads to complete removal of this absorbance (*vide infra*). LMCT transitions from amido groups are expected to fall at lower energy than those of alkoxo groups due to the lower electronegativity of nitrogen.

4.4 Reactions of $(\equiv SiO)_nTi(NEt_2)_{4-n}$ with Alcohols

The reactions of either **3** or **4** with excess *tert*-butyl alcohol vapor cause an immediate color change from yellow to white and nearly complete (ca. 90%) displacement of the amido ligands as $HNEt_2$, eqs 4.4-4.5:

$$(\equiv SiO)_2Ti(NEt_2)_2 + 2\ {}^tBuOH \rightarrow (\equiv SiO)_2Ti(O^tBu)_2 + 2\ HNEt_2 \qquad (4.4)$$

3 **5**

$$(\equiv SiO)Ti(NEt_2)_3 + 3\ {}^tBuOH \rightarrow (\equiv SiO)Ti(O^tBu)_3 + 3\ HNEt_2 \qquad (4.5)$$

4 **6**

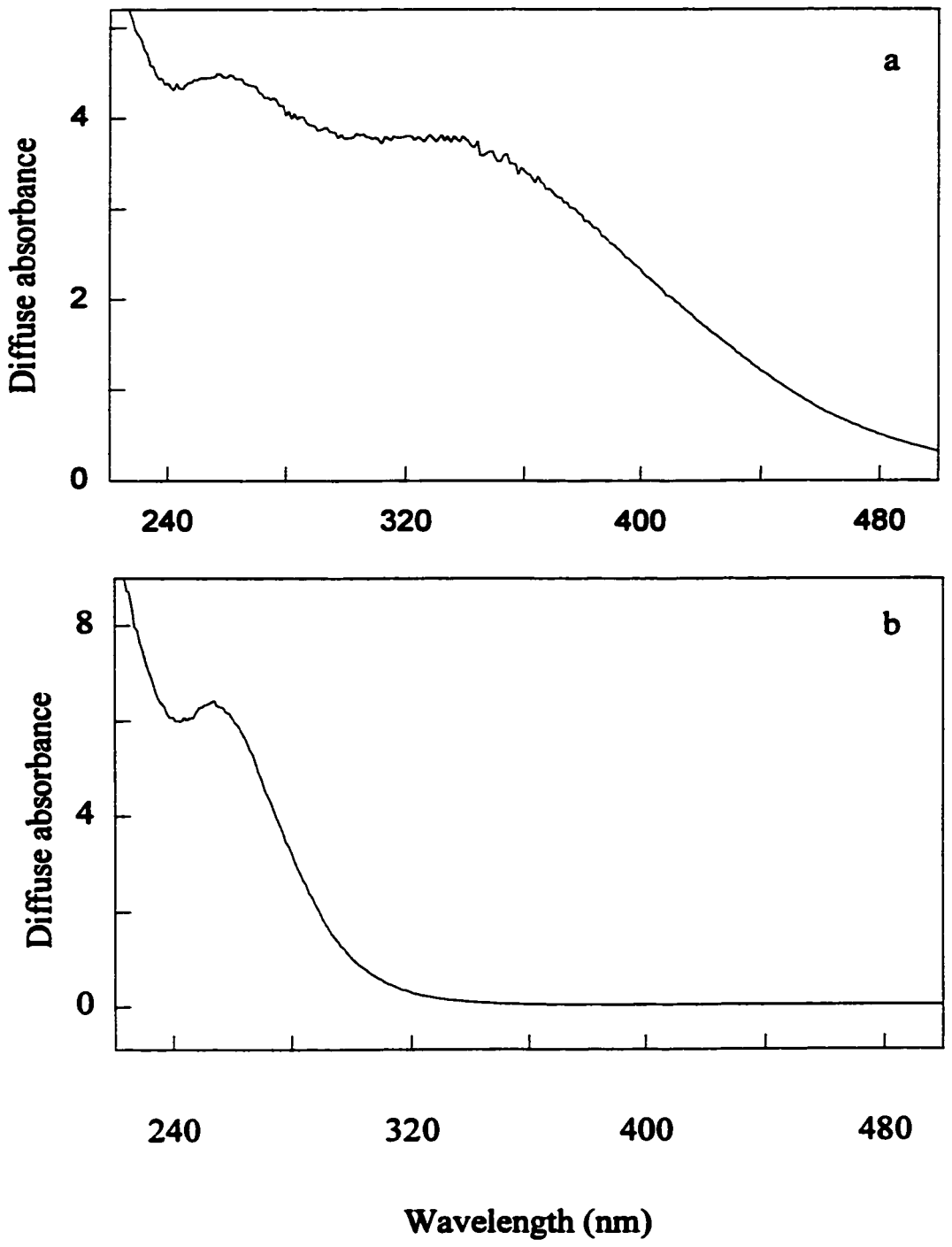

Figure 4.4. UV-visible spectra of (a) silica-200 modified with $Ti(NEt_2)_4$, recorded in diffuse reflectance mode,and (b) sample from (a) exchanged with 2-propanol.

The amount of $HNEt_2$ liberated was quantified by gas-phase IR spectroscopy as 2.0/Ti for **3** (eq 4.4) and 2.8/Ti for **4** (eq 4.5). In the IR spectrum of **4** treated with $(CD_3)_3COD$, the ν(C-H) vibrations of the diethylamido ligands decreased in intensity by 96% upon evacuation, while new bands were observed at 2235, 2135, 2076 and 2054 cm^{-1}, assigned to the ν(C-D) vibrations of perdeuterio-*tert*-butyl groups which are strongly chemisorbed, Figure 4.5. The ^{13}C CP/MAS NMR spectra of both **5** and **6** consist of a major peak at 30.6 ppm, corresponding to the methyl carbons of the *tert*-butyl groups, and a minor, variable intensity peak at 12.8 ppm, assigned to the methylene carbon of a small amount of residual, adsorbed diethylamine, Figure 4.6. The quaternary carbon of the *tert*-butoxo ligand was not observed due to its poor cross polarization. Calcination of **6** in O_2 at 750 °C released 12.7 CO_2/Ti, in agreement with the proposed formula for **6** and a small amount of chemisorbed $HNEt_2$ (<<1 equiv. per Ti). Similar color changes were observed when **3** or **4** was exposed to excess 2-propanol, and diethylamine was again observed in the gas phase.

When the reaction of **4** was performed with $(CD_3)_2CDOD$, the appearance of ν(C-D) modes in the IR spectrum was accompanied by an approximately 80% decrease in intensity of the ν(C-H) vibrations, due to displacement of the amido ligands. The ^{13}C CP/MAS NMR spectra on silica-200 and -500 are qualitatively similar and consist of five peaks at 11.7, 23.8, 43.0, 66.3, and ca. 80 ppm, Figure 4.6b, even after prolonged evacuation of volatiles. The signals at 23.8 and ca. 80 ppm are assigned to the methyl and methine carbons of coordinated 2-propoxide ligands, as for **1** and **2** (Figure 3.1). The peaks at 11.7 and 43.0 ppm are slightly shifted from those of **3** and **4** and are assigned to the methyl and methylene carbons of coordinated diethylamine.

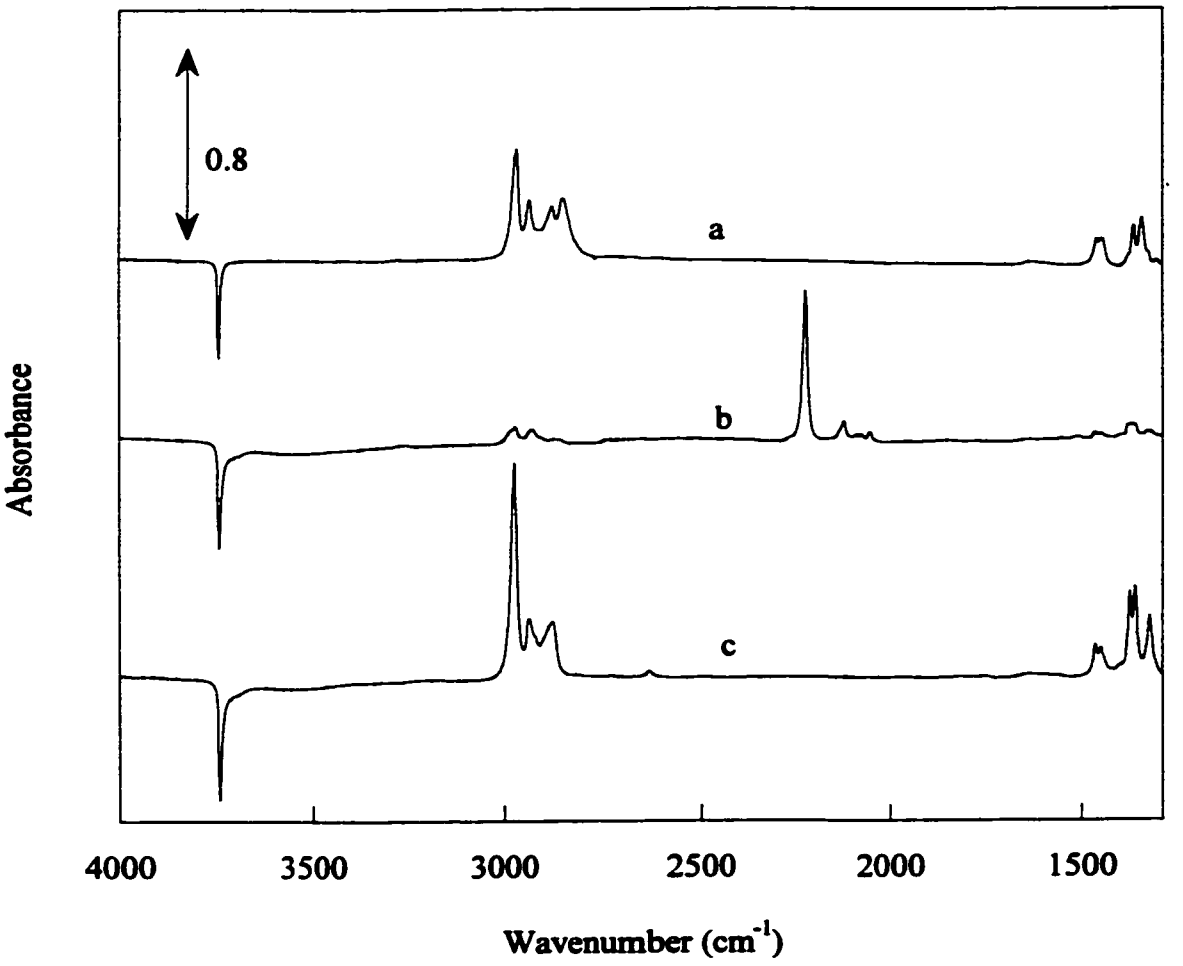

Figure 4.5. *In situ* IR difference spectra of a self-supporting disk of silica-500 treated with (a) $Ti(NEt_2)_4$ to give **4**, followed by (b) $(CD_3)_3COD$ to give **6**, followed by (c) $Ti(O^iPr)_4$ to give **2**. The reference spectrum of silica-500 has been subtracted. At each stage of the experiment, unreacted reagents and volatile products were removed by evacuation before recording the spectrum and adding the next reagent.

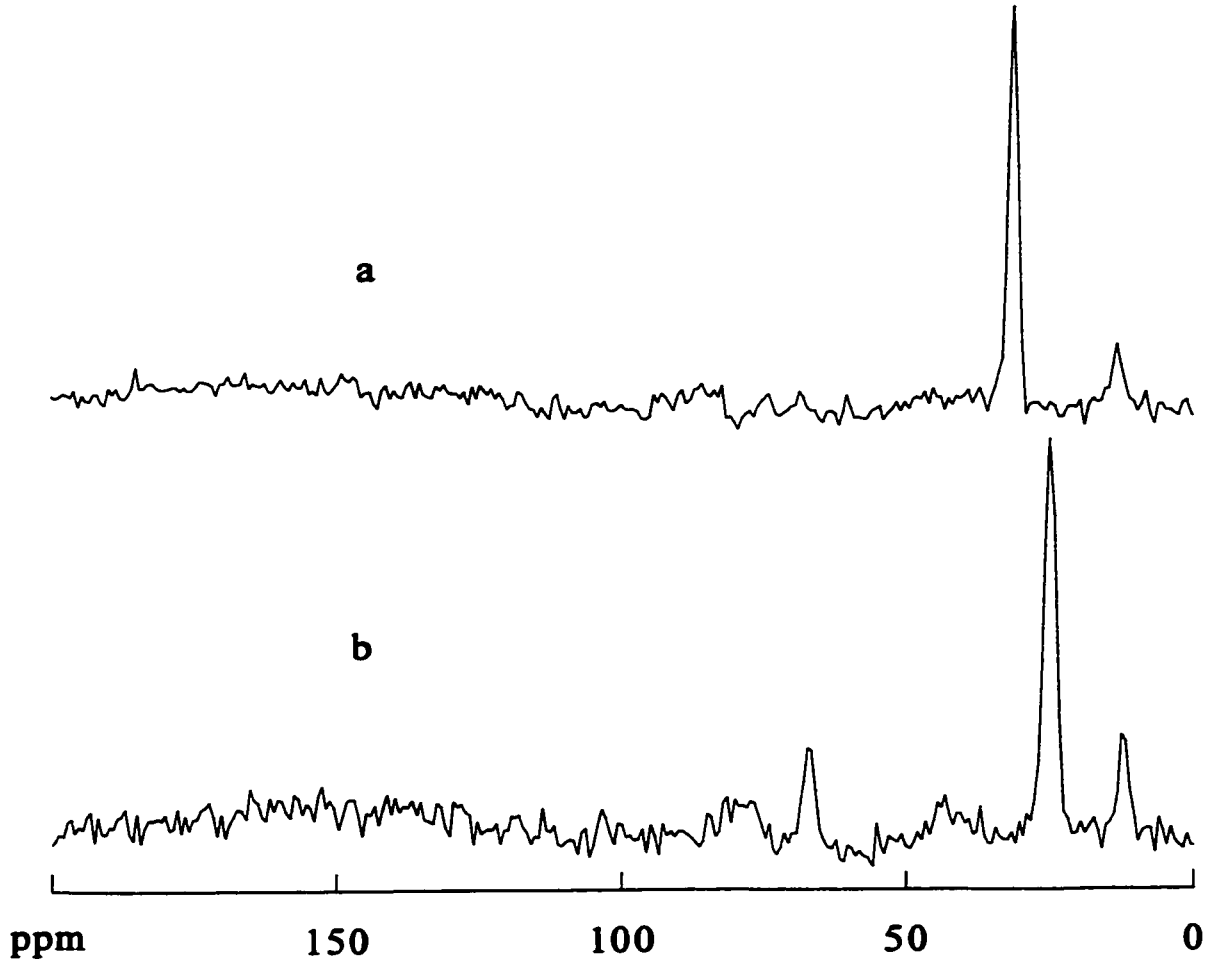

Figure 4.6. ^{13}C CP/MAS spectra of silica-500 modified with $Ti(NEt_2)_4$ to give **4**, followed by (a) tert-butyl alcohol to give **6**, or (b) 2-propanol to give **8**. In each case, unreacted reagents and volatile products were removed by evacuation before the spectrum was recorded. Spin rate, 4 kHz.

Finally, the peak at 66.3 ppm is assigned to the methine carbon of coordinated 2-propanol. In free 2-propanol, this signal appears at 64.7 ppm. The methyl carbon signal of coordinated 2-propanol is presumed to be superimposed on the methyl signal of the 2-propoxide ligands at 23.8 ppm. The exchange reactions are shown in eqs 4.6-4.7:

$$(\equiv SiO)_2Ti(NEt_2)_2 + 2\ {}^iPrOH + L \rightarrow (\equiv SiO)_2Ti(O^iPr)_2L + 2\ HNEt_2 \qquad (4.6)$$

3 **7**

$$(\equiv SiO)Ti(NEt_2)_3 + 3\ {}^iPrOH + L \rightarrow (\equiv SiO)Ti(O^iPr)_3L + 3\ HNEt_2 \qquad (4.7)$$

4 **8**

where L is ^iPrOH, $HNEt_2$, or (apparently in most cases) a siloxane oxygen from the silica surface. We have no direct evidence for this coordinated siloxane ligand, but its presence is inferred in those surface complexes which bind neither free alcohol nor amine.

The UV-visible spectrum of **7**, Figure 4.4b, shows the disappearence of the visible absorption, while the remaining UV band at 254 nm resembles the LCMT band of **1**, Figure 3.3a. Calcination of **8** in O_2 at 750 °C liberated 10.6 CO_2/Ti (expected value, 9 CO_2/Ti for **8**, neglecting the contribution of the ligand L). Therefore, the amount of ^iPrOH and $HNEt_2$ strongly chemisorbed on the surface is less than 1 ligand per Ti. This result is also consistent with incomplete (ca. 80%) loss of the C-H vibrations due to $HNEt_2$ in the IR spectrum of **4** after reaction with $(CD_3)_2CDOD$.

4.5 Reactions of mononuclear surface alkoxide complexes with $Ti(O^iPr)_4$

The modified silicas **5-8** all contain up to 2.0 wt % Ti. When maximum Ti loading is achieved, there are no residual accessible surface hydroxyl groups. However, despite the absence of hydroxyl grafting sites, each of these materials reacts irreversibly with additional $Ti(O^iPr)_4$. The reactions are accompanied in each case by a doubling of the Ti loading on silica, Table 4.2, as well as liberation of 0.5 equiv each of 2-propanol and propene into the gas phase. For example, a sample of **8** treated with excess $Ti(O^iPr)_4$ generated a material containing 0.71 mmol Ti, and released 0.37 mmol ^iPrOH and 0.35 mmol C_3H_6 into the gas phase. A small amount of diethylamine was also detected in the gas phase by GC upon exposure of **5-8** to $Ti(O^iPr)_4$, consistent with the retention of some coordinated $HNEt_2$ on the surface in reactions 4.4-4.7.

When deuterium-labeled **6** reacts with $Ti(O^iPr)_4$, the ν(C-D) vibrations disappear almost completely from the IR spectrum, and new ν(C-H) vibrations, corresponding to unlabeled isopropyl groups, appear, Figure 4.5c. Calcination of the product of this reaction in O_2 liberated 7.5 CO_2/Ti, compared to 7.6 CO_2/Ti generated in the calcination of **2**. The IR spectra of the products of the reactions of **5-8** with $Ti(O^iPr)_4$ are superposable, both qualitatively and quantitatively, upon those of **1** and **2**. The ^{13}C CP/MAS spectra of these materials consist of two peaks at 25.0 and 78.0 ppm, assigned to the methyl and methine carbons of chemisorbed 2-propoxide ligands. The spectra are indistinguishable from those obtained by direct grafting of $Ti(O^iPr)_4$ on the surface hydroxyl groups of silica (Figure 3.1). The net reactions are shown in eqs 4.8-4.9:

$$(\equiv SiO)_2Ti(O^iPr)_2 + Ti(O^iPr)_4 \rightarrow [(\equiv SiO)Ti(O^iPr)_2]_2O + {}^iPrOH + C_3H_6 \qquad (4.8)$$

7 1

Table 4.2. Titanium content of materials prepared by room temperature chemisorption of $Ti(O^iPr)_4$ on $(\equiv SiO)_nTi(O^iPr)_{4-n}$[a,b]

silica support[c]	wt. % Ti before reaction with $(\equiv SiO)_nTi(O^iPr)_{4-n}$	wt. % Ti after reaction with $(\equiv SiO)_nTi(O^iPr)_{4-n}$
silica-500	1.98	3.96
	[d]	3.98
	[d]	3.94
	[d]	3.96
average		3.96 ± 0.02
silica-200	1.94	3.92
	[d]	4.00
	[d]	3.94
average		3.95 ± 0.04

[a] Prepared by the chemisorption of $Ti(NEt_2)_4$ on silica, followed by ligand metathesis with excess ^iPrOH.

[b] On silica-500, n = 1; on silica-200, n = 2.

[c] The appended numbers refer to the temperature, in °C, at which the silica was partially dehydroxylated prior to the first chemisorption reaction.

[d] These are *in situ* IR experiments, therefore the Ti loading resulting from the first grafting reaction was not measured. However, there are no remaining hydroxyl groups (as judged by the absence of ν(SiO-H)) at the time of second grafting reaction.

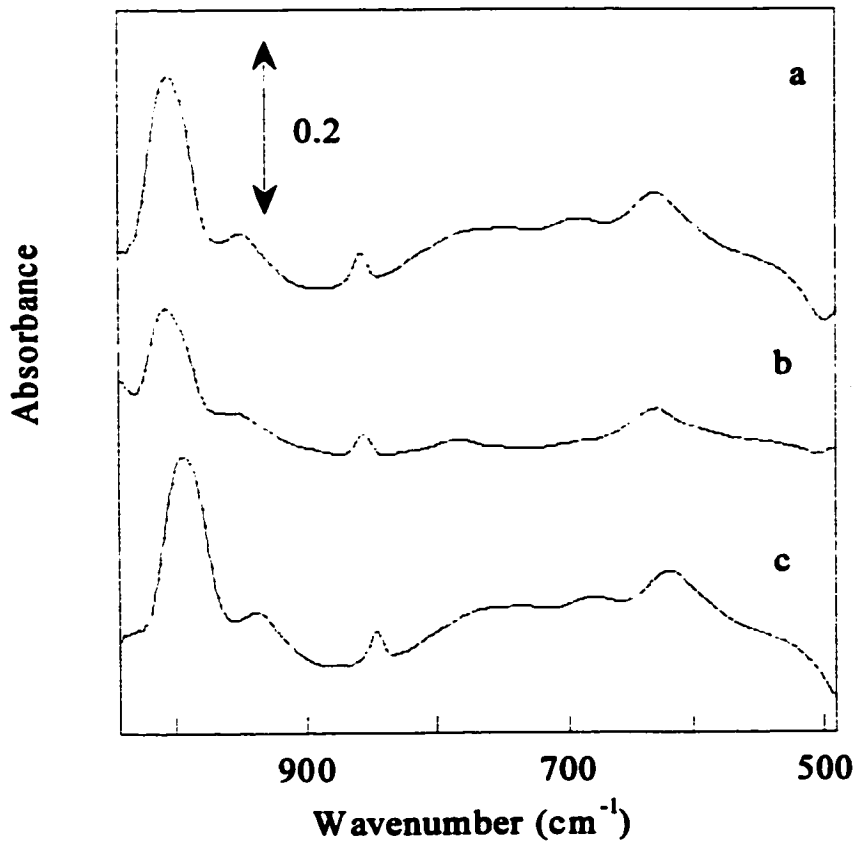

Figure 4.7. *In situ* IR spectra of self-supporting disks of silica-500 treated with (a) $Ti(O^iPr)_4$ to form **2** directly; (b) $Ti(NEt_2)_4$ followed by ligand metathesis with ^iPrOH to form **8**; and (c) previous sample treated with $Ti(O^iPr)_4$ to form **2** by the sequential grafting method.

$$(\equiv SiO)Ti(O^iPr)_3 + Ti(O^iPr)_4 \rightarrow (\equiv SiO)Ti_2(O^iPr)_5(O) + {}^iPrOH + C_3H_6 \qquad (4.9)$$

8 **2**

Careful comparison of the low frequency spectra of mononuclear **8** and dinuclear **2** reveal only one signfiicant difference. A band at 680 cm^{-1} appears in the spectrum of **1** prepared either directly by grafting $Ti(O^iPr)_4$ on unmodified silica, or by reaction of $Ti(O^iPr)_4$ with **8**, Figure 4.6. This band is tentatively assigned as ν_{as}(TiOTi).

4.6 Discussion

The supported dialkylamido complexes **3** and **4** are an indirect route to grafted mononuclear titanium alkoxides via ligand metathesis. The maximum loading of chemisorbed Ti using $Ti(NEt_2)_4$ as the molecular reagent does not exceed the number of surface hydroxyl groups, which react either individually (on silica-500) or in pairs (on silica-200). Thus, on silica-500, 0.42 mmol of Ti is grafted on a surface containing originally 0.40 mmol of OH/g, whereas on silica-200, 0.41 mmol of Ti is grafted on a surface containing originally 0.86 mmol of OH/g (Table 4.1). The reproducible but different stoichiometries of these reactions on each kind of silica resemble those of the reactions of the metal alkyls MR_4 (M is Zr,[5,6] Cr[7]) with silica surfaces.

Consistent with the greater acidity of alcohols relative to amines, the mononuclear amido surface complexes are readily transformed into mononuclear surface alkoxide complexes **5-8**. However, the amine is not quite quantitatively liberated from the surface: a small amount remains bound to the tert-butoxo surface complexes, and slightly

more remains bound to the 2-propoxo surface complexes, both of which are presumably less sterically encumbered than the diethylamido surface complexes **3** and **4**. The ^{13}C NMR spectrum also shows evidence for coordination of some 2-propanol to mononuclear supported titanium 2-propoxide complexes (although not to dinuclear **1** or **2**). In agreement with a previous report,[8] but in contrast to another,[9] we find that alcohol does not cleave the SiO-Ti bond to any significant extent, since the ν(SiO-H) vibration never reappears in the IR spectrum.

The mononuclear supported complexes **5-8** react with 1 equiv of $Ti(O^iPr)_4$ to form the dinuclear surface complexes **1** and **2** on silica-200 and –500, respectively, by a mechanism which likely resembles steps in the proposed grafting mechanism for $Ti(O^iPr)_4$ on silica. The surface dinuclear complexes produced via grafting $Ti(O^iPr)_4$ on **5-8** are identical, spectroscopically and analytically, to those produced by the direct grafting of $Ti(O^iPr)_4$ on unmodified silica. The surface reactions are summarized in Schemes 4.1 and 4.2.

4.7 Conclusion

Silica-supported mononuclear titanium alkoxide complexes are accessible but they must be prepared via an indirect route, involving the reaction of grafted Ti amido complexes with alcohols. They demonstrate a tendency to coordinate additional ligands, as well as to undergo spontaneous condensation with $Ti(O^iPr)_4$. This condensation is the origin of the propene formed during the grafting.

Scheme 4.1. Grafting of Ti complexes on silica-200 surface

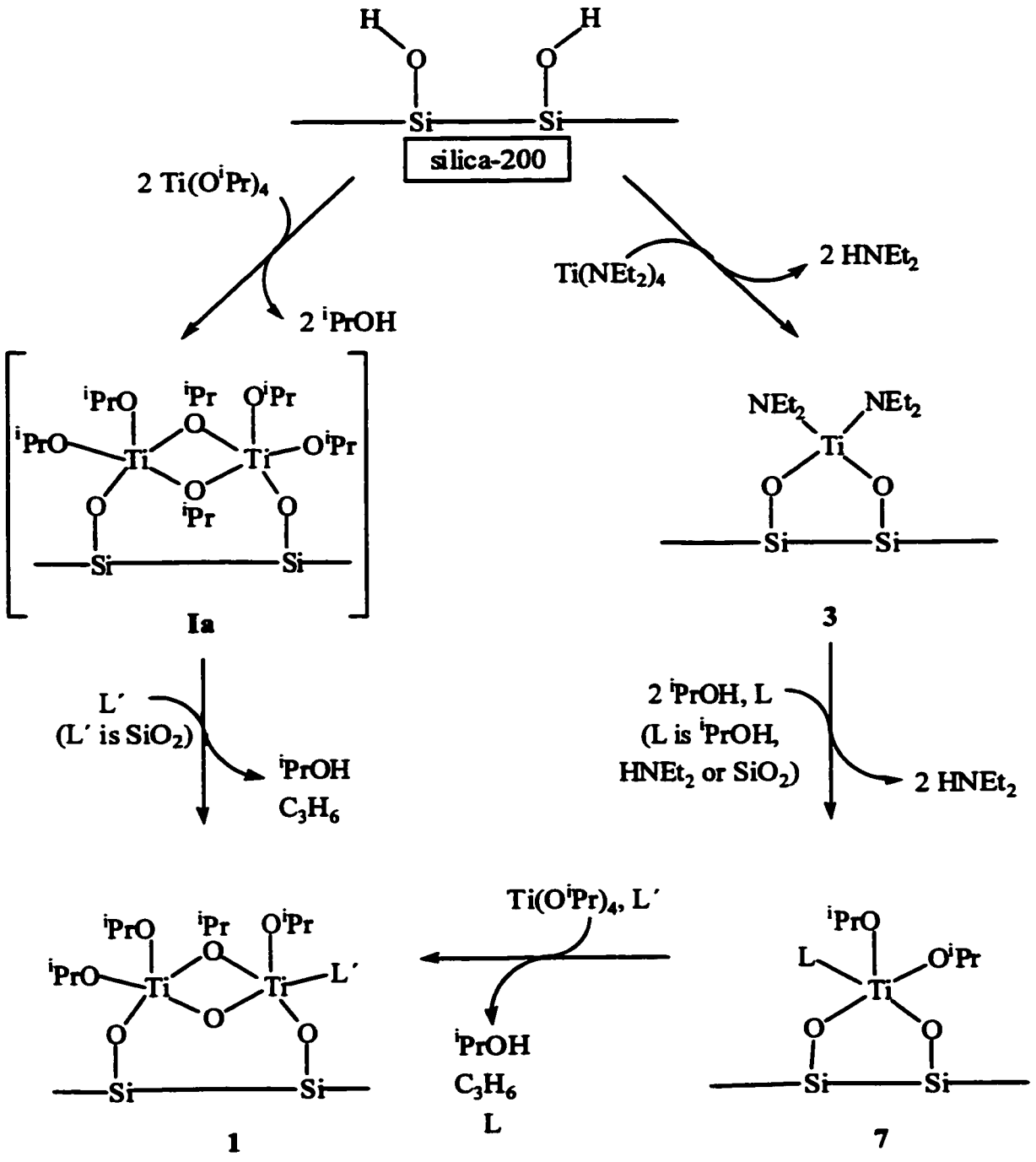

Scheme 4.2. Grafting of Ti complexes on silica-500 surface

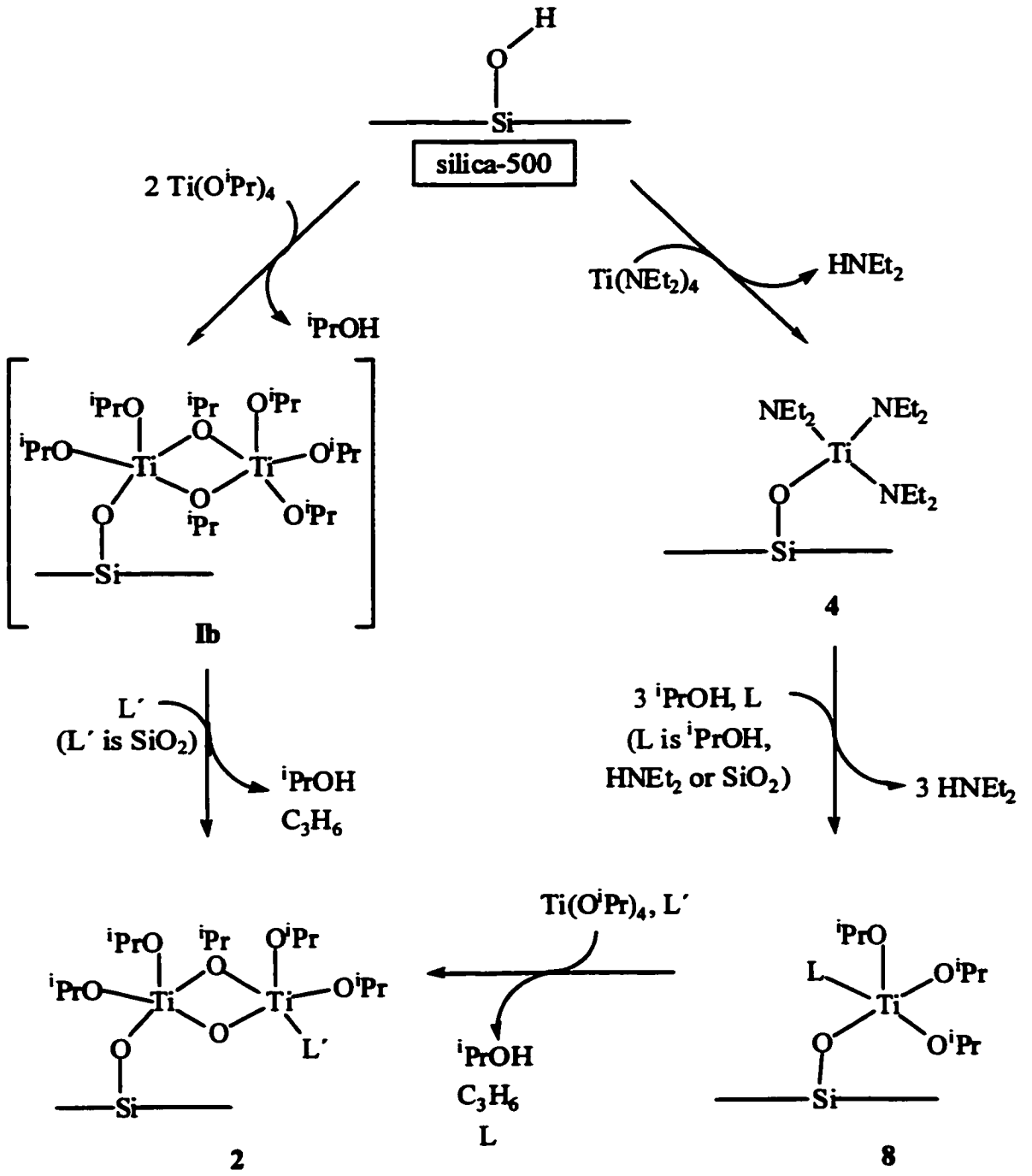

4.8 References

(1) Bradley, D. C.; Gitlitz, M. H. *J. Chem. Soc. (A)* **1969**, 980-984.

(2) Hino, M.; Sato, T. *Bull. Chem. Soc. Jpn* **1971**, *44*, 33-37.

(3) Rice, G. L.; Scott, S. L. *J. Mol. Catal. A: Chem.* **1997**, *125*, 73-79.

(4) Cornac, M.; Janin, A.; Lavalley, J. C. *Polyhedron* **1986**, *5*, 183-186.

(5) Schwartz, J.; Ward, M. D. *J. Mol. Catal.* **1980**, *8*, 465.

(6) Quignard, F.; Lecuyer, C.; Bougault, C.; Lefebvre, F.; Choplin, A.; Olivier, D.; Basset, J.-M. *Inorg. Chem.* **1992**, *31*, 928.

(7) Amor Nait Ajjou, J.; Scott, S. L. *Organomet.* **1997**, *16*, 86-92.

(8) Blandy, C.; Pellegatta, J.-L.; Choukroun, R.; Gilot, B.; Guiraud, R. *Can. J. Chem.* **1993**, *71*, 34-37.

(9) Gao, X.; Bare, S. R.; Fierro, J. L. G.; Banares, M. A.; Wachs, I. E. *J. Phys. Chem. B* **1998**, *102*, 5653-5666.

Chapter 5

Stoichiometric Epoxidation by Silica-supported Ti Complexes

5.1 Introduction

Peroxo- and alkylperoxotitanium complexes are presumed intermediates in the homogeneous and heterogeneous catalytic epoxidations of olefins. High valent, d^0 transition metal complexes activate peroxides heterolytically, thereby facilitating oxygen atom transfer to electron-rich substrates.[1] For heterogeneous Ti catalysts in which the metal is dispersed on the external and/or internal surfaces of silica or an aluminosilicate framework, the fraction of active sites is generally unknown and the stoichiometry of the epoxidation reaction is untestable; reactivities can be compared only in terms of overall activity and selectivity.[2] Detailed information about the properties of individual sites as well as elementary steps in the mechanism are needed in order to create a conceptual foundation for rationalizing catalyst activity as well as for designing new catalysts.

In order to define the stoichiometry of the oxygen transfer step in epoxidation, the number of peroxo ligands coordinated at each Ti site and the number of such sites which are active must be quantified. The mechanism of epoxidation likely begins with coordination of a peroxide ligand at Ti.[3] In Chapters 3 and 4, we described the preparation and quantitative characterization of well-defined mononuclear and dinuclear titanium alkoxide complexes grafted onto silica surfaces. In this Chapter, their transformation to alkylperoxo complexes and the stoichiometric reactivity of such complexes towards simple olefins will be described.

5.2 Reactions of mono- and dinuclear surface complexes with *tert*-butylhydroperoxide

Displacement of alcohol (^{t}BuOH or ^{i}PrOH) from **5-8** by *tert*-butylhydroperoxide at room temperature was observed by IR and GC. A small amount of diethylamine was also detected in the gas phase by GC upon exposure of **5-8** to $Ti(O^iPr)_4$ or ^{t}BuOOH, consistent with the retention of some coordinated $HNEt_2$ on the surface (Chapter 4). The exchange reactions are summarized in eq 5.1-5.2:

$$(\equiv SiO)_2Ti(OR)_{4-n} + 2\ ^tBuOOH \rightarrow (\equiv SiO)_2Ti(OO^tBu)_2 + 2\ ROH \qquad (5.1)$$

5 (R = ^{t}Bu); **7** (R = ^{i}Pr) **9**

$$(\equiv SiO)Ti(OR)_3 + 3\ ^tBuOOH \rightarrow (\equiv SiO)Ti(OO^tBu)_3 + 3\ ROH \qquad (5.2)$$

6 (R = ^{t}Bu); **8** (R = ^{i}Pr) **10**

When the reaction with ^{t}BuOOH was performed with deuterium-labeled **6**, a 97% decrease in the intensity of the ν(C-D) vibrations was observed by IR, while ν(C-H) vibrations assigned to the *tert*-butylperoxo ligands appeared. No regeneration of silica hydroxyl groups was observed. A weak band at 850 cm^{-1} is assigned to the peroxo ν(O-O) vibration, by comparison to the spectrum of $VO(C_7H_3O_4N)(OO^tBu)$ with a band at 890 cm^{-1}.[4] Calcination of **10** in O_2 at 750 °C resulted in the liberation of 11.6 equiv of CO_2/Ti, in reasonable agreement with the expected value (12.0). Both of the mononuclear alkylperoxo complexes **9** and **10** (n = 2 or 1) are stable in a vacuum.

The dinuclear complexes **1** and **2**, obtained either by direct grafting of $Ti(O^iPr)_4$ on silica or by grafting $Ti(O^iPr)_4$ onto the mononuclear complexes **7** or **8**, also react with

^{t}BuOOH with liberation of ^{i}PrOH into the gas phase and formation of alkylperoxo complexes $(\equiv SiO)_nTiOTi(OO^tBu)_{6-n}$, eq 5.3-5.4:

$$(\equiv SiO)_2TiOTi(O^iPr)_4 + 4\ ^tBuOOH \rightarrow (\equiv SiO)_2TiOTi(OO^tBu)_4 + 4\ ^iPrOH \qquad (5.3)$$

1 **11**

$$(\equiv SiO)TiOTi(O^iPr)_5 + 5\ ^tBuOOH \rightarrow (\equiv SiO)TiOTi(OO^tBu)_5 + 5\ ^iPrOH \qquad (5.4)$$

2 **12**

The extent of these reactions is seen more clearly when the ligands of **1** or **2** are perdeuterioalkoxide ligands. When the 2-propoxide ligands of **2** were exchanged for perdeuterio-*tert*-butoxide, the subsequent reaction with ^{t}BuOOH caused the loss of 87% of the ν(CD) vibrations, Figure 5.1, corresponding to essentially complete replacement of the ^{t}BuO ligands by ^{t}BuOO. No regeneration of surface hydroxyl groups was observed.

Calcination of **12** in O_2 at 750 °C led to the formation of 9.5 equiv of CO_2/Ti, in reasonable agreement with the expected value (10.0). The ^{13}C CP/MAS NMR spectrum, Figure 5.2, shows retention of a small amount of 2-propanol on the surface, with minor peaks appearing at 21 and 66 ppm assigned to coordinated 2-propanol (as for **7** and **8**, Chapter 4), as well as signals at 30 and 87 ppm, assigned to the methyl and quaternary carbons of the *tert*-butylperoxo ligands.

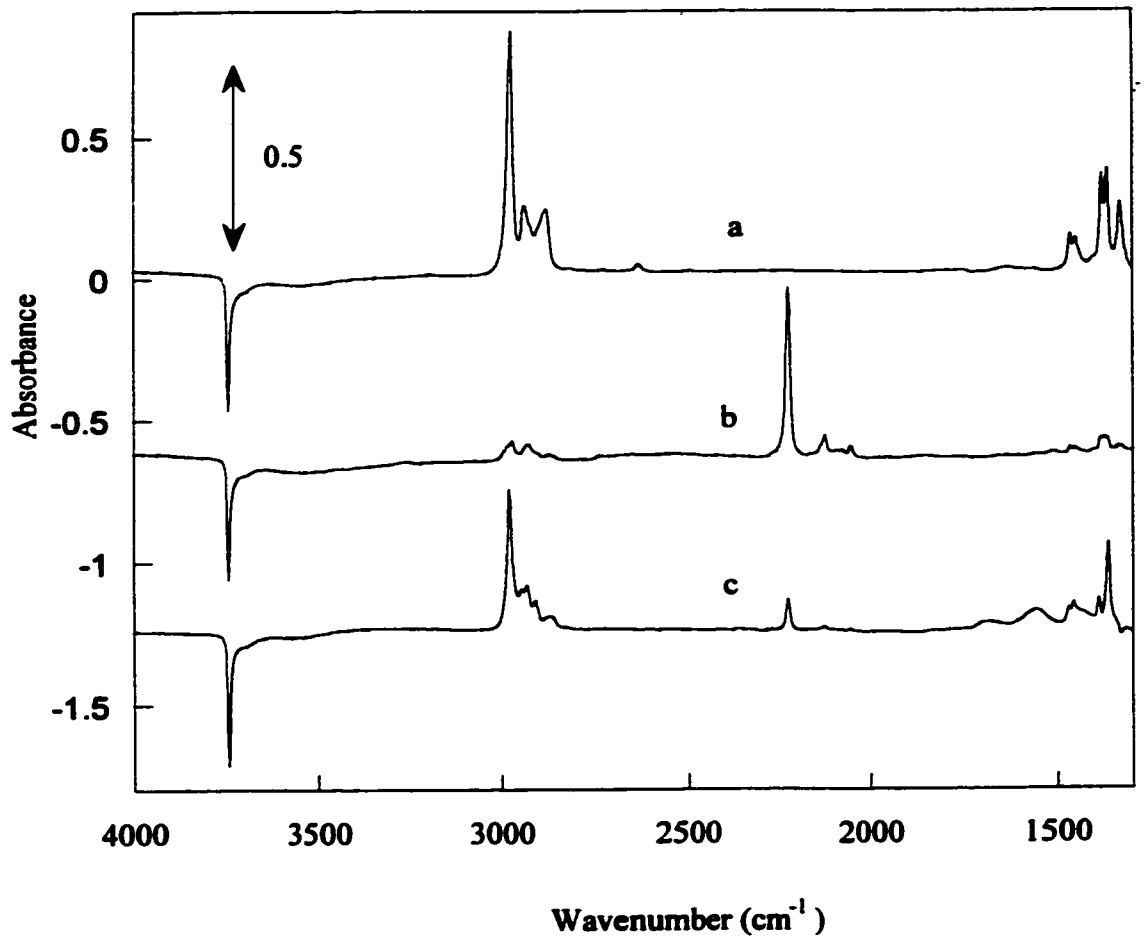

Figure 5.1. *In situ* IR difference spectra of a self-supporting disk of silica-500 (a) treated with $Ti(O^iPr)_4$ to give **2**, followed by (b) $(CD_3)_3COD$, followed by (c) $(CH_3)_3COOH$ to give **12**. The reference spectrum of silica-500 has been subtracted. At each stage of the experiment, unreacted reagents and volatile products were removed by evacuation before recording the spectrum and adding the next reagent.

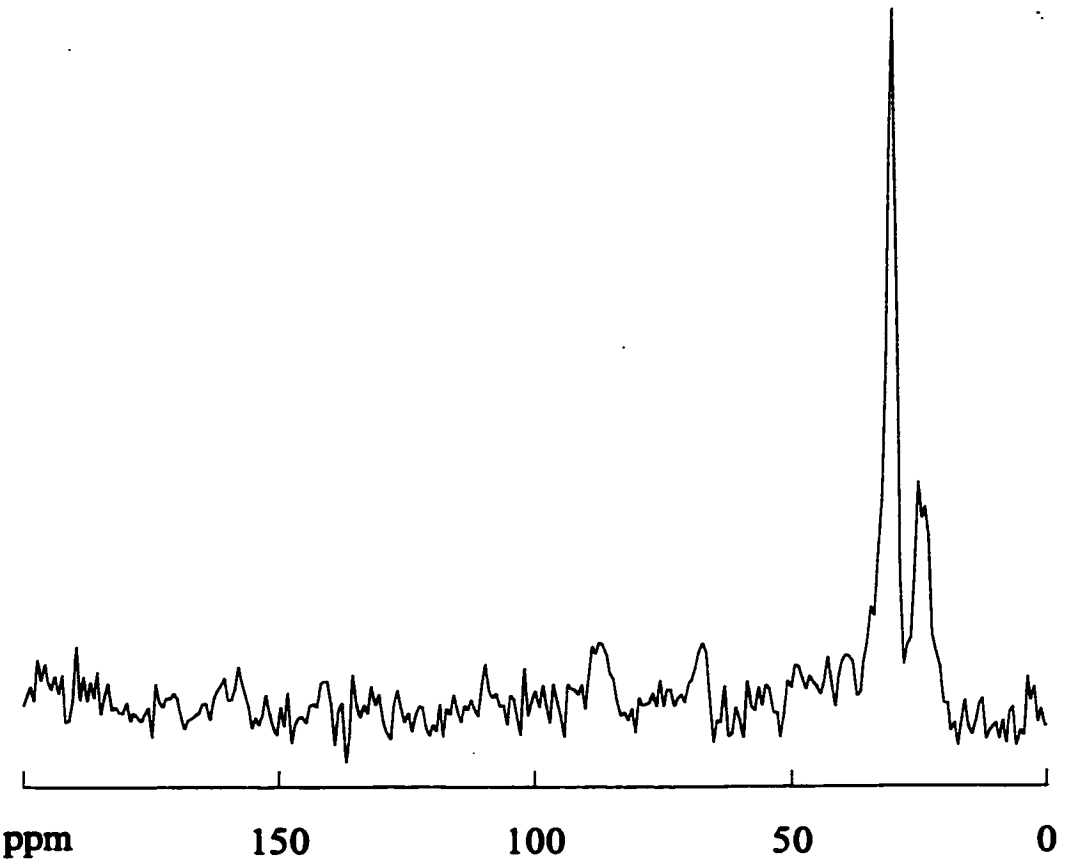

Figure 5.2. ^{13}C CP/MAS spectrum of silica-500 treated with $Ti(O^iPr)_4$ to give **2**, followed by ligand exchange with ^tBuOOH to give **12**. Spin rate, 4 kHz.

The IR spectrum of each *tert*-butylperoxo complex exhibits a vibration at ca. 850 cm^{-1}, assigned to ν(O-O), Figure 5.3. All of the complexes are stable in the presence of excess *tert*-butylhydroperoxide; no regeneration of surface hydroxyls (corresponding to protonolysis of the Si-O-Ti linkages)[5] was observed, nor was O_2 (from the disproportionation of the peroxide)[1] detected.

5.3 Reactions of mono- and dinuclear surface peroxo complexes with olefins

Both of the mononuclear *tert*-butylperoxo complexes **9** and **10** are stable in the presence of cyclohexene vapor at room temperature; *i.e.*, neither cyclohexene oxide nor any other oxidation product was detected by GC. However, addition of cyclohexene vapor at room temperature to either of the dinuclear complexes **11** or **12** caused the immediate appearance of cyclohexene oxide as the sole gaseous product detected by GC/MS. Using techniques previously described to quantify gaseous products of surface reactions (chapters 2 and 3),[6,7] we measured the quantity of epoxide formed by each of the dinuclear *tert*-butylperoxotitanium complexes upon exposure to an excess of olefin in the absence of *tert*-butylhydroperoxide (*i.e.*, stoichiometric gas phase reaction conditions). The results are shown in Table 5.1. After reaction with cyclohexene at room temperature for one hour, cyclohexene oxide was the exclusive product. The quantity of the epoxide recovered was reproducible, both from different samples and after regeneration of the *tert*-butylperoxo complexes in the same sample subsequent to their reaction with cyclohexene. Complex **11**, with four *tert*-butylperoxo ligands per TiOTi unit, generates

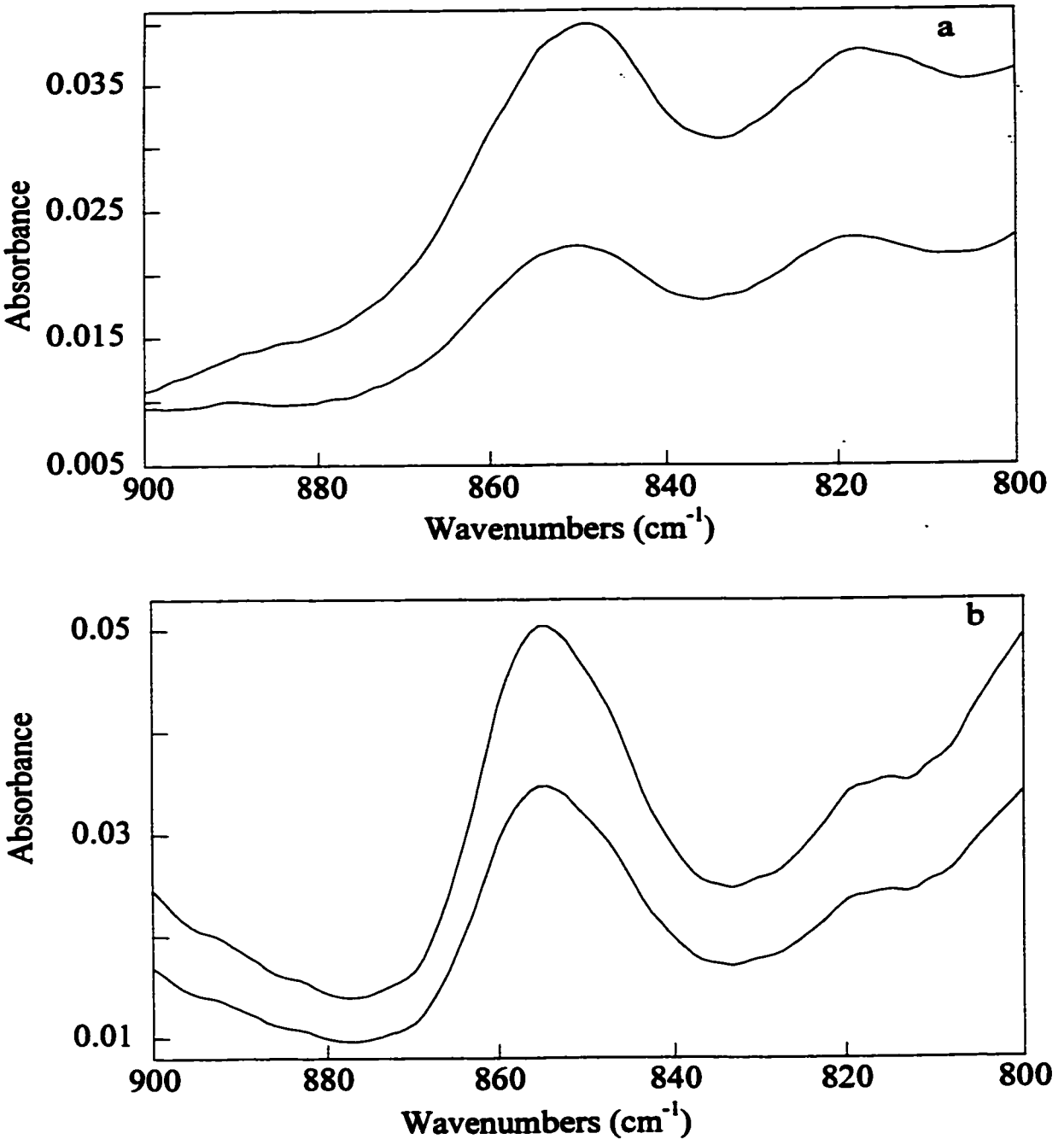

Figure 5.3. IR spectra of silica-supported *tert*-butylperoxo complexes:(a) mononuclear complexes **9** and **10**; (b) dinuclear complexes **11** and **12**. In each frame, the upper line corresponds to the *tert*-butylperoxo complex on silica-500 and the lower line corresponds to the *tert*-butylperoxo complex on silica-200.

Table 5.1. Yield of epoxides upon reaction of excess olefin vapor with dinuclear silica-supported *tert*-butylperoxo complexes of Ti

surface complex	olefin	mmol Ti/g[a]	mmol epoxide/g[a]	epoxide/Ti
$(\equiv SiO)_2TiOTi(OO^tBu)_4$	C_6H_{10}	0.83	1.74	2.10
11	C_6H_{10}		1.71[b]	2.06
	C_6H_{10}	0.83	1.67	2.01
	C_6H_{10}		1.69[b]	2.04
	C_3H_6	0.81	1.62	2.00
$(\equiv SiO)TiOTi(OO^tBu)_5$	C_6H_{10}	0.80	0.74	0.93
12	C_6H_{10}		0.73[b]	0.92
	C_6H_{10}	0.80	0.76	0.95
	C_6H_{10}		0.77[b]	0.96
	C_3H_6	0.79	0.79	1.00

[a] All values are normalized per gram of silica.

[b] Measured after evacuation of volatiles and regeneration of the *tert*-butylperoxo complex with ^tBuOOH, followed by a second addition of excess cyclohexene to the sample in the previous table entry.

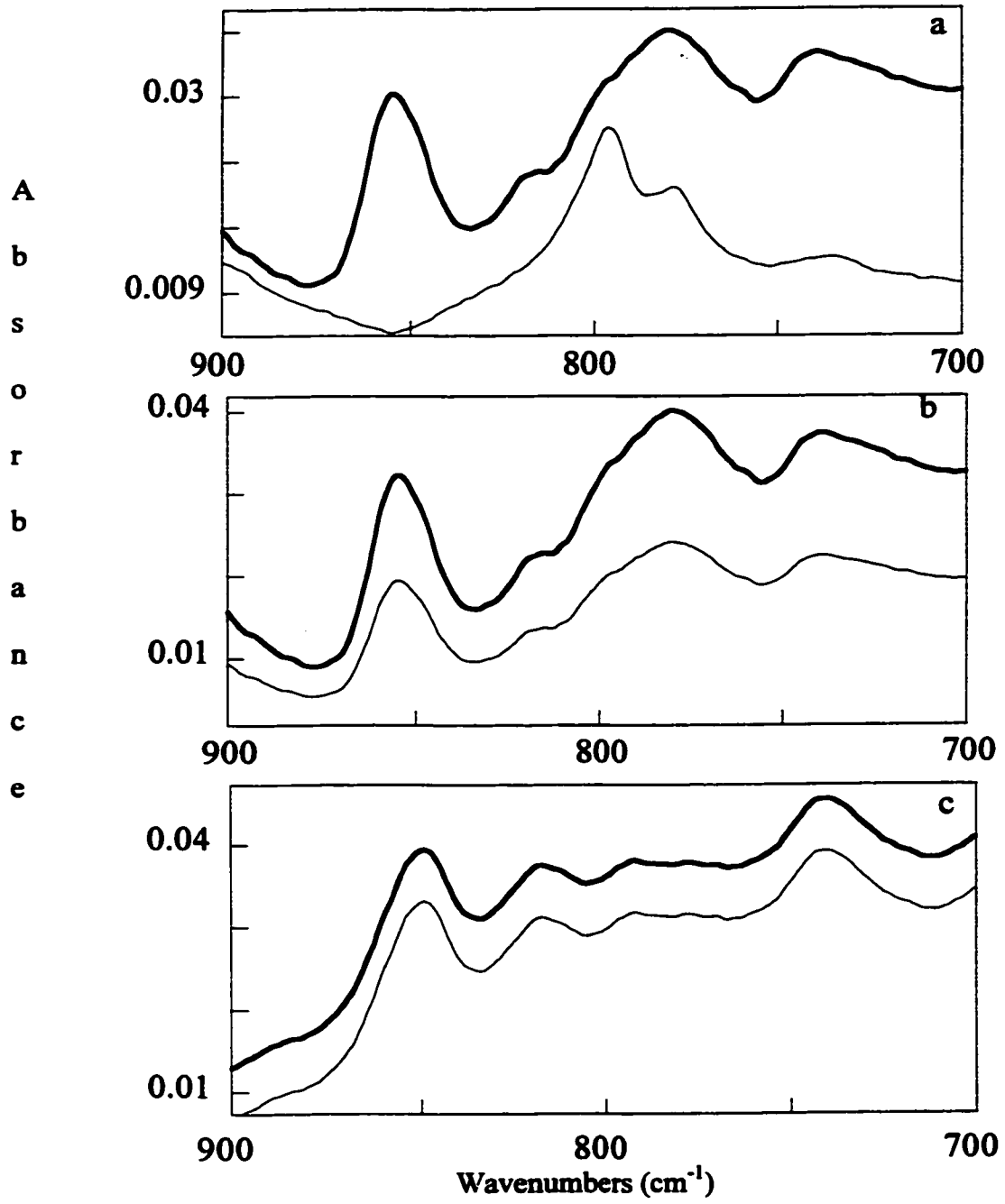

Figure 5.4. *In situ* IR spectra of (a) $(\equiv SiO)_2TiOTi(OO^tBu)_4$, **11**; (b) $(\equiv SiO)TiOTi(OO^tBu)_5$, **12**; (c) $(\equiv SiO)Ti(OO^tBu)_3$, **10** before and after reaction with cyclohexene. In each frame, the heavier line corresponds to the *tert*-butylperoxo complex, the lighter line to the same sample after exposure to excess cyclohexene vapour followed by evacuation of volatiles.

Finally, the ν(O-O) vibration of (≡SiO)Ti(OO^{t}Bu)$_3$, **10**, is unchanged in intensity upon exposure to cyclohexene, Figure 5.4c.

The same reaction stoichiometries were obtained upon reaction with propylene. Thus four equiv. of propylene oxide were recovered when **11** was treated with excess $C_3H_{6(g)}$ at 60°C, whereas **12** yielded only two equiv. of the epoxide under the same conditions, Table 5.1.

5.4 Discussion

The greater acidity of alkyl hydroperoxides relative to that of the alcohols[9] explains the virtually quantitative ligand exchange on supported titanium alkoxide complexes. The alkoxide ligands are almost completely displaced, as shown by a deuterium-labeling IR experiment (Figure 5.1). However, the siloxide linkage is not cleaved by ^{t}BuOOH, in contrast to the reactivity of Ti silasequioxanes.[5] The lack of reactivity of the siloxide "ligand" is as expected, since silica silanols are more acidic than alkylhydroperoxides.

Alkylperoxo ligands bind in an η^2-fashion to early transition metal complexes, leading to an increase in coordination number at Ti.[10] Peroxo complexes of titanium are often seven-coordinate with pentagonal bipyramidal geometries, as in $[Ti(O_2)_3(H_2O)]^{2-}$,[11] and can be binuclear, as in $K_2[Ti(O_2)(C_7H_3O_4N)(H_2O)]_2O$, which contains a linear Ti-O-Ti bridge.[12] There are few structurally characterized η^2-alkylperoxo complexes of d^0 metals, and only one example has been isolated for Ti.[10] VO(OO^{t}Bu)($C_7H_3O_4N$)(H_2O) is a distorted pentagonal bipyramid with an η^2-OO^{t}Bu ligand.[4] An *in situ* NMR study of Ti(OO^{t}Bu)$_n$(O^{i}Pr)$_{4-n}$ with n=1, 2, 3, 4, concluded that all the tert-butylperoxo ligands are

coordinated in an η^2-fashion based on their ^{13}C chemical shifts, even for n=4.[13] We suggest that the surface complexes also contain η^2-alkylperoxo ligands, although we have no spectroscopic evidence for or against this.

The reactivity of the dinuclear alkylperoxo complexes **11** and **12** toward cyclohexene resembles the stoichiometric epoxidation activity of Mo(VI) peroxo complexes such as $MoO(O_2)_2(HMPA)$ in organic solvents.[14] In contrast, mononuclear **9** and **10** show no reactivity toward cyclohexene at room temperature. Interestingly, the formation of a TiOTi species was observed by ^{17}O NMR in the reaction of $Ti(O^iPr)_4$ with cumene hydroperoxide,[15] although the active species for epoxidation was not isolated.

The observed difference in reactivity of the dinuclear *tert*-butylperoxo complexes is presumed to be a consequence of their different compositions. We propose a symmetrical structure for **11**, in which each six-coordinate Ti bears two η^2-alkylperoxo ligands, Scheme 5.1. In contrast, the proposed structure of **12** is unsymmetrical, with only one of the two Ti sites resembling those of **11**. The other site bears three η^2-*tert*-butylperoxo ligands, all of which are apparently unreactive towards olefins, Scheme 5.2. We suggest that the tris(*tert*-butylperoxo)titanium site may not react because of unfavorable steric interactions with the three *tert*-butyl substituents. Consistent with this finding, the isolated (*i.e.*, mononuclear) tris(*tert*-butylperoxo)titanium site **10** also shows no reactivity towards cyclohexene. Steric congestion has been implicated in catalytic performance of related Ti-silsesquioxane model systems.[16] However, electronic differences between the sites cannot be excluded as a reason for the difference in reactivity at this time.

Scheme 5.1. Stoichiometric epoxidation of olefins by $(\equiv SiO)_2TiOTi(OO^tBu)_4$, **11**.

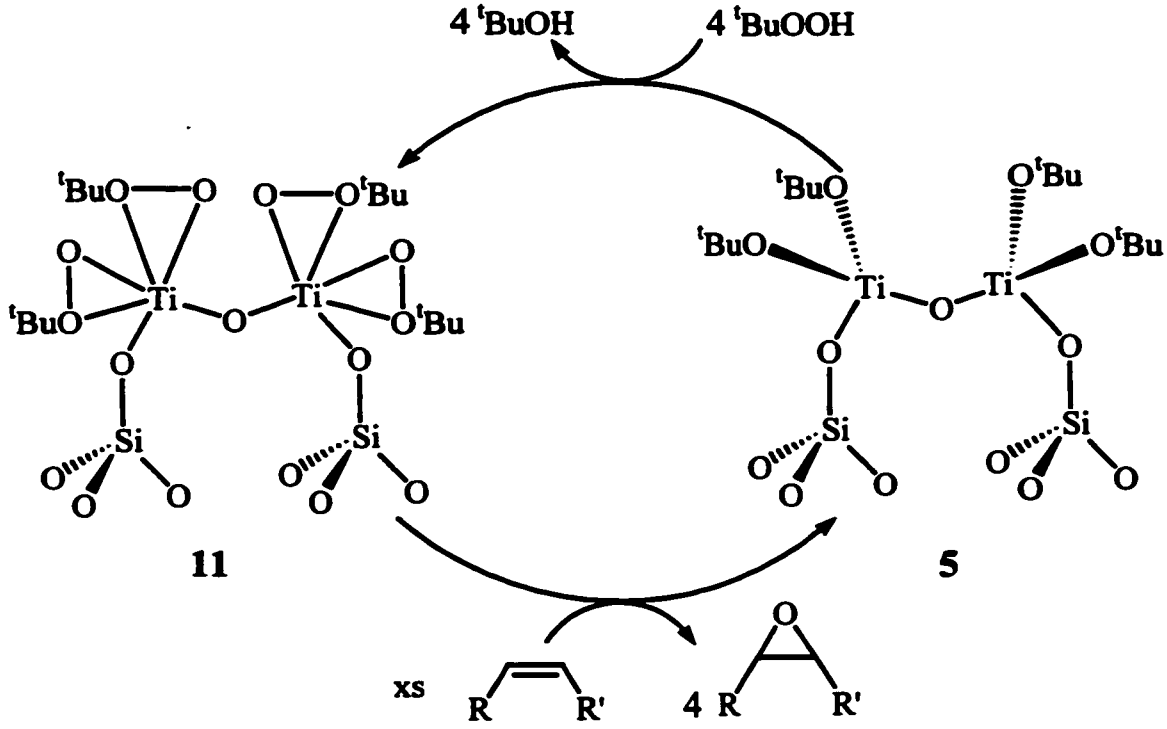

Scheme 5.2. Stoichiometric epoxidation of olefins by (≡SiO)TiOTi(OO^{t}Bu)$_5$, **12**.

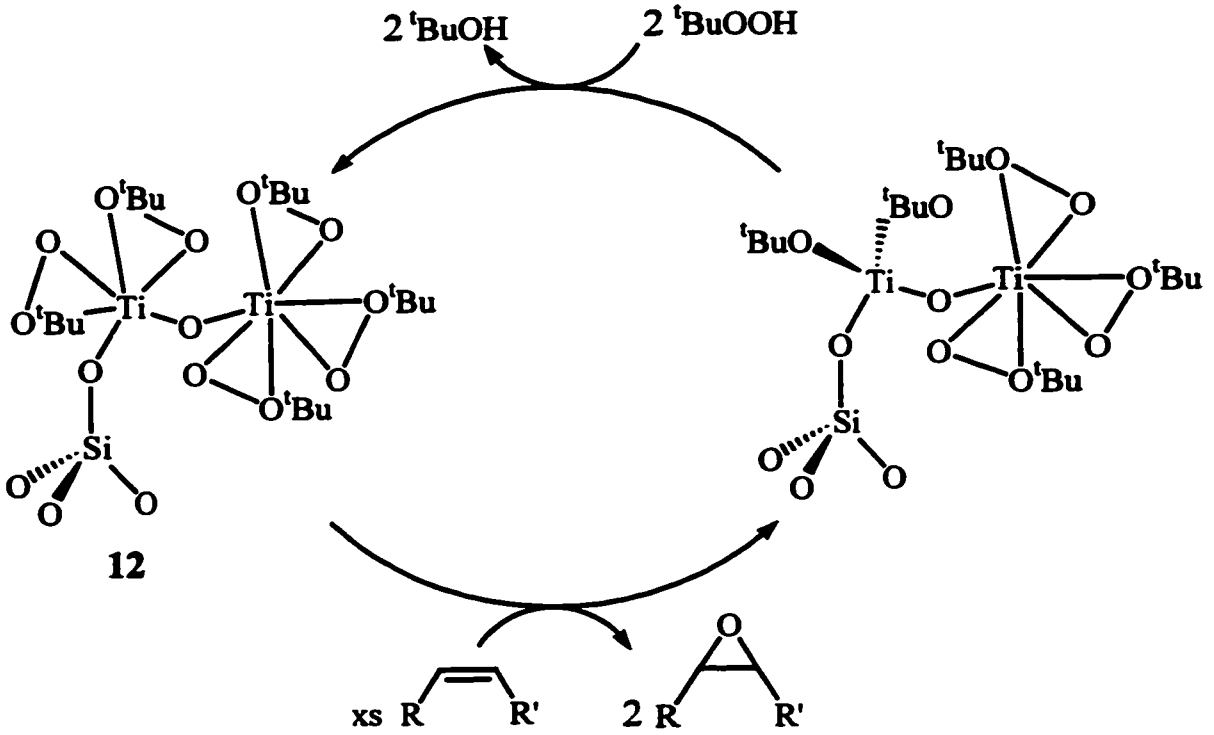

According to this reasoning, the isolated bis(*tert*-butylperoxo)titanium site **9** was expected to be active for epoxidation, but no reaction with cyclohexene was found. The steric constraint imposed by the second siloxide linkage to the surface is, however, considerably greater than the first, since the doubly-anchored complex is effectively held closer to the surface than it would be by a single, flexible siloxide bond.

5.5 Conclusion

Both mono- and dinuclear surface alkoxide complexes react with *tert*-butyl-hydroperoxide; however, it appears that only the dinuclear alkylperoxo complexes react directly with simple olefins. The stoichiometric reactions of cyclohexene with dinuclear silica-supported complexes $(\equiv SiO)_2TiOTi(OO^tBu)_4$, **11**, and $(\equiv SiO)TiOTi(OO^tBu)_5$, **12**, are quantitative. Thus all sites are active, however, not all peroxidic oxygens are available for reaction. The yields of epoxide are four and two equiv. per TiOTi unit, respectively. This result suggests that all the peroxidic oxygens of the bis(peroxo) sites are active, whereas none of the peroxidic oxygens of the tris(peroxo) sites are.

It was unexpected that such closely-related dinuclear peroxometal complexes should show such a dramatic difference in reactivity.[17] Nevertheless, it is clear that for the same Ti loading (maximum 3.9 wt.%) on the same silica support material, the epoxidation efficiency is 100% higher for **11** compared to **12**. These results suggest a possible explanation for the influence of hydroxyl content of oxide supports used to prepare such catalysts on their reactivity.

5.7 References

(1) Jørgensen, K. A. *Chem. Rev.* **1989**, *89*, 431-458.

(2) Arends, I. W. C. E.; Sheldon, R. A.; Wallau, M.; Schuchardt, U. *Angew. Chem. Int. Ed. Engl.* **1997**, *36*, 1144-1163.

(3) Khouw, C. B.; Dartt, C. B.; Labinger, J. A.; Davis, M. E. *J. Catal.* **1994**, *149*, 195-205.

(4) Mimoun, H.; Chaumette, P.; Mignard, M.; Saussine, L.; Fischer, J.; Weiss, R. *Nouv. J. Chim.* **1983**, *7*, 467-475.

(5) Abbenhuis, H. C. L.; Krijnen, S.; van Santen, R. A. *Chem. Commun.* **1997**, 331-332.

(6) Bouh, A. O.; Rice, G. L.; Scott, S. L. *J. Am. Chem. Soc.* **1999**, *121*, 7201-7210.

(7) Rice, G. L.; Scott, S. L. *Langmuir* **1997**, *13*, 1545-1551.

(8) Yudanov, I. V.; Gisdakis, P.; Valentin, C. D.; Rösch, N. *Eur. J. Inorg. Chem.* **1999**, 2135-2145.

(9) Richardson, W. H. In *The Chemistry of Peroxides*; Patai, S., Ed.; Wiley: New York, 1983; p 129.

(10) Boche, G.; Möbus, K.; Harms, K.; Marsch, M. *J. Am. Chem. Soc.* **1996**, *118*, 2770-2771.

(11) Griffith, W. P. *J. Chem. Soc.* **1964**, 5248-5253.

(12) Schwarzenbach, D. *Inorg. Chem.* **1970**, *9*, 2391-2397.

(13) Babushkin, D. E.; Talsi, E. P. *React. Kinet. Catal.Lett.* **1999**, *67*, 359-364.

(14) Mimoun, H.; Roch, I. Seree. de Roch.; Sajus, L. *Tetrahedron* **1970**, *26*, 37.

(15) Finn, M. G.; Sharpless, K. B. *J. Am. Chem. Soc.* **1991**, *113*, 113-126.

(16) Klunduk, M. C.; Maschmeyer, T.; Thomas, J. M.; Johnson, B. F. G. *Chem. Eur. J.* **1999**, *5*, 1481-1485.

(17) Al-Ajlouni, A. M.; Espenson, J. H. *J. Org. Chem.* **1996**, *61*, 3969-3876.

Chapter 6

Reaction of Epoxides with Silica-supported Ti Complexes

6.1 Introduction

Titanium supported on or in siliceous supports such as amorphous silica, mesoporous silicates and zeolites is an effective catalyst for the epoxidation of simple olefins by alkylhydroperoxides. Catalytic reactions are conducted in the liquid phase, and strong solvent dependences have been reported.[1] Although such catalysts are often highly selective for the epoxide, they lose their activity over time. This phenomenon is often attributed to leaching of the titanium from the catalyst into solution, via cleavage of the Ti-O-Si support bonds by the weakly acidic alkylhydroperoxide.[2] Furthermore, some Ti/silicate catalysts are known to be highly sensitive to moisture.[3]

In order to shed light on the nature of the reactions which cause deactivation of the catalyst, we studied the behaviour of alkylperoxotitanium complexes grafted onto silica surfaces under gas phase reaction conditions, without the complication of the solvent. In Chapter 5, we described how, upon exposure of $(\equiv SiO)_2TiOTi(OO^tBu)_4$, **11**, or $(\equiv SiO)TiOTi(OO^tBu)_4$, **12**, to excess olefin at room temperature, in the absence of uncoordinated *tert*-butylhydroperoxide or solvent, 2.0 and 1.0 equiv. epoxide, respectively, were recovered per Ti. In our attempts to render this stoichiometric reaction catalytic, another transformation of epoxide was uncovered, resulting in deactivation of the catalyst.

6.2 Olefin epoxidation under gas phase catalytic conditions

The catalytic gas phase epoxidation of cyclohexene was attempted, in the simultaneous presence of excess cyclohexene and *tert*-butylhydroperoxide vapor (*i.e.*, in the absence of solvent). Catalysts derived from **1** and **2** yielded a stoichiometric amount (2.0 and 1.0 equiv. of epoxide per Ti, respectively) after 0.5-1 hours reaction time. The active sites are stable in the presence of excess *tert*-butylhydroperoxide; no regeneration of surface hydroxyls (corresponding to protonolysis of the Si-O-Ti linkages) was observed. In each case, the yield of epoxide corresponds to precisely one turnover of the "catalyst", defined as the *t*-butylperoxo complexes **11** and **12**, formed upon reaction of **1** and **2** with ^{t}BuOOH. After evacuation of all volatiles, followed by readdition of both reagents, an additional turnover of the catalyst was observed, Table 5.1. This (stoichiometric) cycle may be repeated several times. However, catalytic epoxidation was never observed under gas phase reaction conditions; the second turnover did not take place until the epoxide was removed from the reactor.

We infer that, in the absence of solvent, the epoxide once formed remains coordinated to the active site, eq 6.1-6.2.

$$(\equiv SiO)_2TiOTi(OO^tBu)_4 + \text{xs } C_6H_{12} \rightarrow (\equiv SiO)TiOTi(O^tBu)_4(OC_6H_{12})_4 \qquad (6.1)$$

11

$$(\equiv SiO)TiOTi(OO^tBu)_5 + \text{xs } C_6H_{12} \rightarrow (\equiv SiO)TiOTi(O^tBu)_2(OC_6H_{12})_2(OO^tBu)_3 \qquad (6.2)$$

12

The coordinated epoxide apparently prevents regeneration of the active site with ^{t}BuOOH, unless removed by evacuation.

Although epoxides are not common ligands for transition metals, examples are known in surface chemistry and molecular chemistry. For example, ethylene oxide is adsorbed on the surface of the Ag/SiO_2 epoxidation catalyst,[4] and a thermally stable molecular adduct, $[HB(3,5\text{-}(CF_3)_2Pz)_3]Ag(OC_2H_4)$, has been crystallographically characterized.[5] The latter complex does not lose the epoxide ligand even under reduced pressure. Epoxide complexes of Cd(II) carboxylates were prepared by displacement of THF by cyclohexene oxide and propylene oxide, and the adducts were crystallographically characterized.[6] The binding constants for adduct formation, measured by NMR, demonstrate that epoxides are slightly less basic (and hence weaker ligands) than either THF or dioxane.[7]

The failure to observe catalytic gas phase epoxidation chemistry with **1** and **2** stands in contrast to the well-known propensity of materials prepared in a very similar manner to effect catalytic epoxidation in the liquid phase.[8] Dissociation of the epoxide from the epoxide is presumably assisted by solvation.

6.3 Reaction of the *in situ*-generated epoxide

When the epoxide formed by reaction of **11** with cyclohexene was not immediately removed by evacuation, but was instead left in the reactor in contact with the catalyst for a period of several hours, it was no longer possible to remove it by evacuation. Dramatic and irreversible changes in the IR spectrum of the silica, Figure 6.1, indicate that the epoxide becomes strongly adsorbed on the surface. New, intense bands at 2937, 2866

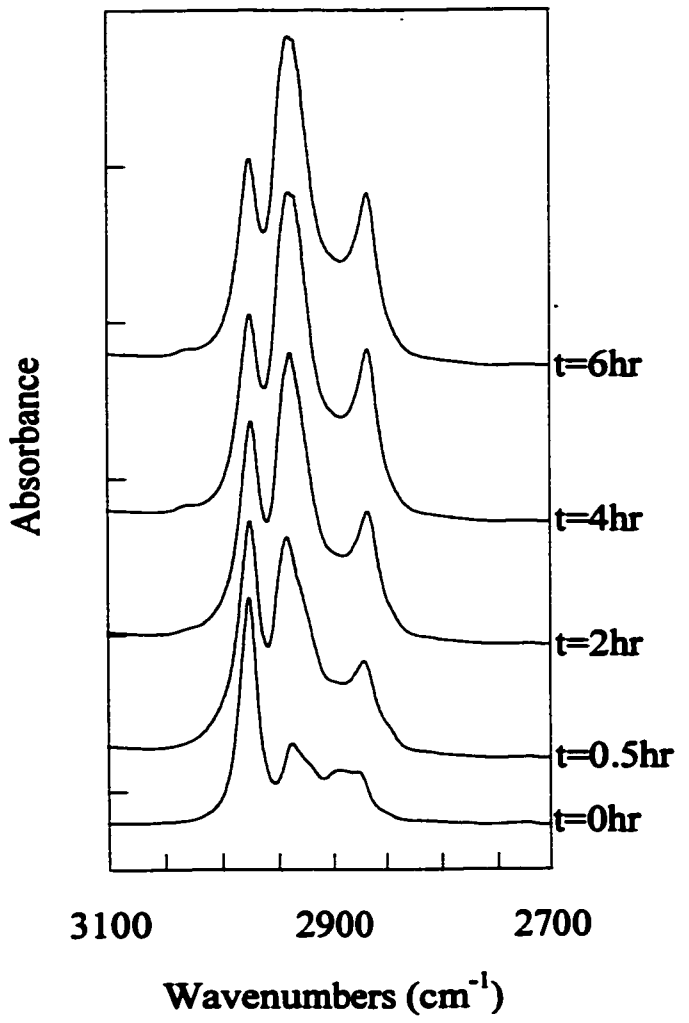

Figure 6.1. Transmission IR spectra of the $Ti(O^iPr)_4$-modified silica surface, initially $(\equiv SiO)_2TiOTi(O^iPr)_4$, at various times after exposure to a ^tBuOOH / cyclohexene mixture. Volatiles were condensed into a side-arm with liquid N_2 before recording each spectrum.

and 1465 cm^{-1} appear, characteristic of the ν(CH) and $\delta(CH_2)$ vibrations of the cyclohexane moiety. Similar spectral changes were observed when epoxidation was effected starting with **12**, when the cyclohexene oxide product was not promptly removed from the reactor.

The rate of the reaction was monitored by observing the increase in intensity of the hydrocarbon vibrations on the surface at constant temperature T = 25°C. The area under the absorbance spectrum from 3050 to 2800 cm^{-1} was integrated and plotted as a function of time. The curve obeys pseudo-first-order kinetics with k_{obs}= 0.00115 ± 0.0002 s^{-1} in a reaction containing 14.6 μmol Ti, Figure 6.2a. The pseudo-first-order rate constants are directly proportional to the amount of Ti present in the reactor, Table 6.1, as shown by the closed circles in Figure 6.3a.

A similar reaction was observed for **2**, with semilar kinetic behavior. However, the slopes of plots of k_{obs} vs. n_{Ti} for the reactions catalyzed by **1** and **2** are significantly different. The reaction of **2** has a slope corresponding to a second-order rate constant of 122 s^{-1} $(mol\ Ti)^{-1}$. In contrast, the reaction catalyzed by **1** has a slope of only 79 s^{-1} $(mol\ Ti)^{-1}$. Both have intercepts insignificantly different from zero. After reaction of the Ti/silica catalyst with the *in situ*-generated epoxide, and the associated spectral changes described above, the material becomes inactive towards cyclohexene. Thus, evacuation of all volatiles followed by readdition of *t*-butylhydroperoxide and cyclohexene resulted in no further formation of epoxide.

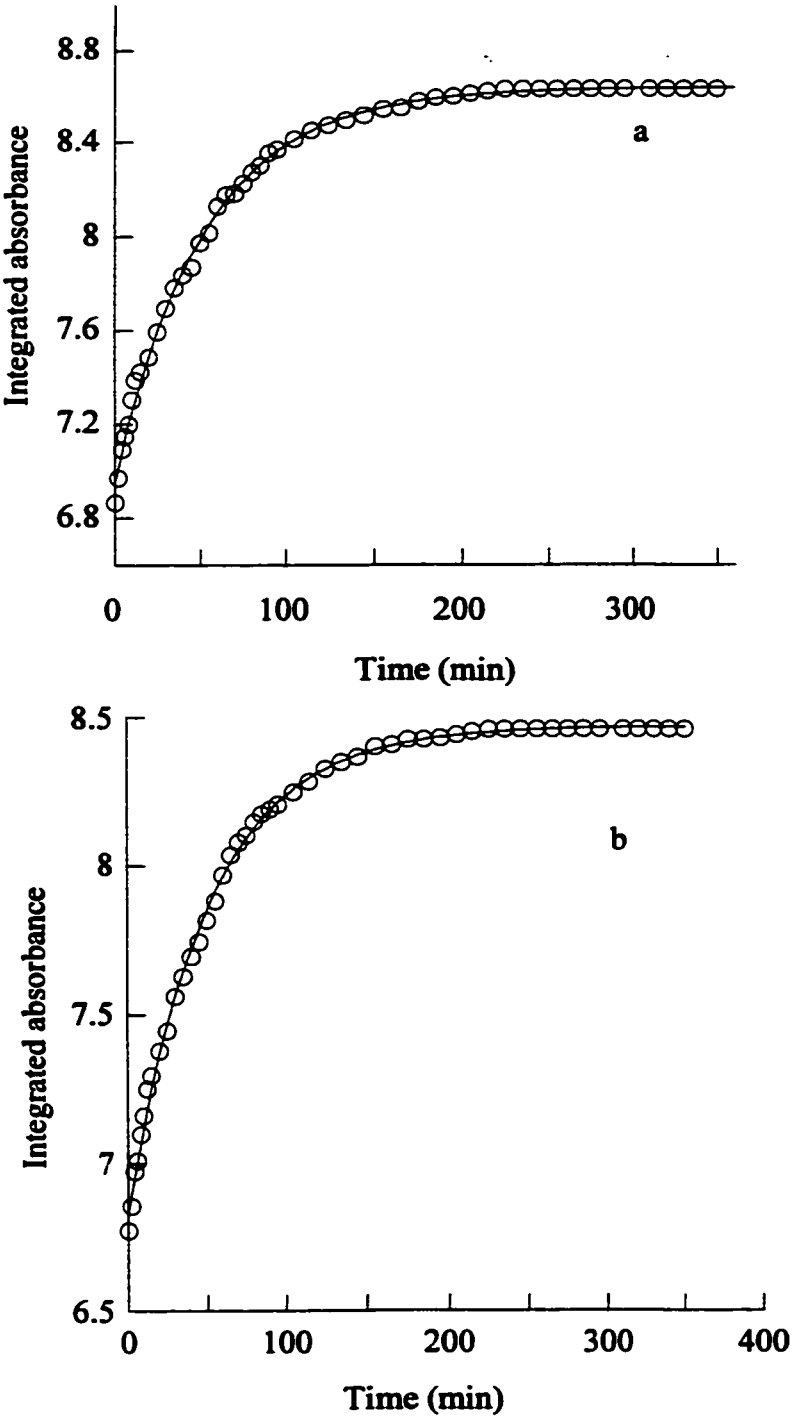

Figure 6.2. Time-resolved growth of the C-H stretching bands upon addition to $(\equiv SiO)_2TiOTi(O^iPr)_4$ of (a) a ^{t}BuOOH/cyclohexene mixture and (b) cyclohexene oxide. The solid lines are fits to the integrated first-order rate equation. Each reaction contained 14.6 μmol Ti.

Table 6.1. Pseudo-first-order rate constants for the reaction of cyclohexene oxide with silica-supported Ti complexes at 25°C

surface complex	Reaction mixture	n_{Ti}/μmol	k_{obs}/s^{-1}
$(\equiv SiO)_2TiOTi(OO^tBu)_4$	$C_6H_{10}/^tBuOOH$	6.89	0.00055±0.00003
		10.2	0.00084±0.00009
		12.9	0.00103±0.00005
		14.6	0.00117±0.0001
	$C_6H_{10}O$	14.6	0.00115±0.0001
		16.4	0.00131±0.0001
$(\equiv SiO)TiOTi(OO^tBu)_5$	$C_6H_{10}/^tBuOOH$	1.21	0.00014±0.00001
		5.9	0.00072±0.00006
		10.2	0.00124±0.0004
$(\equiv SiO)Ti(O^iPr)_3$	$C_6H_{10}/^tBuOOH$	6.6	0.0013±0.0001

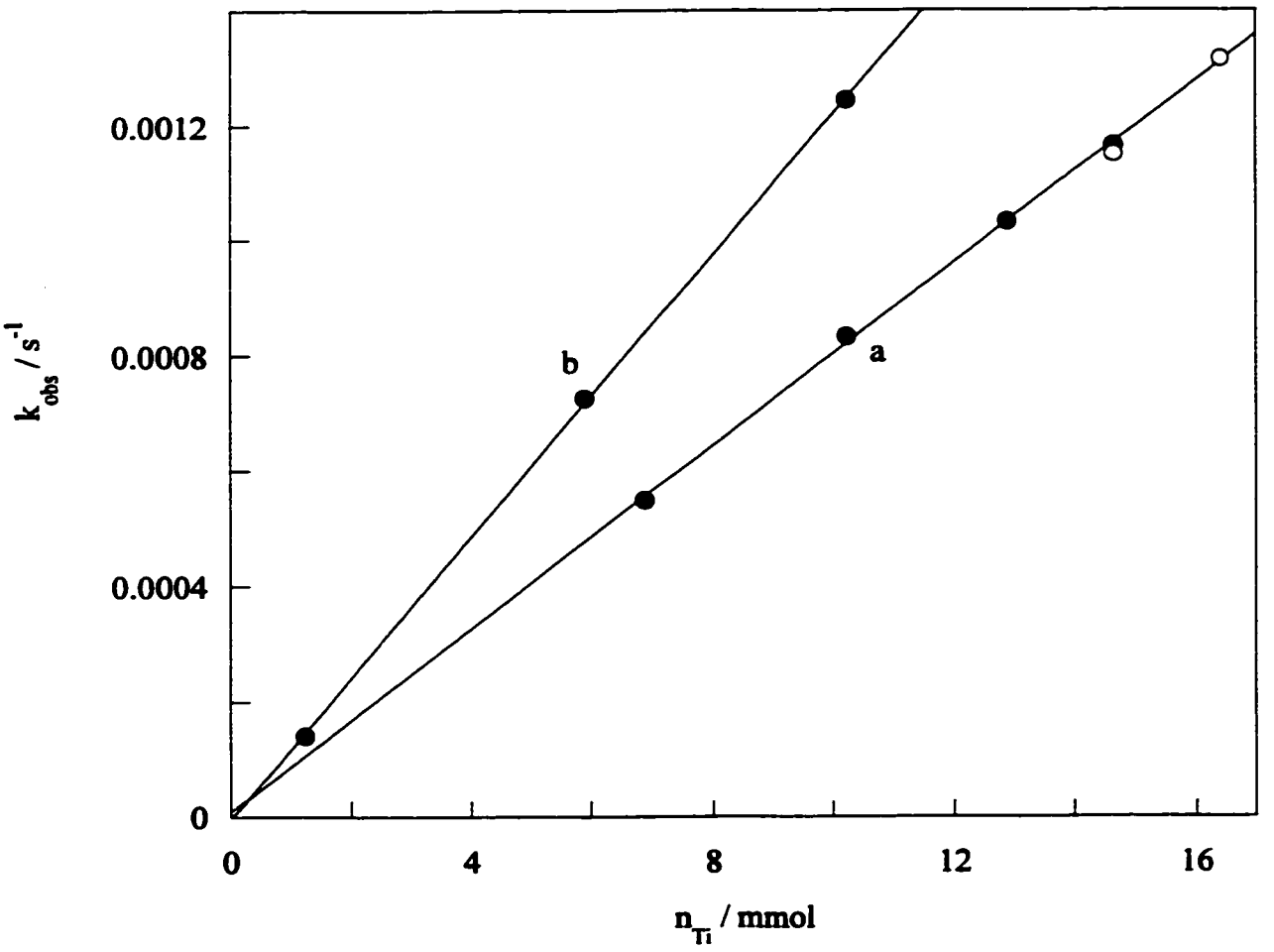

Figure 6.3. Dependence of the pseudo-first-order constants for reaction of cyclohexene oxide, at 25°C, with $(\equiv SiO)_nTiOTi(O^iPr)_{6-n}$, on the quantity of Ti present in the reactor. Closed circles correspond to experiments in which the epoxide was formed *in situ*; open circles are experiments in which the epoxide was added directly to the reactor. The two datasets correspond to materials with (a) n=2; (b) n=1.

6.4 Reaction of the active sites with added epoxide

Identical IR spectral changes were observed when a sample of $(\equiv SiO)_2TiOTi(O^iPr)_4$, **1**, containing 14.6 μmol, which had never been exposed to either *tert*-butylhydroperoxide or cyclohexene, was treated with cyclohexane oxide at 25°C. A pseudo-first-order increase in intensity of the hydrocarbon bands was observed, Figure 6.2b. Furthermore, the pseudo-first-order rate constant for this reaction, $k_{obs} = 0.00115 \pm 0.0002\ s^{-1}$, corresponds precisely to that obtained in the absence of added epoxide, but in the presence of a cyclohexene/^{t}BuOOH mixture. Thus, the rate constants for the epoxide reaction, shown by open circles in Figure 6.3a, fall directly on the line describing the rate of the olefin reaction. This finding demonstrates that the reaction corresponds to a rate-determining transformation of the epoxide, which is preceded by rapid epoxidation in the case of cyclohexene/^{t}BuOOH mixtures. The rate law for this reaction is mixed second-order, eq. 6.3.

$$-d[C_6H_{10}O]/dt = k[C_6H_{10}O]\, n_{Ti} \qquad (6.3)$$

Although the mononuclear Ti site **6** does not effect epoxidation of cyclohexene, it nevertheless undergoes the same reaction as the dinuclear Ti sites with cyclohexene oxide. Addition of 30 Torr cyclohexene to a sample of **6** (6.62 μmol Ti) at room temperature resulted in a pseudo-first-order increase of the C-H intensity, with an observed rate constant $k_{obs} = 0.0013 \pm 0.0001\ s^{-1}$. This reaction is significantly faster than that of **2**.

6.5 Characterization of the chemisorbed cyclohexene oxide

A sample of **2** containing 12.4 μmol Ti was allowed to react at room temperature with excess cyclohexene oxide for 24 hours, at which time all volatiles were evacuated. Complete combustion of the organics in 450 Torr O_2 at 700 °C led to the formation of 1209 μmol CO_2. After subtracting the quantity of CO_2 expected from the combustion of 2.5 isopropyl groups per Ti (93 μmol), the amount of CO_2 remaining corresponds to 15.0 equiv. of cyclohexene oxide per dinuclear Ti site, or 3.0 epoxides per original alkoxide ligand, eq 6.4.

$$(\equiv SiO)TiOTi(O^iPr)_5 + \text{xs } C_6H_{12}O \rightarrow (\equiv SiO)TiOTi(O^iPr)_5(OC_6H_{12})_{15} \qquad (6.4)$$

2

The corresponding experiment with a sample of **1**, containing 11.2 μmol Ti, led to the formation of 873.6 μmol CO_2. After subtracting the quantity of CO_2 expected from the combustion of 2.0 isopropyl groups per Ti, 67.2 μmol, the amount of CO_2 remaining corresponds to 12.0 equiv. of cyclohexene oxide per dinuclear Ti site, eq 6.5.

$$(\equiv SiO)_2TiOTi(O^iPr)_4 + \text{xs } C_6H_{12}O \rightarrow (\equiv SiO)_2TiOTi(O^iPr)_4(OC_6H_{12})_{12} \qquad (6.5)$$

1

Once again, this corresponds to a reaction of 3.0 epoxides per original alkoxide ligand.

The solid-state ^{13}C CP/MAS spectra of the material resulting from the reaction of cyclohexene oxide with **2** consists of four resonances at 22, 25, 34 and 78 ppm, Figure

6.4a. This spectrum can be compared to the spectrum of **2**, Figure 3.1, with only two signals at 25 and 78 ppm corresponding to the methyl and methine carbons of the isopropyl groups. However, the signal-to-noise ratio is considerably higher in Figure 6.4a, reflecting a greater amount of hydrocarbon on the silica surface.

The additional signals observed in Figure 6.4a are assigned to CH_2 signals of the chemisorbed cyclohexene oxide groups. According to the ^{13}C NMR spectrum of cyclohexene oxide itself, features are expected at δ 52.7 ppm $O(CHCH_2CH_2)_2$, 24.8 ppm $O(CHCH_2CH_2)_2$ and 20.1 ppm $(OCHCH_2CH_2)_2$.[9] The absence of a signal at 53 ppm in figure 6.4a indicates that cyclohexene oxide is not intact. The presence of a real signal upfield of the 25 ppm isopropyl peak is shown by the dipolar dephasing experiment. The band sharpens considerably as all signals except that of the isopropylmethyl are suppressed, Figure 6.4b.

A ^{13}C spectrum was also recorded following addition of a cyclohexene/^{t}BuOOH mixture to **2**, Figure 6.5. The spectrum again shows four resonances at 22, 25, 34 and 78 ppm, indicating formation of the same product. Simulation of the ^{13}C NMR spectrum of cyclohexene oxide oligomers gave signals at 83, 29 and 22 ppm. The signal at 83 ppm (OCH) is likely overlaid with methine signal of the isopropyl groups, at 78 ppm, while the 29 and 22 ppm signals are observed as high and low field shoulders on the methyl signal of the isopropyl groups, at 25 ppm. Finally, organic products were extracted from the surface with CH_2Cl_2. A solution NMR spectrum was recorded of the soluble organic material after evaporation of the solvent and redissolution in CD_2Cl_2. The ^1H spectrum, Figure 6.6, shows several broad peaks from 0.9 to 2.2 ppm corresponding to methylene protons and a peak at 3.5 ppm corresponding to the methine proton of the olgomer.[10]

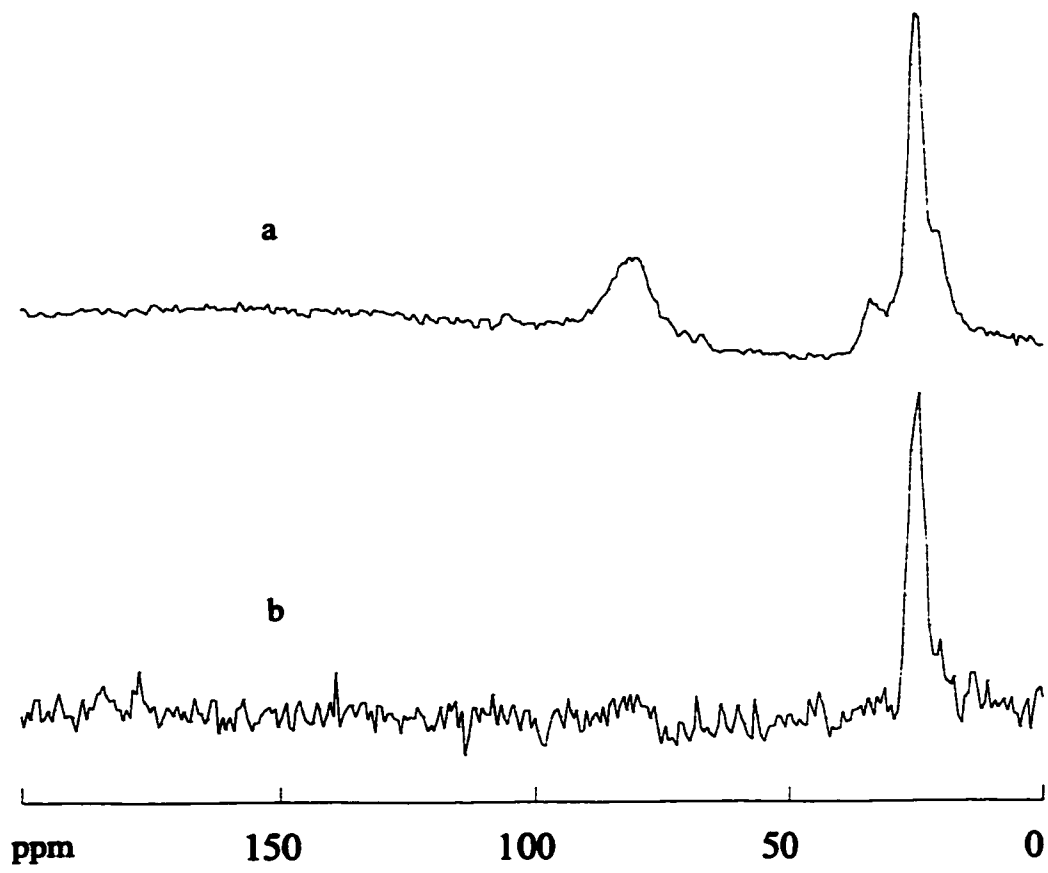

Figure 6.4. ^{13}C spectra of (≡SiO)TiOTi(O^iPr)$_5$, **2**, after addition of cyclohexene oxide and evacuation of volatiles: (a) CP/MAS spectrum; (b) dipolar dephased spectrum. Spin rate, 4 kHz.

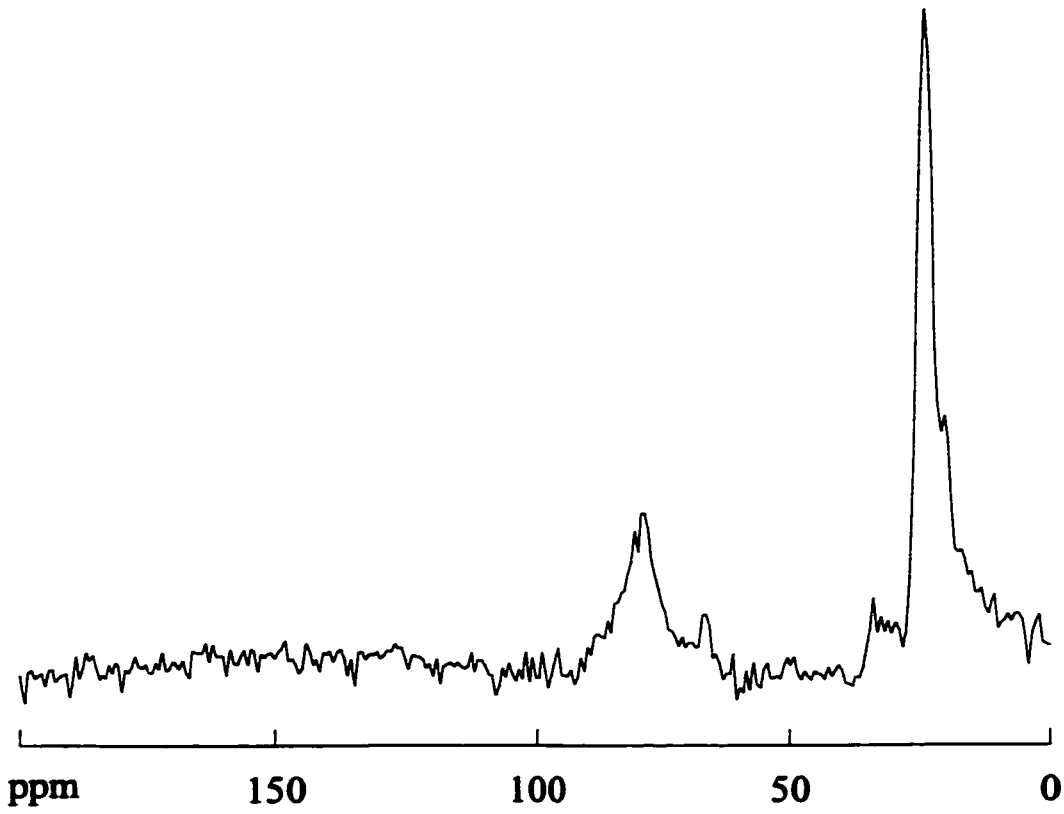

Figure 6.5. ^{13}C CP/MAS spectrum of (≡SiO)TiOTi(O^{i}Pr)$_5$, **2**, after addition of cyclohexene/ ^{t}BuOOH.

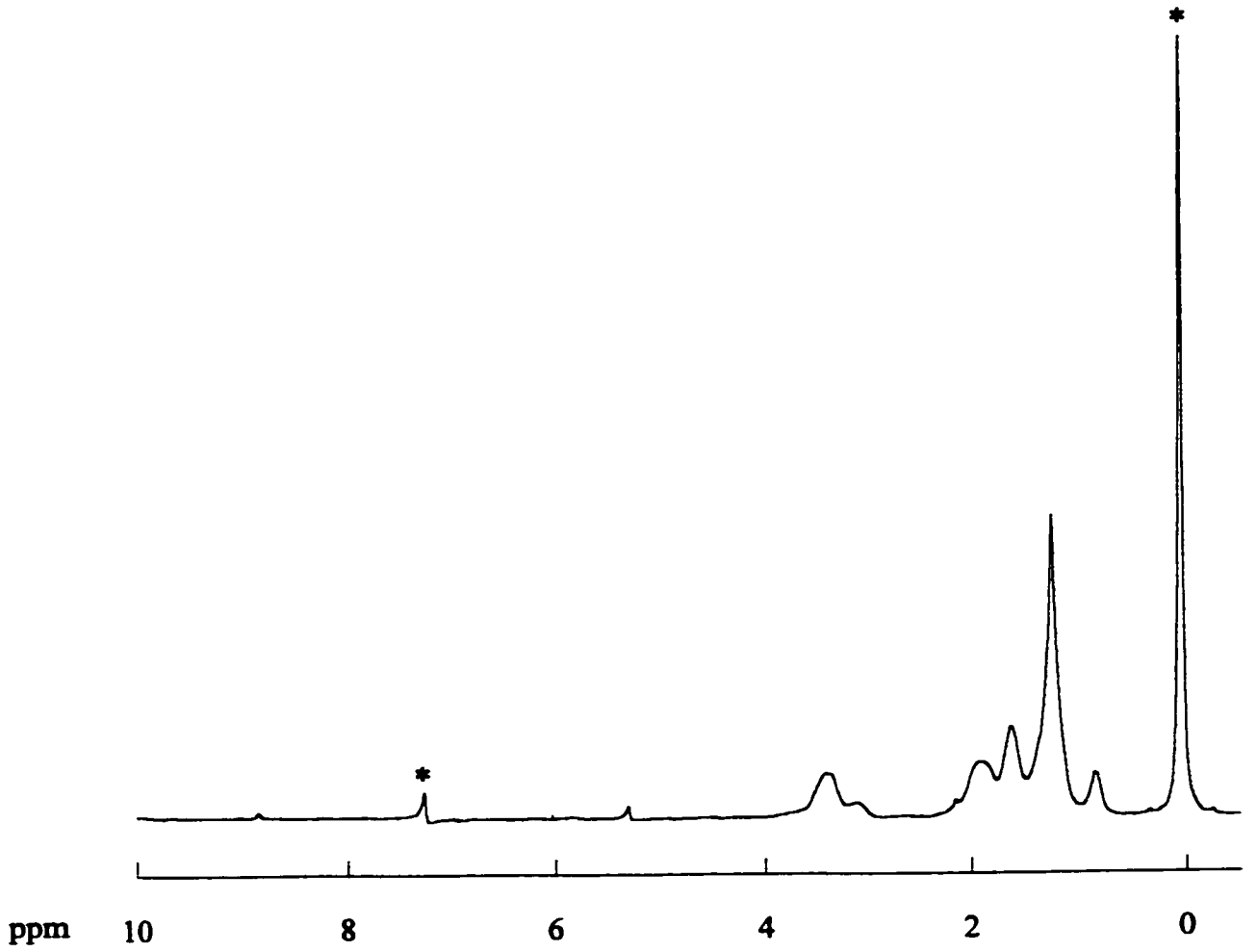

Figure 6.6. ^{1}H NMR spectrum of organic products extracted after reaction of cyclohexene oxide with **2**.

From these experiments, we conclude that silica-supported organotitanates oligomerize cyclohexene oxide. The combustion results further imply that the materials are selective trimerization agents for cyclohexene oxide, and that the reaction sites are the alkoxide ligands themselves.

6.6 Mechanism of epoxide trimerization

Lewis acids are known to catalyze the homopolymerization of epoxides to polyethers,[11] as well as the copolymerization of epoxides with CO_2 to polycarbonates.[12] The mechanism is generally assumed to be a coordination polymerization, in which nucleophilic attack of a coordinated alkoxide ligand causes ring-opening of the epoxide, Scheme 6.1. Insertion of the epoxide leads to the formation of a new alkoxide ligand, which can then react with another equivalent of the epoxide.

$Ti(O^iPr)_4$ is reported to catalyze the polymerization of epoxides in the presence of phenol.[13] Phenoxide ligands were suggested to increase the Lewis acidity of the Ti center, which enhances its ability to coordinate the epoxide. A similar role may be played by the siloxide ligands of the silica-supported organotitanates. However, it is not known why epoxide trimerization occurs so selectively, instead of random oligomerization. However, it is most interesting that all the alkoxide ligands participate in the trimerization reaction with epoxides, whereas only specific sites effect the epoxidation reaction (Chapter 5). The triether ligands, being potentially chelating, are

Scheme 6.1. Mechanism of epoxide trimerization

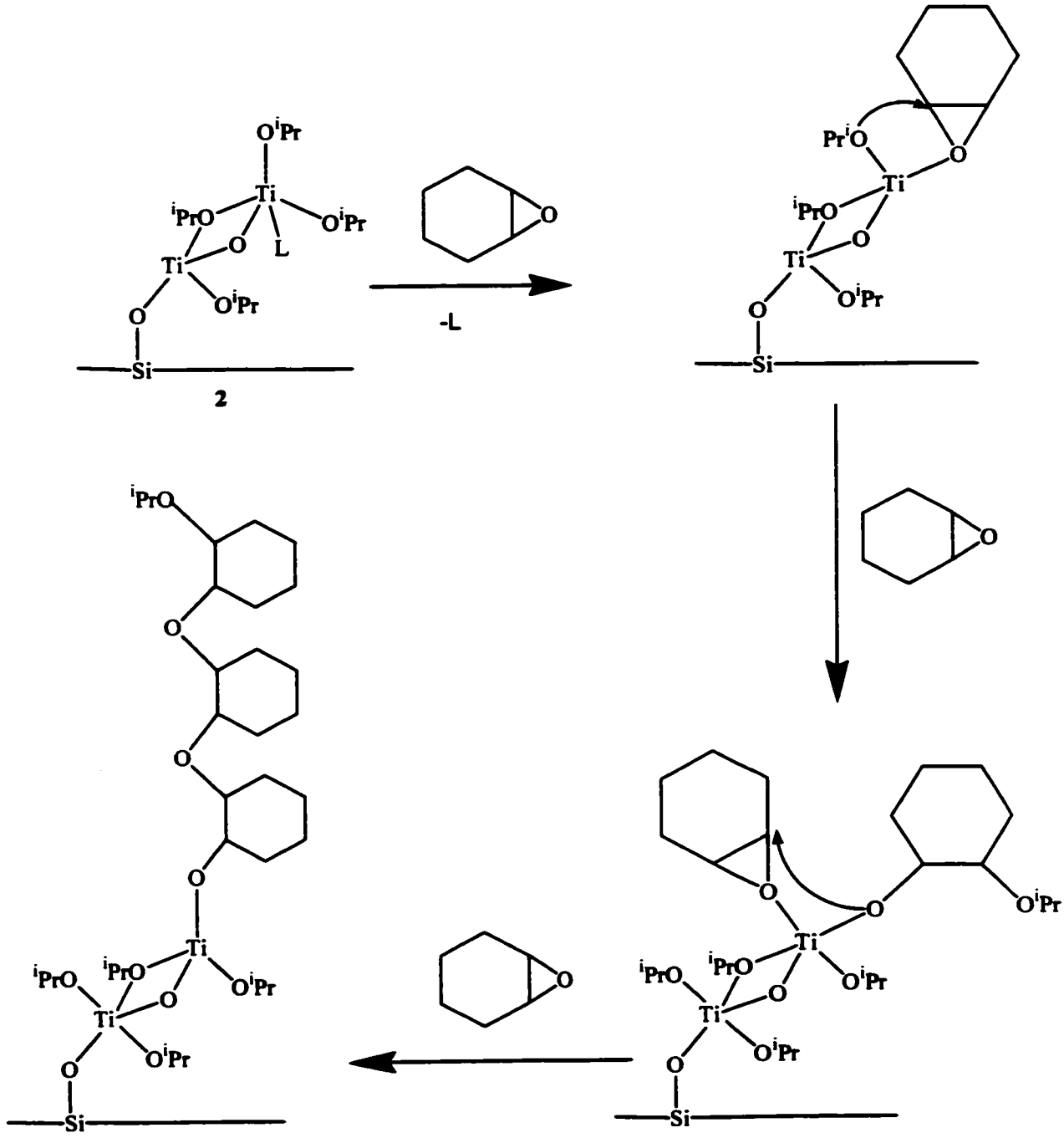

undoubtedly more difficult to displace by ^{t}BuOOH than monodentate alkoxide ligands, thereby shutting off the epoxidation reaction.

6.7 Conclusion

The oxidation of cyclohexene by *tert*-butylhydroperoxide, catalyzed by silica-supported Ti complexes, $(\equiv SiO)_nTiOTi(OO^tBu)_{6-n}$ (n = 1 or 2), yields cyclohexene oxide stoichiometrically as the exclusive product at short reaction times. However, the gas phase reaction is not catalytic, and at longer contact times, the yield of cyclohexene oxide decreases, without the appearance of other volatile oxidation products. It was discovered that the epoxide reacts with the catalyst to form trimers which block the active sites and inhibit further epoxidation reactions. Such reactions may represent important deactivation processes for supported Ti catalysts. Materials which are less active or even inactive in epoxidation are more active in epoxide trimerization.

6.8. References

(1) Crocker, M.; Herold, R. H. M.; Orpen, A. G.; Overgaag, M. T. A. *J. Chem. Soc., Dalton Trans.* **1999**, 3791-3804.

(2) Chen, L. Y.; Chuah, G. K.; Jaenick, S. *Catal. Lett.* **1998**, *50*, 107-114.

(3) Sheldon, R. A.; Dakka, J. *Catal. Today* **1994**, *19*, 215-246.

(4) Fernandes, E. F.; Benesi, A. J.; Vannice, M. A. *J. Phys. Chem* **1994**, *98*, 8498.

(5) Rasika, H. V.; Wang, Z. *Inorg. Chem.* **2000**, *39*, 3724-3727.

(6) Darensbourg, D. J.; Holtcamp, M. W.; Khandelwal, B.; Klausmeyer, K. K.; Reibenspies, J. H. *J. Am. Chem. Soc.* **1995**, *117*, 538-539.

(7) Darensbourg, D. J.; Niezgoda, S. A.; Holtcamp, M. W.; Draper, J. D.; Reibenspies, J. H. *Inorg. Chem.* **1997**, *36*, 2426-2432.

(8) Jørgensen, K. A. *Chem. Rev.* **1989**, *89*, 431-458.

(9) Pawar, D. M.; Noe, E. A. *J. Am. Chem. Soc.* **1998**, *120*, 1485-1488.

(10) Kuran, W.; Listos, T. *Macromol. Chem. Phys.* **1994**, *195*, 401-411.

(11) Kuran, W.; Listos, T. *Polish J. Chem.* **1994**, *68*, 643-656.

(12) Darensbourg, D. J.; Zimmer, M. S.; Rainey, P.; Larkins, D. L. *Inorg. Chem.* **2000**, *39*, 1578-1585.

(13) Fukuchi, Y.; Kuboki, T.; Takahashi, T.; Noguchi, H.; Saburi, M.; Uchida, Y. *J. Polym. Sci. Polym. Lett. Ed* **1988**, *25*, 269-272.

Chapter 7

General Conclusions

It is crucial to understand the structures of active sites in order to understand surface reaction mechanisms. Towards this goal, we prepared silica-supported titanium(IV) complexes whose uniform structures make them homogeneous in nature and render their reactions more amenable to mechanistic studies.

We demonstrated by directly grafting $Ti(O^iPr)_4$ onto partially dehydroxylated silica that only dinuclear surface complexes are formed, by spontaneous silica-induced condensation of $Ti(O^iPr)_4$. This finding explains Fraile *et al*'s original report that such materials are relatively hydrolytically insensitive compared to the $Ti(O^iPr)_4$ precursor. We also developed an indirect route to prepare the protolytically-sensitive mononuclear silica-supported Ti alkoxide complexes by grafting first the amide complexes $(\equiv SiO)_nTi(NEt_2)_{4-n}$ (n = 1 or 2), which then undergo ligand exchange reactions with alcohols. We showed that reactions of the mononuclear surface alkoxide complexes with $Ti(O^iPr)_4$ yield dinuclear species which are identical to those prepared by the direct reaction of $Ti(O^iPr)_4$ with silica. It was possible to transform both mono- and dinuclear supported alkoxide complexes to the corresponding alkylperoxotitanium surface complexes by reaction with *tert*-butylhydroperoxide. Surprisingly, only the dinuclear alkylperoxo titanium surface complexes react with olefins to generate epoxide under mild conditions. This may be a consequence of steric constraints or an electronic effect related to the Ti-O-Ti feature.

We showed that the active sites react with cyclohexene oxide generated *in situ* or added directly. The reactions are pseudo-first-order, with k_{obs} linearly dependent on the amount of catalyst present. The reaction is a selective epoxide trimerization, in which all alkoxide ligands participate. Mononuclear $(\equiv SiO)Ti(O^iPr)_3$, which is inactive in epoxidation, is the most active for trimerization. Dinuclear $(\equiv SiO)TiOTi(O^iPr)_5$, which is less active than dinuclear $(\equiv SiO)_2TiOTi(O^iPr)_4$ in epoxidation, is 1.5 times faster in trimerization. This reaction permanently deactivates the sites for epoxidation. These findings are, of course, strictly valid only for grafted Ti/Silica catalysts. We do not know whether they can be extended to other heterogeneous Ti catalysts (*e.g.* framework-substituted materials). However, it seems clear that the current acceptance of a single kind of mononuclear active site for all Ti in such catalysts should be critically reevaluated.